Development of an Experimental Device For Monitoring Frost Heave In Soils

by

Heidi McKnight-Whitford

Submitted in partial fulfilment of the requirements
for the degree of Master of Applied Science

at

Dalhousie University
Halifax, Nova Scotia
May 2013

© Copyright by Heidi McKnight-Whitford, 2013

DALHOUSIE UNIVERSITY

DEPARTMENT OF CIVIL AND RESOURCE ENGINEERING

The undersigned hereby certify that they have read and recommend to the Faculty of Graduate Studies for acceptance a thesis entitled "Development of an Experimental Device For Monitoring Frost Heave In Soils" by Heidi McKnight-Whitford in partial fulfilment of the requirements for the degree of Master of Applied Science.

Dated: May 9, 2013

Research Co-Supervisors: _____

_____

Readers: _____

_____

DALHOUSIE UNIVERSITY

DATE: May 9, 2013

AUTHOR: Heidi McKnight-Whitford

TITLE: Development of an Experimental Device For Monitoring Frost Heave In Soils

DEPARTMENT OR SCHOOL: Department of Civil and Resource Engineering

DEGREE: MASc CONVOCATION: October YEAR: 2013

Permission is herewith granted to Dalhousie University to circulate and to have copied for non-commercial purposes, at its discretion, the above title upon the request of individuals or institutions. I understand that my thesis will be electronically available to the public.

The author reserves other publication rights, and neither the thesis nor extensive extracts from it may be printed or otherwise reproduced without the author's written permission.

The author attests that permission has been obtained for the use of any copyrighted material appearing in the thesis (other than the brief excerpts requiring only proper acknowledgement in scholarly writing), and that all such use is clearly acknowledged.

_____

Signature of Author

To:

Mom, Dad, Anthony, Maggie, Paul, Vanessa, Joshua, and Riggs

Thank you for all of the love and support.

TABLE OF CONTENTS

LIST OF TABLES

LIST OF FIGURES

ABSTRACT

The goal of this research is to develop a laboratory freeze cell and experimental methods to monitor frost heave in soil samples. This will allow the ability to identify the mechanisms of ice lens formation under one-dimensional, open system freezing conditions. This dissertation will describe past research examining frost heave in soils and discuss research gaps associated with the measurements performed. Based on the literature, the development of the test apparatus is described, particularly with respect to some of the unique measurements being performed to assess frost heave. The use of thermocouple probes, pore pressure transducers for suction measurements, and Particle Image Velocimetry (PIV) in the test procedure will be discussed. An explanation of the test procedure will be advanced with the assistance of some preliminary tests on a clayey specimen. Future work can enhance the testing methods and develop improved procedures for measuring frost heave in soil samples.

LIST OF ABBREVIATIONS USED

AEV	Air Entry Value
cm	Centimeters
kPa	Kilopascals
mm	Millimeters
NPT	National Pipe Thread
PIV	Particle Image Velocimetry
PPTs	Pore Pressure Transducers
SP	Segregation Potential
TCs	Thermocouples
Tc	Cold side temperature
Tp	Pore freezing temperature
Ts	Segregation freezing temperature
Tw	Warm side temperature
USCS	Unified Soil Classification System

ACKNOWLEDGEMENTS

I would like to express my deepest gratitude to my supervisor, Dr. Craig Lake, for his unwavering guidance and support. Dr. Lake was an exceptional supervisor who always kept my research moving forward, and maintained patience even when mine wore thin. Without his technical contributions and moral support, this research could not have been completed. I would also like to thank my co-supervisor, Dr. Andy Take for his tremendous technical input and his continuous encouragement to think critically.

Thank you to NSERC for providing financial support that helped make this research possible.

I am very grateful to my committee members, Dr. Chris Barnes, and Dr. Brian Taylor for taking the time to review my thesis.

I would like to extend my appreciation to the civil engineering technicians and support staff at Dalhousie University and Queen's University. Special thanks to Brian Liekens for his ongoing technical support, and Brian Kennedy for his time spent machining custom parts for my freeze cell.

Thank you also to my fellow graduate students, as well as undergraduate research assistants, at Dalhousie University and Queen's University for their contributions.

CHAPTER 1 INTRODUCTION

1.1 THESIS INTRODUCTION

As a result of frost heave, cover and barrier systems for waste containment applications may undergo damage, leading to hydraulic performance related issues. Problems encountered include increased effective void ratio and hydraulic conductivity of the barrier system and the potential for contaminant release into the environment. Frost heave is also responsible for damage to buildings and other civil engineering infrastructure, when not accounted for properly.

The goals of this research are to develop a laboratory freeze cell experiment to measure suction development during frost heave damage in clayey material specimens, and use Particle Image Velocimetry (PIV) to identify the mechanisms of ice lens formation. An experimental apparatus and test methodology are developed, and their validity confirmed through obtaining repeatable test data.

Chapter 1 of this dissertation provides a literature review of the mechanisms of ice lens formation, as well as experimental setups and test procedures that have been used to study these mechanisms. Chapter 2 describes the apparatus, materials, and methods of the experimental setup. Chapter 3 displays the experimental results, using the newly developed freeze cell, and provides a discussion of these results. Chapter 4 provides a discussion of the test procedure developed and Chapter 5 states conclusions and offers recommendations for future work.

1.2 LITERATURE REVIEW

1.2.1 Ice Lens Formation

When frost susceptible soils are subjected to sub-zero temperatures, they undergo pore water freezing and subsequent heave due to ice lens formation. When pore water freezes, a suction gradient develops that induces water migration from the unfrozen soil, through the frozen fringe, where it accumulates and freezes. The frozen fringe, which acts as a zone of impeded flow caused by the partial freezing of pore water, is a frozen zone of soil located between the active ice lens and the unfrozen soil (Nixon 1991).Water migrates through the frozen fringe in a thin layer of unfrozen water that remains close to the soil particles. During freezing, water undergoes a nine percent expansion, initiating heave in the soil.

Konrad and Morgenstern (1980) postulated that at the onset of freezing of a fine-grained soil, the rapid change in temperature across the soil depth creates ice lenses that are not visible. As the freezing front (active ice lens) advances, the temperature gradient decreases, and thin ice lenses appear. The frost front continues to advance at decelerating rates, forming thicker ice lenses at increased spacing. Under constant temperature boundary conditions, a final ice lens forms when the frost front stops advancing (see Figure 1.1). Once the freezing front becomes stationary, the final ice lens goes through a period of growth, resulting from an accumulation of continued water migration (Konrad & Morgenstern 1982a). The suction developed in the soil due to this ice formation results in water movement towards the higher suction area of the soil (i.e. the ice lens), provided water is available.

If frost penetration is controlled at slow rates, such as in ramped freezing tests, it is expected that a linear temperature profile would be maintained throughout the soil. If frost penetration rates are too quick, however, the thickening frozen fringe will impede heat flow through the fringe and a bilinear temperature gradient will develop (see Figure 1.1). This can occur in the early stages of step freezing tests, until steady-state

conditions are reached. The temperature at the base of the final ice lens is very close to 0 ºC (Konrad & Morgenstern 1980).

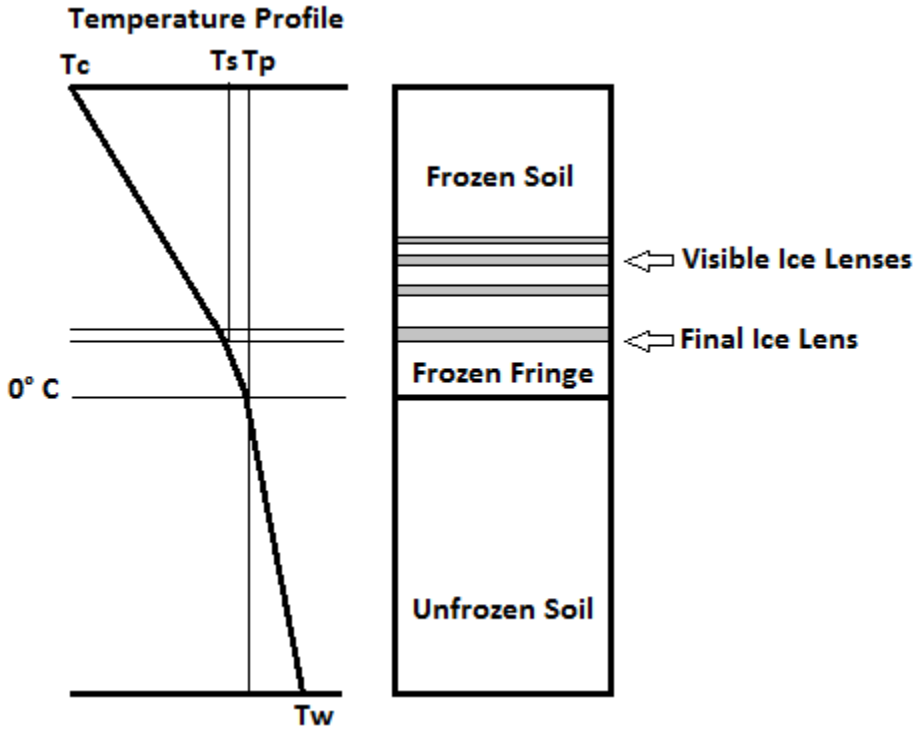

Figure 1.1 Schematic of ice lens formation

In Figure 1.1, Tc and Tw represent the cold side and warm side temperatures at the boundary conditions, respectively. Ts represents the segregation freezing temperature at the freezing front. This is the temperature at which migratory water freezes. Tp represents the pore freezing temperature, which is the highest temperature at which ice can grow in the soil pores. The frozen fringe is located in the zone between Ts and Tp (Konrad 1994).

The ice lenses that form during the freezing of a soil are made up of in-situ pore water, and water that migrates to the freezing front, which freezes and undergoes a nine percent expansion. As an ice lens grows, a pressure is applied to the boundary conditions, causing subsequent heave in the soil (Konrad and Morgenstern 1980). Direct measurement of surface heave can be misleading during these tests, however, by underestimating frost heave and not accounting for freezing induced consolidation of the unfrozen soil that also

takes place. Quantifying the volume of ice lens formation gives a more accurate prediction of overall heave (Konrad and Seto, 1993). PIV has been used by Arenson et al. (2007) to measure this ice lens growth. This study was used as a proof test to see if PIV would be useful in frost heave tests. Promising results were an indication that the study should be extended.

There is experimental evidence to suggest that when water migrates toward the growing ice lens, vertical ice veins form first, followed by horizontal ice lenses. It was proposed by Arenson et al. (2006), that the vertical veins may form when large suction stresses develop in the frozen fringe and overcome the tensile strength of the soil, causing cracks (see Figure 1.2). Between the soil and ice along the vertical veins, a very thin film of water forms a channel. These channels allow water to continue to migrate, through the partially frozen soil to the growing ice lens, significantly faster than if it were to travel through the partially frozen pores of the frozen fringe. This helps explain the growth of horizontal ice lenses despite a decreased hydraulic conductivity in the frozen fringe (Arenson et al. 2006).

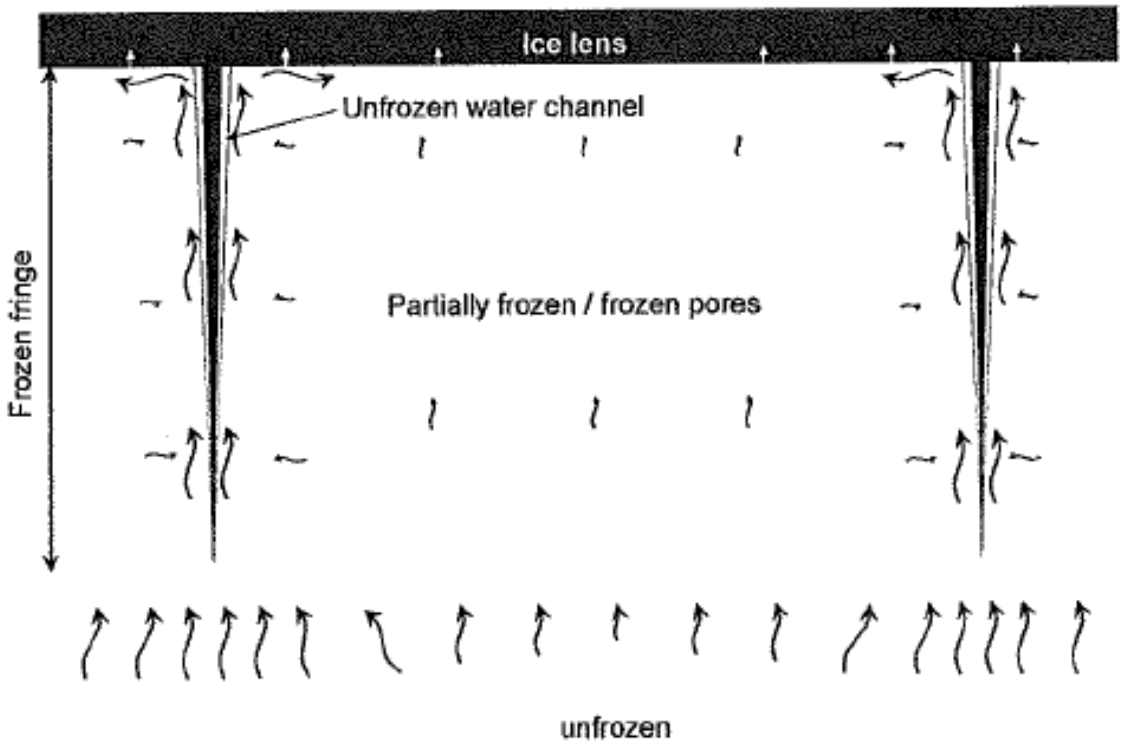

Figure 1.2 Water migration in freezing soils (Arenson et al. 2008)

Arenson and Sego (2004) conducted one-dimensional step-freezing experiments on poorly graded coarse grained sand and were able to watch the location of the freezing front and the unfrozen water within the frozen fringe using a fluorescent tracer. Fluorescence can be traced using UV light, and does not change the freezing point of water. They found that colder temperatures caused more advanced freezing and a thicker frozen lens at the end of the test. In addition, large thermal gradients lead to more trapped unfrozen water than low gradients, which allowed soil to cool more slowly (Arenson and Sego, 2004).

Arenson et al. (2006) observed that changing the temperature gradient on a specimen also changed the thickness of ice lenses, the distance between the lenses, and the thickness of the frozen fringe. Ice lens thickness increased and the distance between lenses decreased with decreasing temperature gradient. Time-lapse photography, and a fluorescent tracer were used to observe the formation and growth of ice lenses (Arenson et al. 2006).

1.2.2 Segregation Potential

From an experimental perspective, segregation potential (SP) is the ratio of porewater flux (v_u) entering the unfrozen soil and temperature gradient (T_G) in the frozen fringe, at the formation of the final ice lens (Konrad and Morgenstern, 1981) as shown in Equation 1.1. SP describes the relationship between heat and mass transfer in a freezing soil, allowing for the prediction of frost heave susceptibility (Konrad 1982a).

$$SP = \frac{v_u}{T_G}$$

Equation 1.1

Konrad and Seto (1993) used an alternative approach to determine segregation potential, by back calculating from surface heave measurements.

SP decreases throughout the freezing process, either with a decreasing rate of cooling in the frozen fringe (see Figure 1.3), or with increasing suctions at the frost front (see Figure 1.4) (Konrad and Morgenstern 1981).

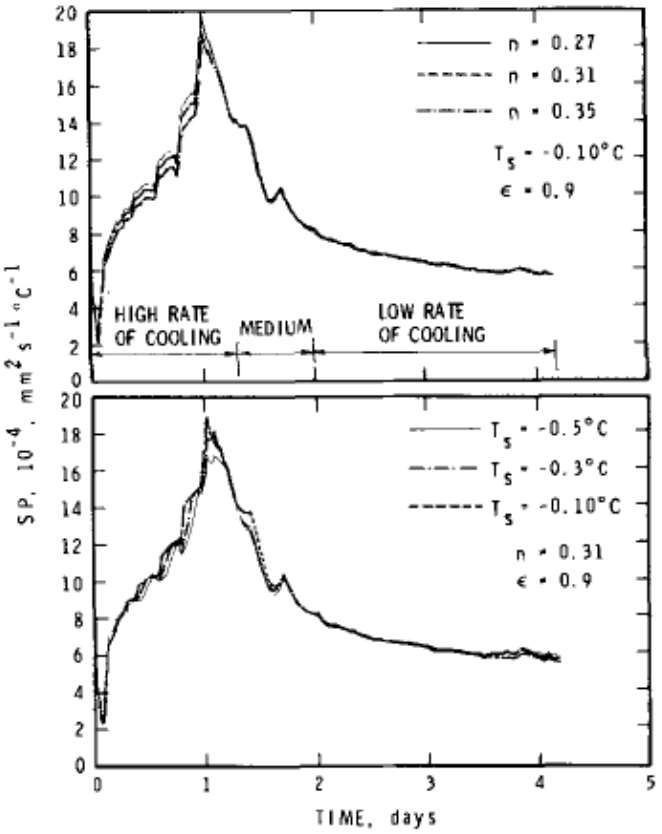

Figure 1.3 Segregation potential vs rate of cooling (Konrad, 1987)

Reprinted, with permission, from ASTM Geotechnical Testing Journal, Volume 10, Issue 2, copyright ASTM International, 100 Barr Harbor Drive, West Conshohocken, PA 19428.

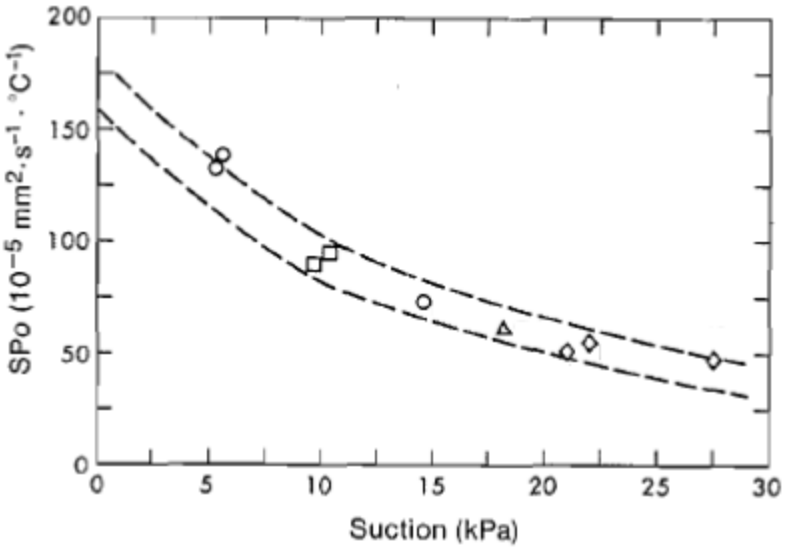

Figure 1.4 Segregation potential vs suction at the frost front for Devon silt (modified from Konrad and Morgenstern 1981)

During transient freezing, SP changes with time. The value of SP at the end of the transient freezing process, when the rate of cooling is zero, is usually reported (Yuzuru et al. 1998). Table 1.1 following, lists the segregation potential of soils reported by Saarelainen (1996).

Table 1.1 Segregation potential of soils

Frost Susceptibility Class	Segregation Potential (mm^2/°C*d)
Negligible	< 12
Low	12-96
Moderate	96-192
High	> 192

1.2.3 Development of Suction

Large suctions can develop in a soil, during freezing, at the ice-water interface at the freezing front. Measuring and understanding the suction values is important for understanding processes that take place during the freezing of a soil such as water migration, freezing induced consolidation, and segregation potential. Suction that

develops in the frozen fringe is the driving force of water migration (Konrad and Morgenstern 1980). Figure 1.5 suggests the suction profile that develops in a freezing soil.

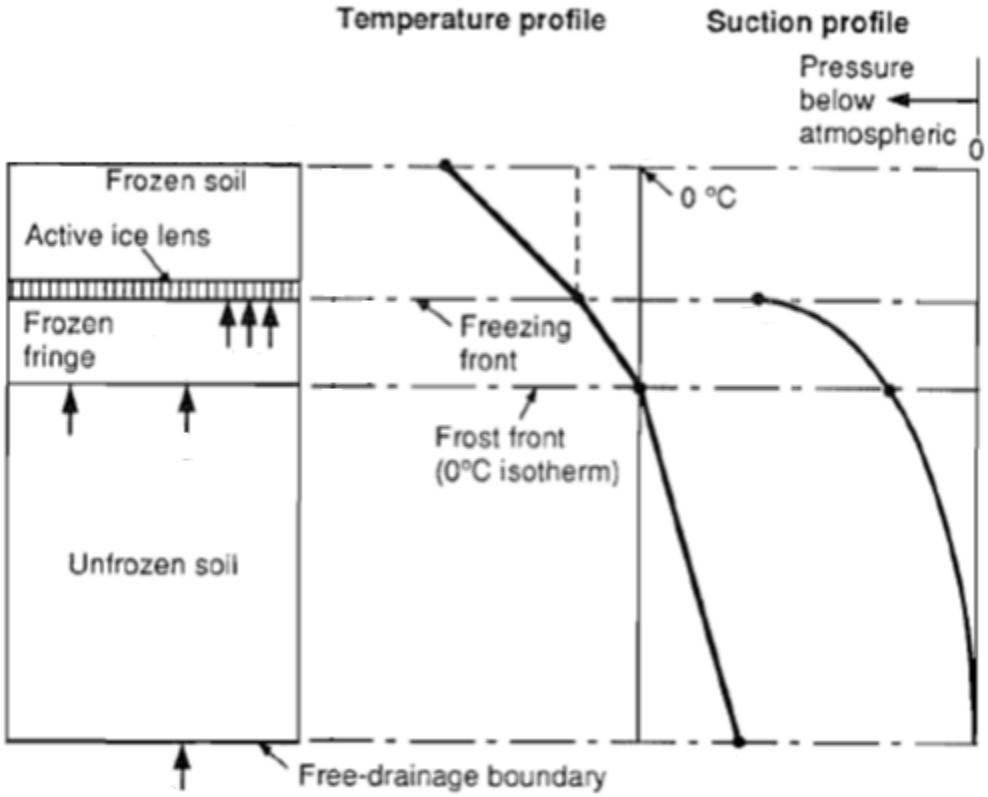

Figure 1.5 Schematic of hydrodynamic and thermal processes in freezing soils (modified from Konrad & Seto 1994)

Konrad and Morgenstern (1981) showed that, for a uniform soil sample, the suction that developed at the frozen fringe was affected only by the warm-side temperature. Konrad and Morgenstern (1982a) predicted that the suction at the frost front of Devon silt could not exceed -80 kPa, without cavitation.

In past research, attempts at measuring soil suction have largely been made using tensiometers which are usually limited to measuring suctions of -80 kPa, and back pressure techniques which offer indirect results (Konrad and Seto 1993). Figure 1.6 shows the distribution of suction, measured using backpressure, in a natural, undisturbed Champlain Sea clay from a one dimensional, laboratory step-freezing test. The numeric

labels on the curves represent the elevation (in mm) from which the measurements were taken.

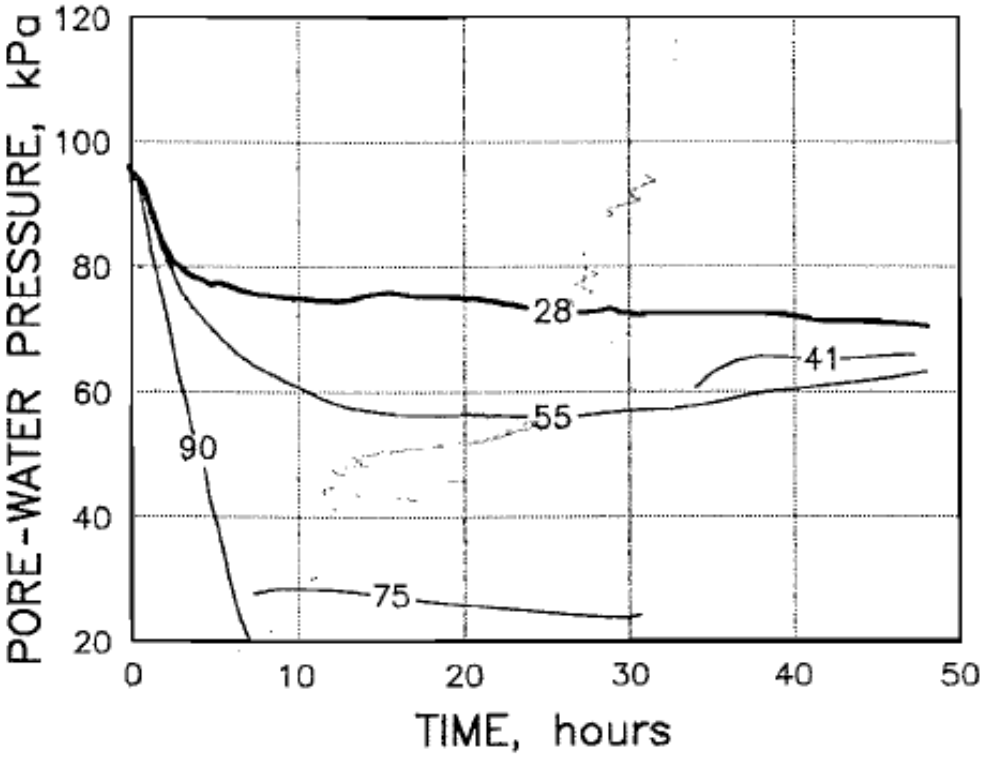

Figure 1.6 Evolution of pore water pressure (Konrad & Seto 1994)

Take and Bolton (2003), suggested using a pore pressure and tension transducer for the reliable measurement of soil suctions ranging from -100 kPa to -400 kPa. This high capacity device consists of a pressure transducer, modified and fitted with a high air-entry filter, which when properly saturated, is capable of reliable soil suction measurement. This technique offers many advantages to freeze cell experiments such as the ability to directly measure the suction in a soil with time and relate it to other measurements such as temperature, water intake, and location of freezing front. To the knowledge of the author, this technique has not been used to measure soil suctions in any published freezing test experiments. A detailed explanation of the device, and how it works, is found in Take and Bolton (2003).

1.2.4 Freeze Cell Experiments

Freeze cell experiments have been used to study the mechanisms of ice lens formation, measure the suction that develops in freezing soils, and classify a soil in terms of its segregation potential. To the knowledge of the author, however, there have been no studies that have accurately accomplished all of this with one experimental setup.

Konrad and Morgenstern (1980) used a freezing cell to conduct experiments on Devon silt, a highly frost susceptible soil. Soil samples were consolidated before being placed into the freezing cell. A number of thermistors were placed in the cell wall, to measure the temperature profiles in the soil, and the cell was heavily insulated. Tests were conducted in a cold room at +0.5°C. A constant temperature below 0°C was held at the cold side boundary, and a constant temperature above 0°C was held at the warm side boundary. Temperature, water migration into and out of the cell, and total heave were monitored during the test, until a stationary frost front developed. The location of the frost front was determined from the thermistor data. The final location of the frost front was determined through inspection of the sample after the termination of the test. Suction values were estimated through the use of the Clausius-Clapeyron equation, as indicated by Konrad and Morgenstern (1980), not direct measurement.

Penner (1985) conducted experiments using a freeze cell apparatus that he adopted and modified from a model developed by Penner and Ueda (1977). He conducted ramped freezing tests on various natural soils. Figure 1.7 shows a schematic of Penner's frost cell. Samples were made 100 mm long by 100 mm in diameter, placed in a lubricated cell, and frozen from the bottom up. Temperature boundary conditions were maintained using temperature baths. The external water source level was maintained at the porous plate on top of the sample. Surface heave was measured using a direct-current displacement transducer. The temperature gradient was measured using thermistors in the sidewall of the cell.

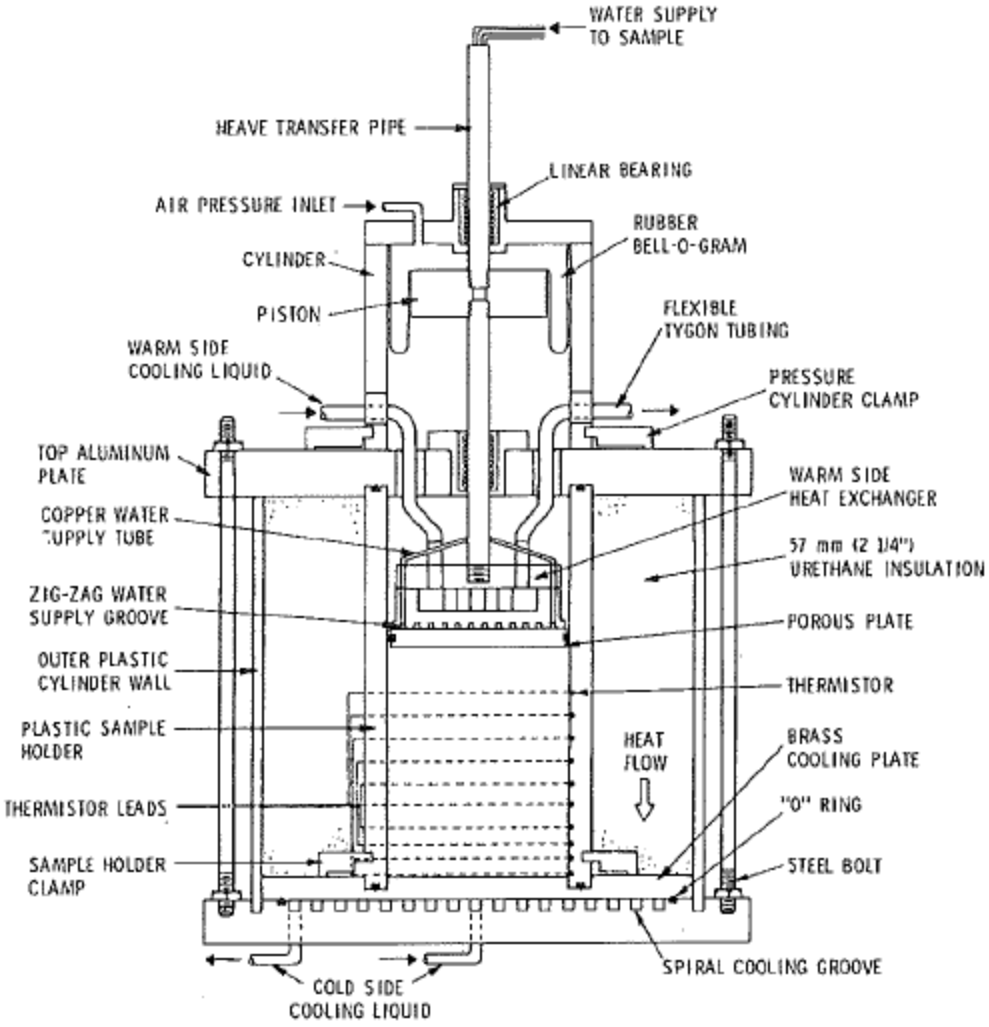

Figure 1.7 Schematic of frost cell used by Penner (1986)

Konrad and Seto (1993) used a freezing cell to conduct experiments on undisturbed Champlain Sea clay samples (see Figure 1.8). The cell consisted of a 102 mm inside diameter, 30 mm thick, 250 mm high split-mould greased with petroleum jelly. Stainless steel porous plates were placed on the top and bottom of the samples. Temperature boundary conditions were maintained using thermoelectric baths that circulated glycol-water mixtures to the top and bottom boundaries of the cell. Thermistors were equally spaced along the cell wall to measure temperature profiles. Water intake was measured manually using a graduated burette. Sample displacement was recorded using a direct current displacement transducer. Pore-pressure sensors were used to measure pore water pressure using a back pressure technique. The back pressure technique avoids the

problems of measuring negative water pressures by superimposing a positive pressure datum so that suctions are still measured as positive pressures.

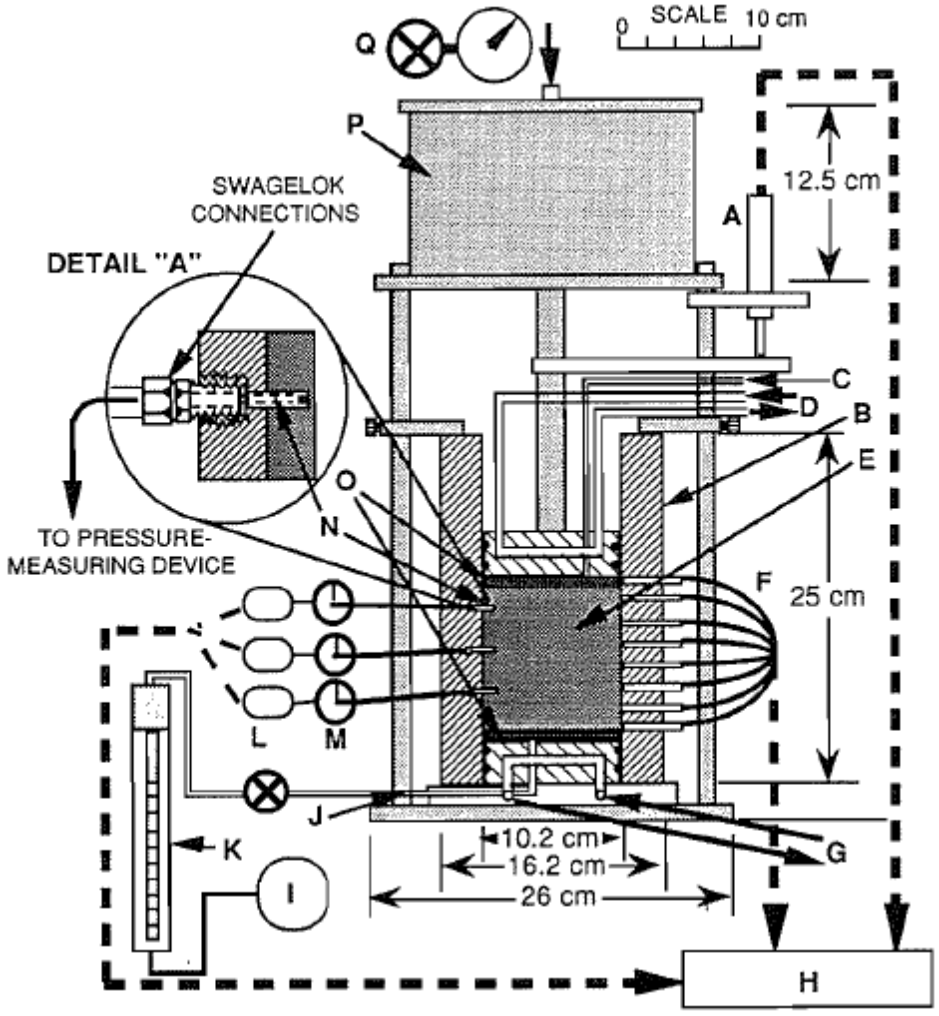

Figure 1.8 Schematic of frost cell used by Konrad and Seto (1993)

Xia (2006) used a freeze cell to conduct one dimensional, open-system, step freezing tests on Devon silt. Samples were consolidated to 100 mm in diameter and 120 mm in height. Temperature boundary conditions were maintained by circulating a liquid from constant cold baths, through the top and bottom plates. Drainage was allowed to occur through the bottom plate, and displacement of the top plate was measured during freezing and consolidation. Temperature gradient was measured using four thermistors in the sidewall of the cell. A digital camera was used to capture images through the Perspex cell

wall, in order to monitor ice lens formation. Figure 1.9 shows a schematic of the one dimensional freezing cell used by the author.

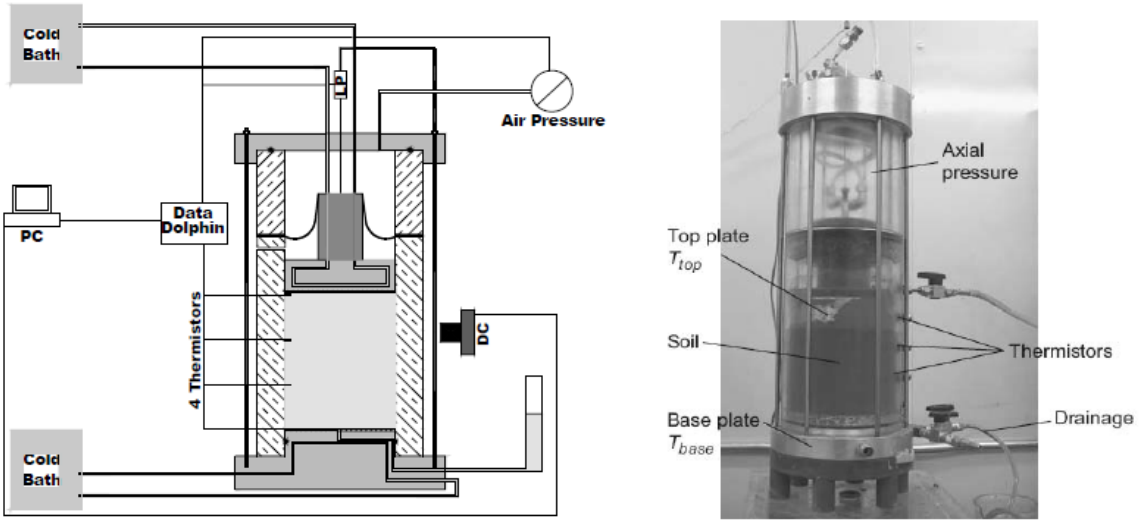

Figure 1.9 Schematic of one dimensional freezing cell used by Arenson et al. (2006)

Upon the review of freeze cell experiments conducted by others, a new freeze cell was developed to study the mechanisms of ice lens formation using suction monitoring probes, thermocouples, and PIV analysis simultaneously.

1.2.5 Particle Image Velocimetry (PIV)

PIV has been used by Arenson et al. (2007) to measure ice lens growth and axial soil strains in laboratory experiments. Digital images, captured during soil freezing, are analyzed in Matlab using image analysis tools, and a specialized PIV application developed for measuring strains in geomaterials (geoPIV) by White et al. (2003).

In geoPIV, images of the soil sample are subdivided into subsets and each subset is found in subsequent images captured during the freezing process. Each subset contains colour information that makes it uniquely identifiable in subsequent images. Figure 1.10 shows how the light colour of ice lenses (white pixels) were used by Arenson et al. (2007) to

extract ice lens structure and determine ice distribution from a series of images of a frost susceptible silt.

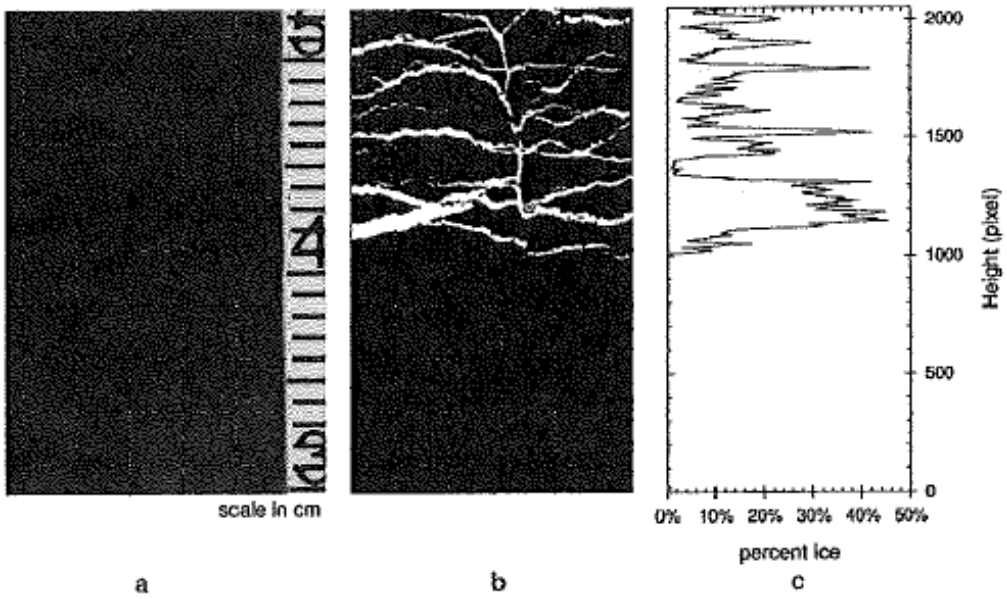

Figure 1.10 Images displaying ice distribution a) original image; b) extracted ice lens structure; c) ice distribution with height (Arenson et al. 2007)

It was noted by Arenson et al. (2007) that the formation of new ice lenses, during their freezing tests, caused changes to the subsets rendering them untraceable. Images were analyzed in reverse order to overcome the issue during their tests. In order to avoid subsets becoming untraceable, it was recommended that adequate texture and lighting be available to improve PIV measurements.

Azmatch et al. (2008) used PIV and time-lapse photography to observe the freezing process in Devon silt. They observed that soil heaving due to freezing was preceded by freezing induced soil consolidation. They also observed that during ice lens formation, vertical tension cracks and vertical ice veins, formed before horizontal ice lenses. They concluded that ice lens patterns and growth rates strongly depend on freezing boundary conditions, and soil characteristics, such as tensile strength (Azmatch et al. 2008).

1.3 SUMMARY

Suctions below -100 kPa have never been recorded in frost heave tests. The objective of this research is to implement a combination of testing techniques, using newly developed technology, to measure suction, axial strain and void ratio, temperature gradients, water migration, frost front location, and frost heave, simultaneously in freezing clays. Results will be directly compared to identify the relationships that exist among these characteristics. The newly developed freeze cell offers an experimental setup and procedure that produces accurate reliable results. Conclusions of this research will offer an improved understanding of the mechanisms of ice lens formation.

CHAPTER 2 APPARATUS, MATERIALS, AND METHODS

2.1 FREEZE CELL APPARATUS

A cylindrical freeze cell, adopted and modified from Xia (2006), was used in this thesis to replicate one-dimensional freezing. These open system freezing tests, with water freely supplied at the warmer end, were performed on clayey specimens. Specimens were frozen in the axial direction, from the top of the specimen downward, with fixed temperature boundary conditions at each specimen end. Figure 2.1 illustrates a schematic of the freeze cell. Each major part of the cell is described below with a bolded label that corresponds to the figure. Figure 2.2 shows a scale drawing of the freeze cell.

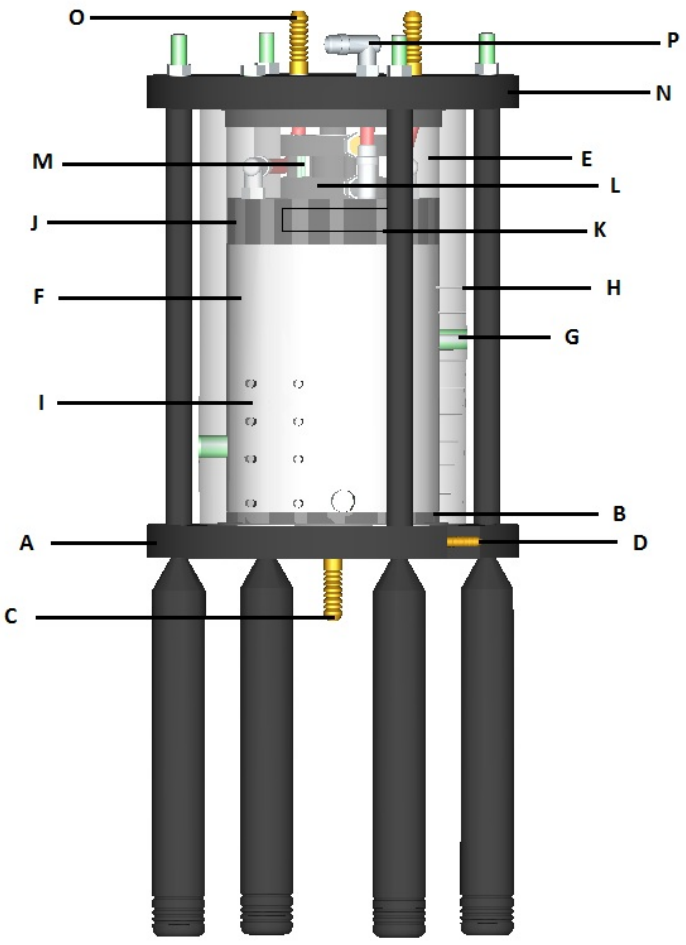

Figure 2.1 Schematic of freeze cell

The main body of the cylindrical freeze cell consists of a 165.1 mm (6.5 inch) diameter stainless steel plate, 19 mm (0.75 inch) thick, which forms the bottom plate of the cell **(A)**. The bottom plate has a 101.6 mm (4 inch) diameter, 6.35 mm (0.25 inch) high platform machined into the center of the top side of the plate. Resting on top of this platform is a 101.6 mm (4 inch) diameter, 6.35 mm (0.25 inch) thick, porous ceramic stone with an air entry value (AEV) of 100 kPa (14.5 psi or 1 bar) **(B)**. A 9.53 mm (0.375 inch) diameter hole was drilled through the center of the base plate to provide a water connection **(C)**. The water connection is used to establish constant, uniform saturation of the porous ceramic stone as well as provide the specimen with free access to water. In addition, there is a 6.35 mm (0.25 inch) pathway drilled laterally through the center of the bottom plate **(D)**. Water is circulated through the pathway in the bottom plate, using a peristaltic pump, to maintain a temperature of +2°C at the bottom of the specimen.

Resting on the bottom plate is a hollow, 101.6 mm (4 inch) inside diameter, 12.7 mm (0.5 inch) thick, Perspex cell **(E)**. The cell is 219.08 mm (8.625 inches) high and is designed to hold a 127 mm (5 inch) long clay specimen **(F)**. Four 0.75 inch National Pipe Thread (NPT) holes are drilled in the Perspex at varying locations and heights around the Perspex cell, where pore pressure transducers (PPTs) are screwed in **(G)**. See Table 2.2 for exact locations of PPTs. The PPTs allow for measurement of the development of suction in the clay specimen throughout the freezing tests. Eleven 1.57 mm (0.062 inch) holes are tapped in the Perspex at varying locations and heights around the Perspex cell, where thermocouples (TCs) are inserted into the specimen **(H)**. See Table 2.1 for exact locations of TCs. Acrylic latex caulk plus silicone is applied in and around these holes, prior to testing, to create a seal. The TCs measure the temperature within the specimen throughout the freezing tests.

A 76.2 mm (3 inch) wide by 127 mm (5 inch) high “window” on the outside of the Perspex cell exists, where no PPTs or TCs are present **(I)**. This window allows for digital images to be taken of the specimen, throughout the tests. PIV is used with the images, to digitally quantify the movement of ice lenses through the soil.

Resting on the top of the specimen is a 101.6 mm (4 inch) diameter, 19.05 mm (0.75 inch) thick stainless steel top plate **(J)**. There is a 6.35 mm (0.25 inch) pathway drilled laterally through the center of the top plate **(K)**. Glycol is circulated through the pathway in the top plate, using a Thermo Electron Circulator HAAKE DC30 liquid chiller with a K10 bath, to maintain a boundary temperature of -8°C at the top of the specimen. Attached to the top of this plate is a 50.8 mm (2 inch) outside diameter NITRA pneumatic, double acting, compact air cylinder with a 27 mm (1.063 inch) bore, which can be used to apply a confining pressure to the specimen **(L)**. There is a pressure connection on the pneumatic actuator connected to a compressor **(M)**. For the tests reported in this thesis, the air cylinder was not pressurized (i.e. 0 kPa applied to specimen).

There is a 15.24 mm (0.6 inch) air space above the top of the pneumatic air cylinder, above which rests a 12.7 mm (0.5 inch) thick stainless steel cover **(N)** on top of the Perspex. There are two 9.53 mm (0.375 inch) diameter holes drilled in the top cover to allow the glycol tubing to travel to the top plate **(O)**. There is also one 12.7 mm (0.5 inch) diameter hole to allow the pressure connection from the compressor to travel to the pneumatic air cylinder **(P)**.

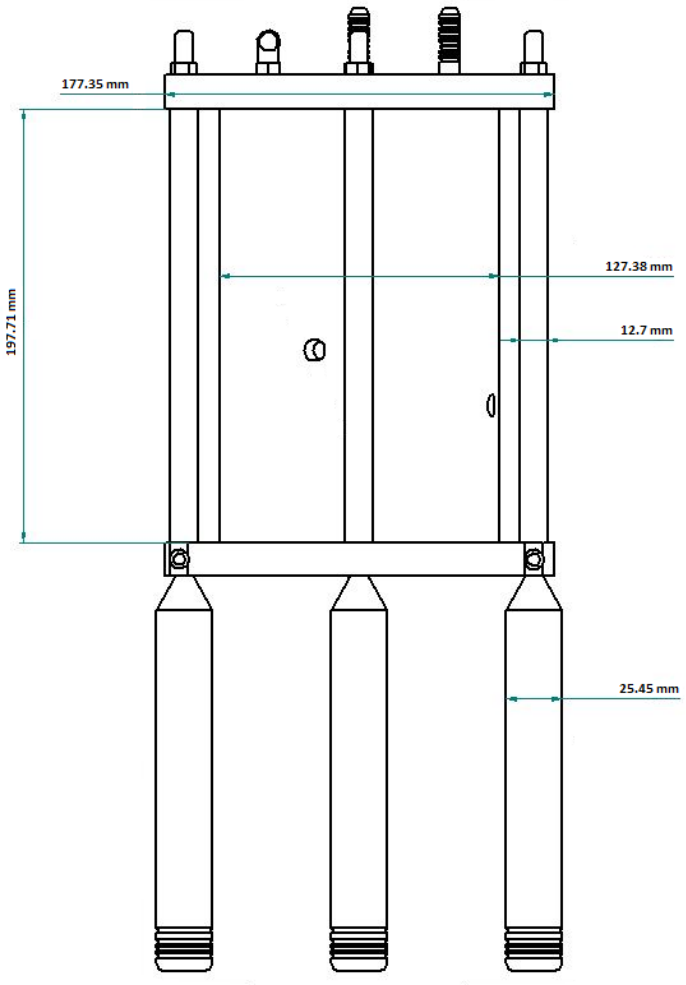

Figure 2.2 Scaled Schematic of freeze cell

2.2 MONITORING EQUIPMENT

2.2.1 Temperature Monitoring

Throughout the test, the temperature gradient across the height of the specimen was measured using TCs with +/-0.5 °C accuracy (Conax Technologies 2013). Eleven Conax, ungrounded, Type T, TCs, with stainless steel sheaths were used. The TC sheaths measure 304.8 mm (12 inches) in length, and 1.58 mm (0.062 inches) in diameter. TCs were located at approximately 12.7 mm (0.5 inches) spacing along the height of the specimen. TCs were inserted 50.8 mm (2 inches) into specimen, so that the tip of each

TC recorded the temperature at the center of the specimen. Temperature values were recorded every second throughout the test using DASYLab acquisition software. Table 2.1 indicates the exact placement of the TCs in the specimen, during freezing tests. The ambient temperature was maintained at +2°C, during the tests, by a cold room with +/-1°C accuracy.

Table 2.1 Thermocouple Locations

Thermocouple No.	Elevation (mm)
01	126.5
02	114.5
03	103.5
04	91.5
05	78.5
06	65.5
07	53.0
08	41.5
09	28.5
10	15.5
11	4.0

Note that the datum is located at the bottom of the specimen.

2.2.2 Suction Monitoring

During the test, suction developed in the freezing soil, and was measured using pore pressure transducers (PPTs). Four DRUCK, PDCR-4010-A093 (Thermx Southwest), high performance millivolt output pressure transducers, with 0.04% full scale accuracy, were modified to measure negative pressures. Following the modifications of Beddoe et al. (2010), a 6.3 mm (0.248 inch) diameter hole was drilled in the ends of the PPTs, where ceramic tips were glued. Of the four PPTs, one used a 500 kPa (five bar) AEV ceramic, one used a 300 kPa (three bar) AEV ceramic, and two used 100 kPa (one bar) AEV ceramics. The measured pressure capability of each ceramic tip was chosen based on predicted suction values at each PPT location. The PPTs were located at elevations of

25.4 mm (1 inch), 50.8 mm (2 inches), 76.2 mm (3 inches), and 101.6 mm (4 inches) from the base of the specimen. Suction values were recorded every second throughout the test using DASYLab. Figure 2.3 illustrates PPTs modified with ceramic tips.

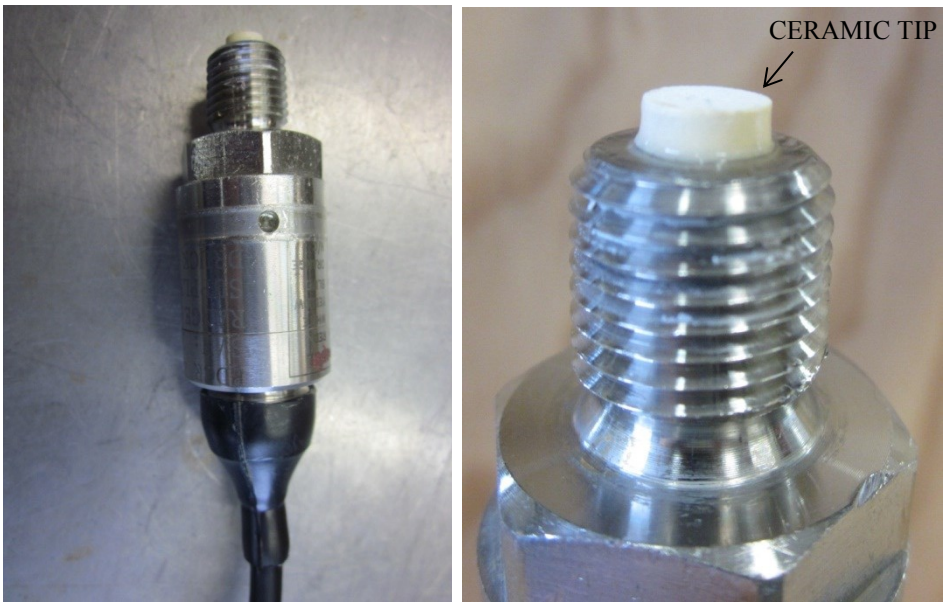

Figure 2.3 PPTs modified with ceramic tips

PPTs are typically used for measuring positive pressure. To measure negative pressures (suction) the ceramic tips must be saturated and placed in contact with the specimen during a test (Take and Bolton, 2003). Suction created in the soil, makes water inside the saturated ceramic and probe want to "pull out", creating a tension on the bladder, indicating a negative pressure reading. Table 2.2 indicates the exact placement of the PPTs in the specimen, during freezing tests.

Table 2.2 Pore Pressure Transducer Locations

Pore Pressure Transducer	Elevation (mm)	AEV of Ceramic Tip (kPa)
01	25.4	100
02	50.8	100
03	76.2	300
04	101.6	500

Note that the datum is located at the bottom of the specimen.

2.2.3 PIV Image Capture

Images used for the PIV analysis were captured through the PIV window, using a Canon Rebel XTi camera, with an 18-55 mm lens. The focus distance was constant at 250 mm (9.84 inches) yielding an image size of 114.3 mm (4.5 inches) by 76.2 mm (3 inches).

Digital images were recorded at specific time intervals throughout the test, using a remote image capturing device. To eliminate glare on the Perspex, in the images, the flash in the camera was turned off, and the overhead lighting in the refrigerated room was left on. To eliminate moisture buildup on the surface of the Perspex PIV window, it was treated with an anti-fog spray prior to the beginning of the test.

2.2.4 Water Intake Monitoring

Water intake of the specimen was measured throughout the test using a reservoir monitored by a force transducer. A 146 mm x 183 mm (5.75 inch x 7.20 inch) plastic reservoir containing a known head of water of was mounted to an Interface, MB-10, 4.54 kg (10 lb) force transducer. DASYLab was used to record the volume of water in the reservoir every second throughout the test. This data provided instantaneous, and cumulative, water intake and/or output rates of the specimen.

2.2.5 Data Acquisition System

Data from the temperature, suction, and water intake monitoring equipment described in this chapter was captured using the DASYLab data acquisition system. A worksheet was created in DASYLab that recorded raw and filtered data from the four PPTs and the force transducer, as well as raw data from the TCs. A total of 16 analog inputs using a USB-1616HS and an AI-EXP48 were used to take the data measurements.

2.3 TEST PROCEDURE (METHODOLOGY)

There were two different test procedures performed for this research. Both procedures were identical except for the top and radial stress boundary conditions on the specimen. In Procedure A, the specimen was allowed to freeze to the cell walls, as well as the stainless steel top plate that provided the top temperature boundary condition. This applied a confining stress on the specimen, rendering it fixed and impeding any heave related to freezing. In Procedure B, the cell walls and stainless steel top plate were generously coated with a silicone lubricant, preventing the specimen from freezing to the cell, and allowing frost heave to occur. This chapter describes the two test procedures in detail.

Specimens used in this thesis were prepared by combining 75% U.S. Silica ground silica (sil-co-sil 75), and 25% IMERYS Speswhite china clay (kaolin), by dry mass at a moisture content of approximately 24%. Each of these soil materials used were 100% passing the 0.075 μm sieve. Under the Unified Soil Classification System (USCS), this soil was classified as CL – lean clay. Atterberg limits, and proctor information on the specimen material, can be found in Appendix A. The materials were combined by hand until a homogenous mixture was achieved. This material was double bagged in heavy plastic sample bags and left to cure overnight in a refrigerated room at +2°C.

After hydration, the specimen was compacted in place in the Perspex freeze cell, in a refrigerated room at +2°C. The steel top plate and cover were removed from the cell and a plastic collar was secured on the top of the Perspex cell. This collar acted similar to the collar on a proctor mold, by keeping the bottom plate and Perspex cell "locked" together. For Test Procedure B, the cell was coated with a silicone lubricant, prior to compaction. The specimen was compacted in the cell in general accordance to ASTM D698-07. The Perspex cell, however, was 12.7 mm (0.5 inches) taller than a proctor mould, so the three lifts were modified accordingly to achieve a final specimen height of approximately 127 mm (5 inches). In addition to increasing the height of each lift during compaction, the material that contacted the Perspex in the PIV window was coated in Ottawa sand that

was dyed black, prior to compaction in the cell. This provided texture to the outside of the specimen which allowed for a more accurate PIV analysis of ice lens formation during freezing (i.e. the image processing technique of PIV requires variations in soil colour, sometimes called image texture, to identify subsets in subsequent images).

Test specimens were prepared and compacted into the freeze cell. A moisture content test was performed on the excess specimen material to confirm soil properties. It was suspected that the moisture test performed on excess material overestimated the moisture content in the specimens. This was verified by preparing three mock specimens that were compacted into the cell then extruded without undergoing freezing. Moisture contents were determined from the excess material after compaction, and compared to moisture profiles determined from the extruded, unfrozen specimens. Results indicated that the moisture tests performed on the excess material consistently overestimated the moisture content of the specimen by approximately 0.4%. To accommodate for this, 0.4% was subtracted from the initial moisture content values determined for each specimen. Once the specimen was in place in the cell and the top cover was secured, a three stage testing procedure began.

STAGE A

Prior to each test, the PPTs used to measure suction were saturated using the equipment shown in Figure 2.4. Details on the saturation process can be found in Take and Bolton (2003). Once all PPTs were saturated, they were placed in a bowl of water in a cold room at +2°C. This allowed the PPTs to maintain saturation until suction measurement began.

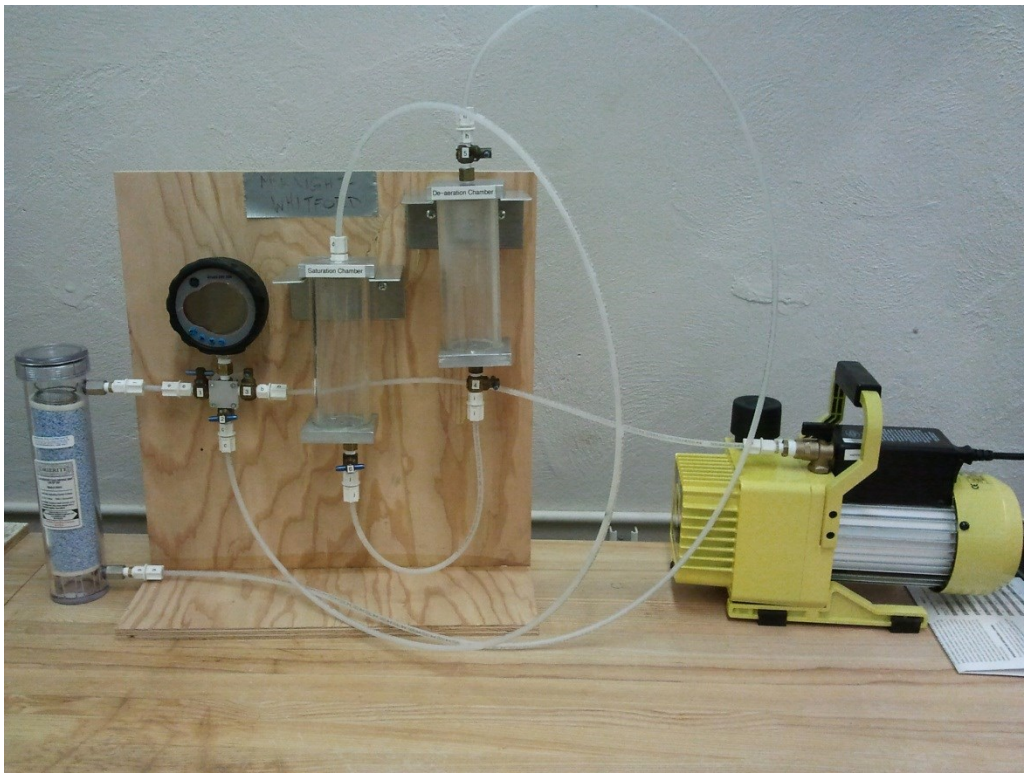

Figure 2.4 Saturation Equipment

During Stage A, the PPTs were installed in the freeze cell. During installation, the PPTs were removed from the bowl of water and screwed into the designated holes drilled in the cell wall. Full contact between the ceramic filter on the PPTs and the specimen material was required for accurate measurement of suction. Pore water pressure data was recorded from the time the PPTs were resting in the bowl of water, through the installation process, and until they equilibrated to an initial suction value. This data showed us how much the soil was disturbed during PPT installation and how long it took to see equilibrium of these effects. The initial suction value of the soil was also established. Figure 2.5 shows an example of the pressure distribution in the specimen during Stage A.

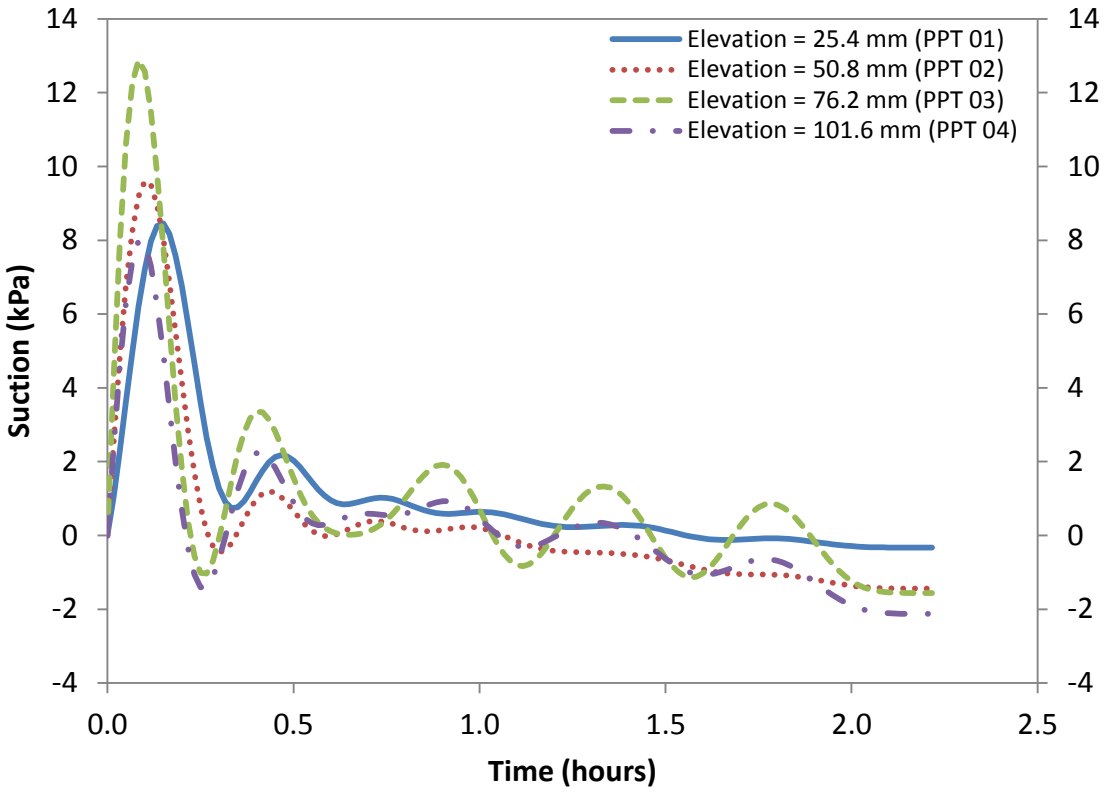

Figure 2.5 Example of pressure distribution during Stage A

STAGE B

During Stage B, the TCs were installed in the freeze cell. TCs were installed by inserting the steel sheathe through the designated holes in the cell wall, and extending the tips to the center of the specimen. The holes in the cell wall were then sealed using caulking. To ensure effective use of the caulking as a seal, it must be applied at temperatures above +5°C. To accommodate this, the cold room temperature was increased from +2°C to +10°C while the TCs were installed, and until the caulking was set. Once the caulking was set, the cold room temperature was decreased to +2°C and time was allowed for the specimen to reach thermal equilibrium, at approximately +2°C, prior to the final test stage. Figure 2.6 shows an example of the temperature distribution in the specimen as it approached thermal equilibrium during Stage B.

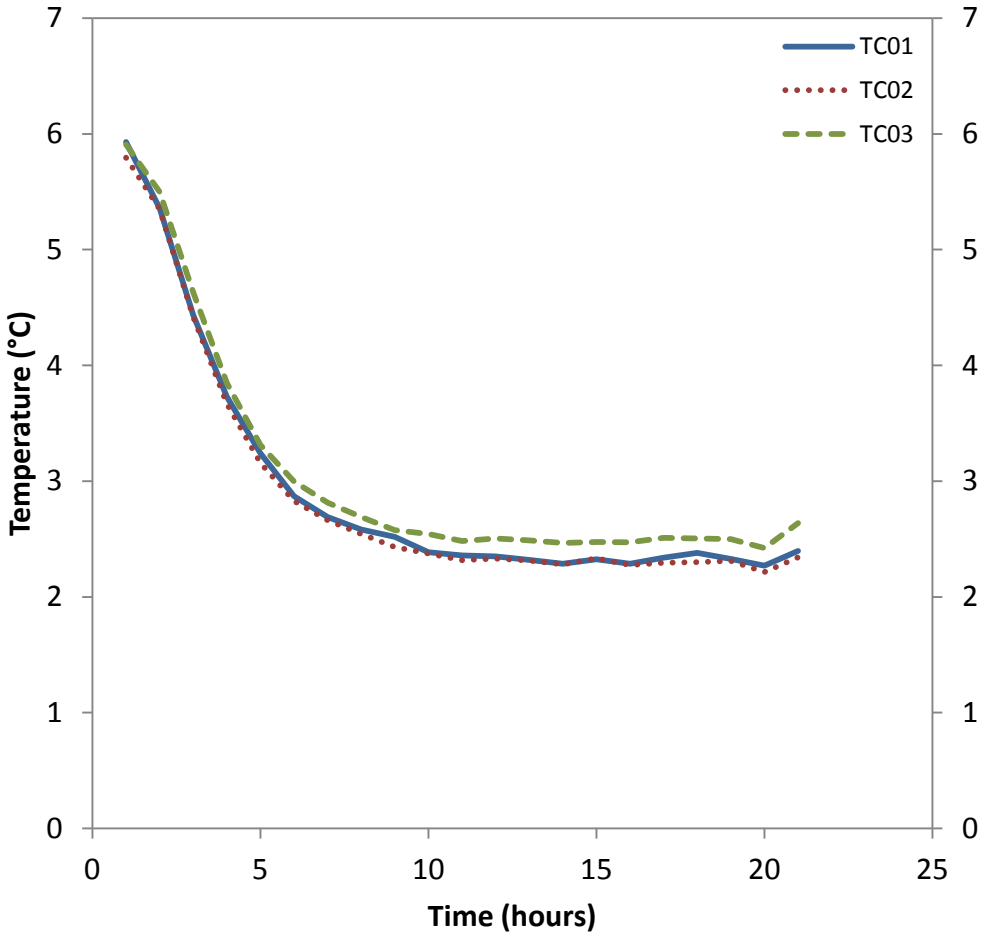

Figure 2.6 Example of temperature distribution during Stage B

STAGE C

During Stage C, one dimensional freezing of the specimen took place. Thermal insulation was placed around the exterior of the freeze cell, excluding the designated PIV window. The water source was hooked up by attaching tubing that runs from the bottom of the water reservoir, to a fitting on the base of the cell. Air was removed from the water line, and the reservoir was filled to a head of 30 mm (1.18 inches) above the base of the specimen. This head of water was chosen to ensure that the specimen would have access to water during the entire test, and was only slightly high enough to allow water to be forced into the specimen from the reservoir. Glycol was circulated through the top plate at a temperature of -8°C, and water was circulated through the bottom plate at a

temperature of +2°C, to maintain constant temperature boundary conditions. Once the temperature boundary conditions were applied, the camera, which was pointed at the PIV window on the cell, began taking images at 30 minute intervals throughout the test. Preliminary analysis of the tests using Test Procedure A indicated that a lot of the freezing action and changes that took place in the specimen, occurred in the first 5 hours of the test. As a result, images were taken more frequently at the beginning of later tests using Test Procedure B.

The DasyLab acquisition software used to record the temperature data from the eleven TCs, suction data from the 4 PPTs, as well as the mass of water in the water reservoir began recording data every second during Stage C. Freezing progressed to steady state temperature conditions.

2.4 POST PROCESSING OF DATA

Following the termination of a test, the specimen was extruded from the cell, and divided into horizontal slices. Slice thickness ranged from 11 mm to 50 mm, depending on the frozen/unfrozen state of the slice material and its proximity to the final ice lens. Moisture content, and void ratio profiles were determined from the slices.

Data collected during Stage C was processed using MATLAB, to determine the results of the tests. Suction data from the PPTs, temperature data from the TCs, and water intake data from the force transducer, were filtered using a 9^{th}- order Low Pass Butterworth Filter and reduced to a manageable number of data points; one per hour.

GeoPIV8 was run on the images of the specimen in order to determine vertical strain and rate of heave throughout the test. The initial void ratio of each specimen was measured and the change in void ratio (Δe) was calculated from the vertical strain values, using Equation 2.1.

$$\Delta e = \varepsilon_v(1 + e_0)$$

Equation 2.1

Where Δe is the change in void ratio; ε_v is the vertical strain; and e_o is the initial void ratio.

Strain was determined using GeoPIV8 by analyzing the images on a pixel level. Each image was divided into 64 x 64 pixel subsets, whose movement was traced from image to image. There were thirteen subsets per row. The number of rows was specific to each test and ranged from sixteen to twenty-two for the results illustrated in Chapter 3. Figure 2.7 shows an example of how subsets were assigned to an image. Strain was determined by tracking the vertical movement (change in distance) of the subsets in a row, relative to the subsets in the nearest rows. A strain value was determined at the midpoint between each set of rows, for each image. Since there were thirteen subsets per row, there were thirteen values of strain calculated between each set of rows. A median value for each row was chosen from the thirteen, and reported as the strain value.

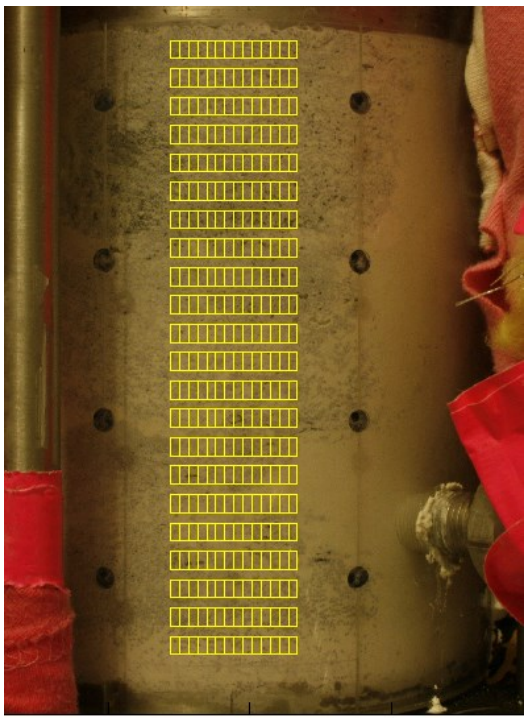

Figure 2.7 Example of PIV subsets used in the testing procedure

Void ratio was also determined from the final moisture content profiles of the specimens. The depth of the frost front (0°C isotherm) was determined by interpolating the location of 0°C from the TC data throughout the test, as well as through visual inspection of the images.

2.5 SUMMARY

A freeze cell apparatus, equipped with PPTs for measuring suction, and TCs for determining temperature gradients, and images for mapping ice lens formation, in a clay specimen, form the experimental setup. The apparatus was used to study the behaviour of clay specimens during one dimensional, open system freezing tests. Chapter 3 of this dissertation provides an analysis of the various test results as well as discussion.

CHAPTER 3 RESULTS OF TEST PROCEDURE

Results obtained from three different tests will be presented in this chapter. Test L05_S01 was performed using Test Procedure A, for a duration of 24 hours. Test L06_S01 was performed using Test Procedure B, for a duration of 26 hours. Test L07_S02 was also performed using Test Procedure B but the duration of the test was extended to 45 hours, in order to provide an extended observation of the frost heave process. Table 3.1 lists the different types of data that were obtained from each test. It should be noted that various tests were performed, using Test Procedure A, prior to those discussed in this chapter. Results from these tests, although not presented in this thesis, were used to help develop the experimental process described in the previous chapter.

Table 3.1 List of tests performed and data obtained

	Test No.		
	L05_S01	L06_S01	L07_S02
Test Procedure Used	A	B	B
Measured Moisture Content Data	✓	✓	✓
Measured Void Ratio Data	✓	✓	✓
Measured Degree of Saturation Data	✓	✓	✓
TC Temperature Data	✓	✓	✓
PPT Suction Data	✓	✓	×
Water intake Data	✓	✓	×
PIV Strain Data	✓	✓	✓
PIV Void Ratio Data	✓	✓	✓
PIV Depth of Frost Front Data	✓	✓	✓
PIV Frost Heave Data	×	✓	✓
Segregation Potential	×	✓	×

3.1 L05_S01 (PROCEDURE A)

3.1.1 Water Content and Void Ratio

The initial moisture content of the specimen prior to freezing conditions was 24%. After undergoing freezing, the moisture content of the frozen soil increased to an average of 29%, while the moisture content of the unfrozen soil decreased to an average of 19%. This trend in moisture redistribution was expected, since water migrated from the unfrozen soil, towards the ice lens during freezing. Figure 3.1 illustrates the initial and final measured moisture profiles of the specimen, before and after the test.

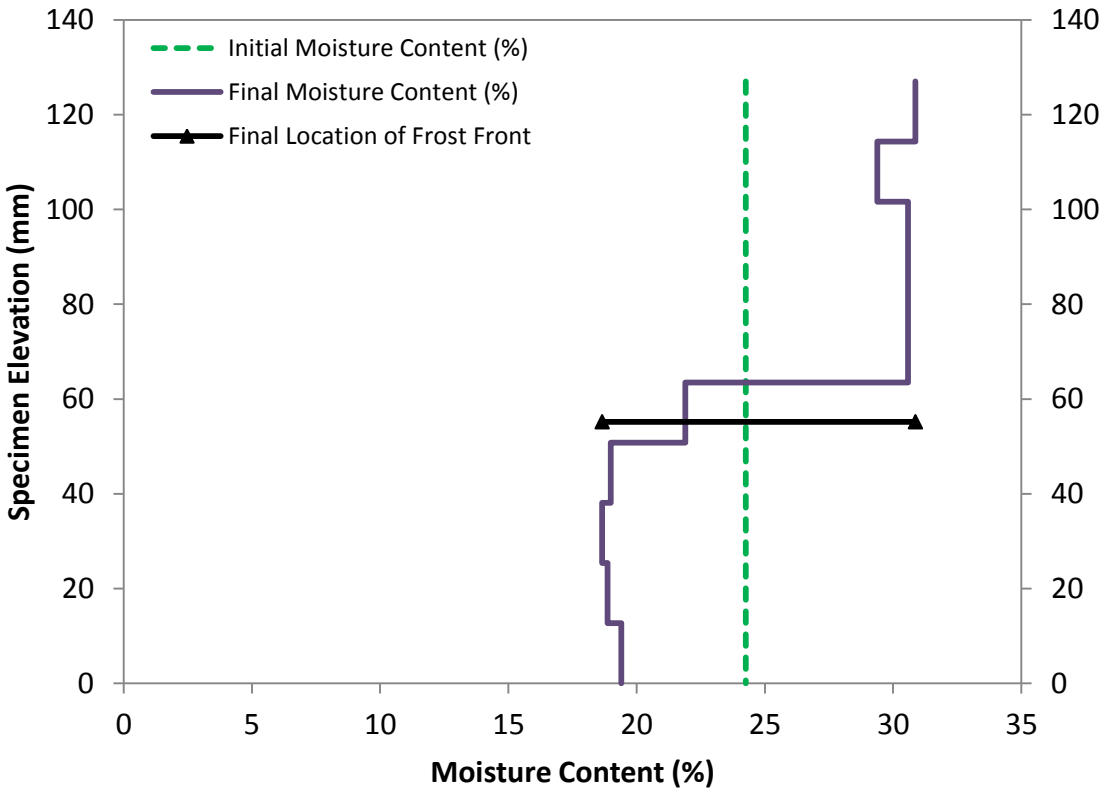

Figure 3.1 L05_S01 Specimen Elevation vs. Moisture Content

As shown in Figure 3.2, the initial void ratio of the specimen prior to freezing conditions (calculated via phase relationships) was approximately 0.77. After undergoing freezing, the void ratio of the frozen soil increased to an average of 1.05, while the void ratio of the

unfrozen soil decreased to an average of 0.54. This trend was similar to that shown for the moisture content profile. As water migrates to the ice lens, accumulates and freezes, the frozen soil undergoes an increase in void ratio due to the expansion of freezing pore water into ice. Similarly, the water migration from the unfrozen soil towards the ice lens, creates a suction induced consolidation in the unfrozen soil, causing a decrease in void ratio. Figure 3.2 illustrates the initial and final void ratio profiles of the specimen, before and after the test. It should be noted for Figure 3.1 and Figure 3.2 that data was obtained with only approximate slice thicknesses, and hence there is likely some error present in these profiles, although the general trends are likely true.

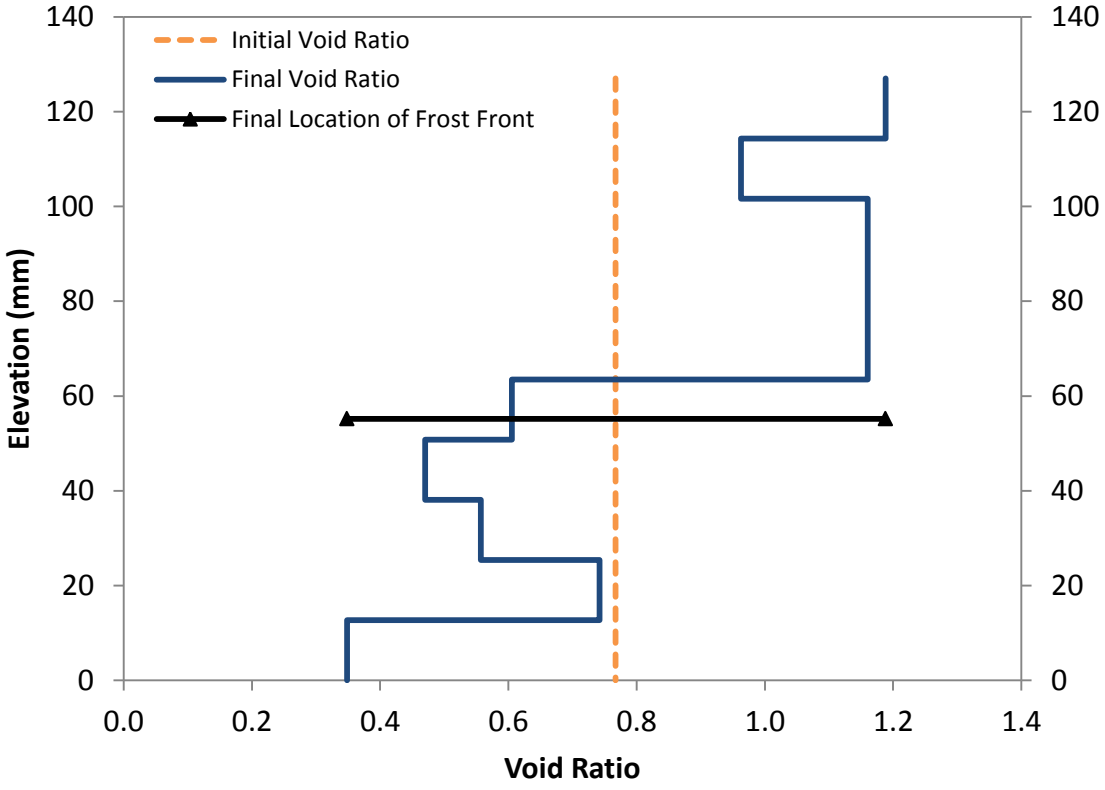

Figure 3.2 L05_S01 Specimen Elevation vs. Void Ratio

3.1.2 Temperature Results

Figure 3.3 and Figure 3.4 illustrate the temperature profiles at various elevations throughout the specimen during hours 0 to 5, and hours 5 to 24, respectively. At the beginning of Stage C (0 hours), the initial temperature in the specimen was measured between +2.1°C and +2.8°C. As freezing progressed, the temperature at the bottom of the specimen gradually increased to +4.1°C. The temperature at the top of the specimen decreased to -6.9°C. The thermal profile across the specimen approached linearity at 15 hours into the test. The slight increase in temperature at the bottom of the specimen, compared to the bottom boundary condition, was attributed to the peristaltic pump used for circulating the water through the bottom plate.

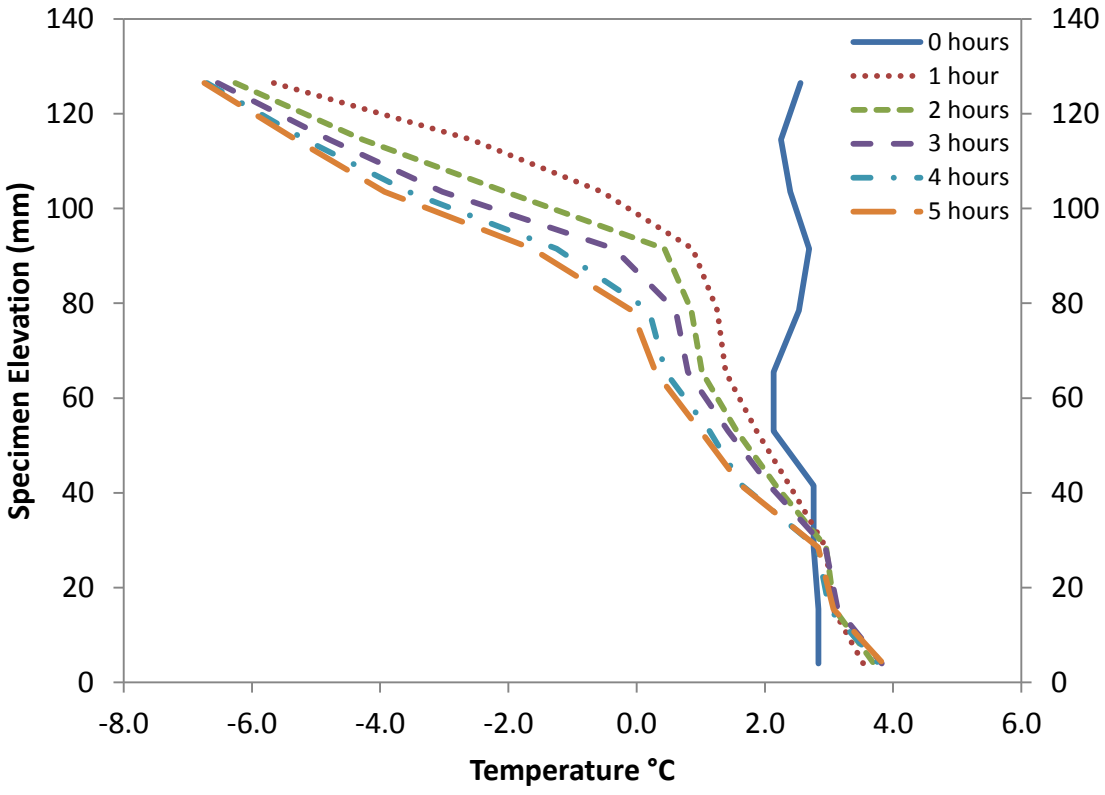

Figure 3.3 L05_S01 Specimen Elevation vs. Temperature for 0 to 5 hours

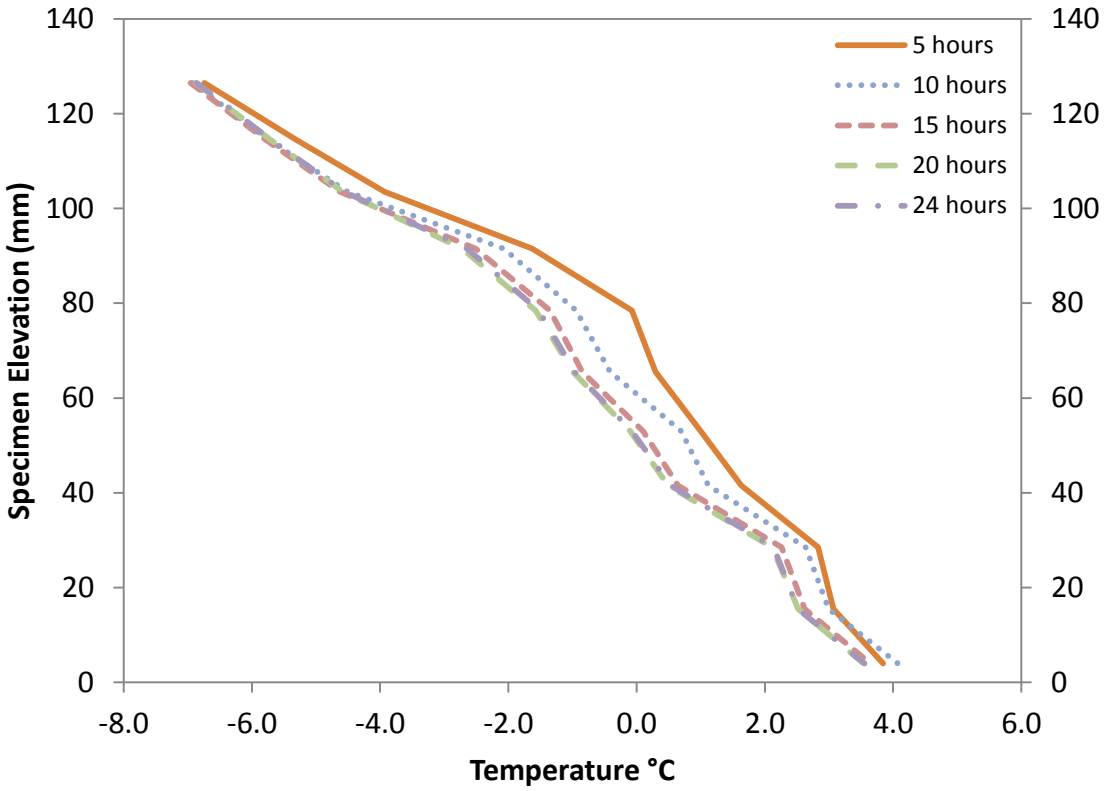

Figure 3.4 L05_S01 Specimen Elevation vs. Temperature for 5 to 24 hours

3.1.3 Suction Results

Figure 3.5 illustrates the suction versus time profiles in the specimen during Stage C. Figure 3.6 and Figure 3.7 illustrate the suction versus elevation profiles in the specimen during hours 0 to 5, and hours 5 to 24, respectively. The initial suction reading in all PPTs was approximately 0 kPa. During the first hour of the test, PPT 01 and PPT 02 showed slight increases in pore water pressure, due to freezing induced consolidation. The low permeability of the soil caused a lag in pore water pressure dissipation at the beginning of the test, resulting in the buildup of pore water pressure. PPT 01, which was at an elevation of 25.4 mm, reached a maximum suction of -28 kPa, four hours into the test. The suction then decreased to approximately -9 kPa by hour 15, where it remained for the duration of the test. PPT 02, which was at an elevation of 50.8 mm, reached a maximum suction of -21 kPa, eight hours into the test. The suction then gradually

decreased during the remainder of the test, reaching approximately -14 kPa when the test was terminated at 24 hours. Both PPT 01 and PPT 02 remained in the unfrozen zone of soil for the entire test. PPT 03, which was at an elevation of 76.2 mm, reached a maximum suction of -565 kPa, 5.67 hours into the test, then cavitated and proceeded to freeze. PPT 04, which was at an elevation of 101.6 mm, reached a maximum suction of -496 kPa, 1.92 hours into the test, then cavitated and proceeded to freeze. Both PPT 03 and PPT 04 were in the frozen zone of soil at the termination of the test. In past research, attempts at measuring soil suction have only reported suctions as low as -80 kPa (Konrad and Seto 1993).

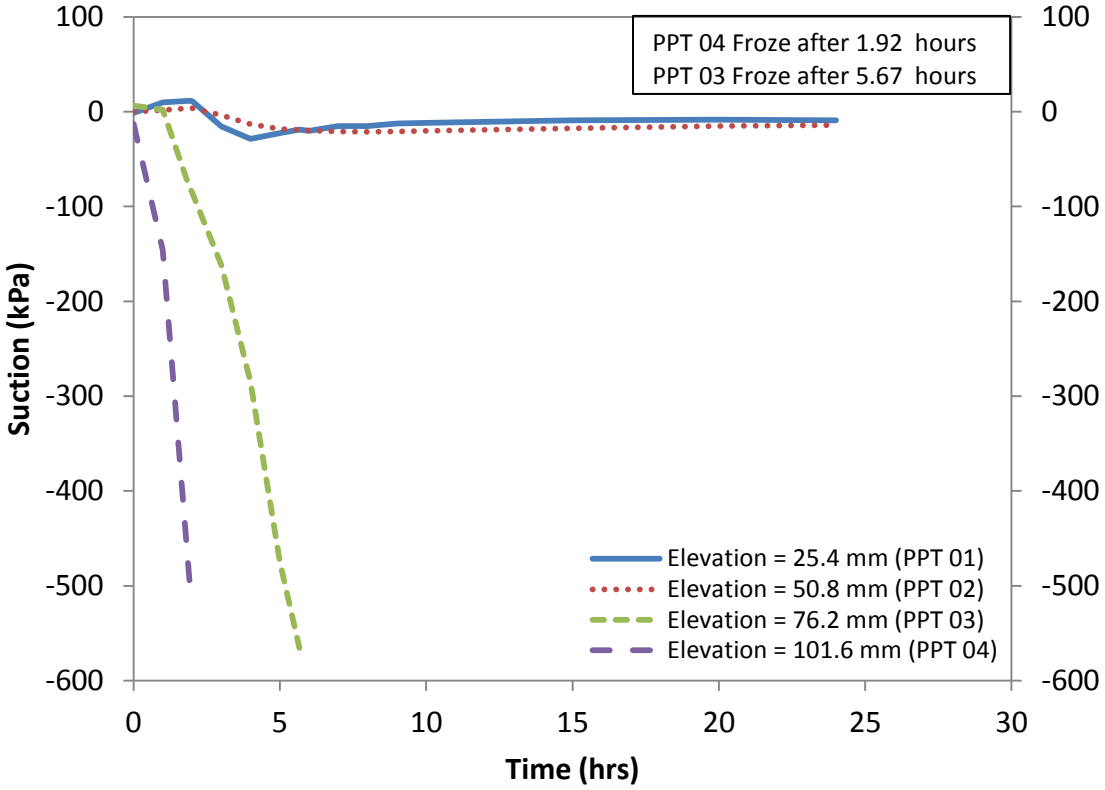

Figure 3.5 L05_S01 Suction vs. Time

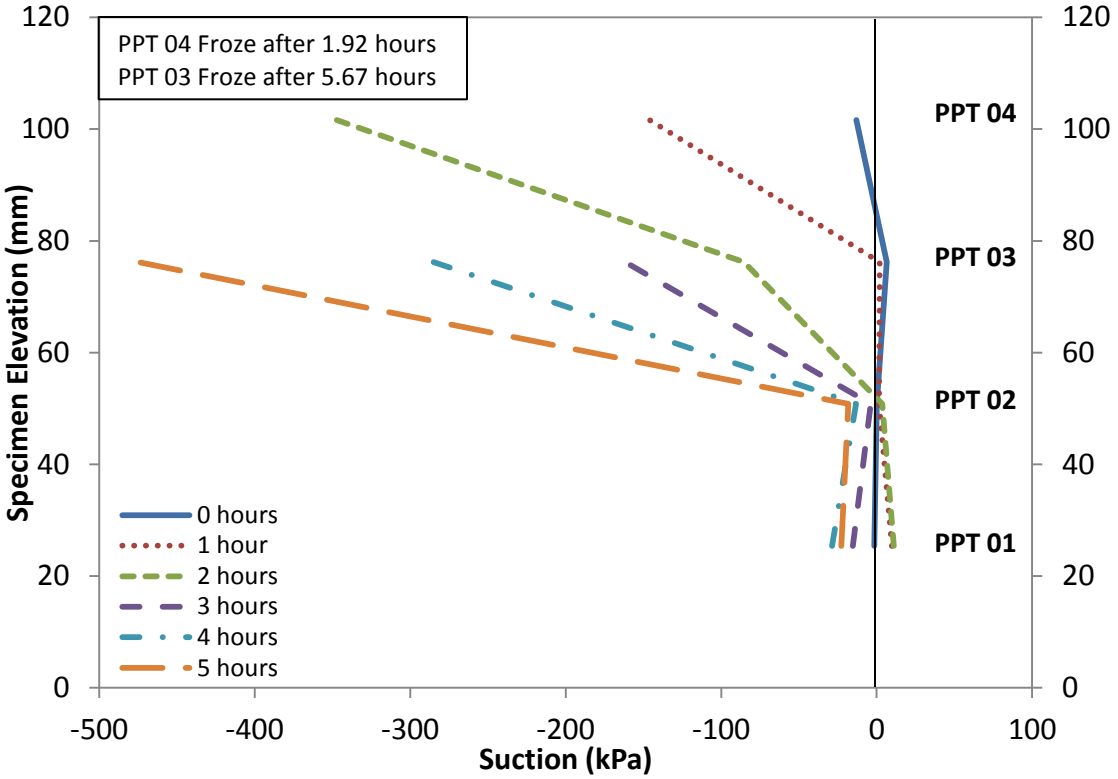

Figure 3.6 L05_S01 Specimen Elevation vs. Suction for 0 to 5 hours

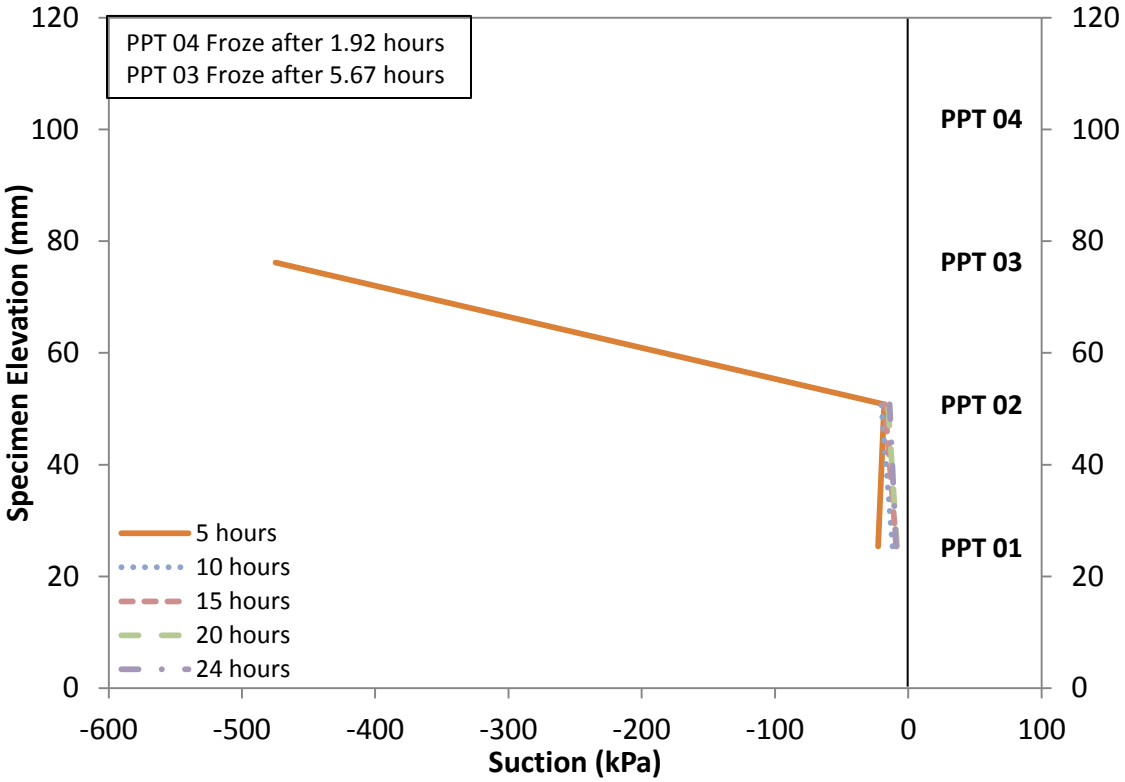

Figure 3.7 L05_S01 Specimen Elevation vs. Suction for 5 to 24 hours

3.1.4 Water Intake Results

During this test, the specimen was allowed to freeze to the cell wall and top plate, initiating a confining stress that restricted heave. This unknown transient confining stress created an increase in pore water pressure at the bottom of the specimen, making it difficult for the specimen to intake water (i.e. very small gradient). Figure 3.8 illustrates the water intake of the specimen during Test L05_S01. The specimen took in approximately 6 ml of water during the first hour, and then expelled it by three hours into the test. At this time, the specimen began a period of somewhat steady water intake that continued until the test was terminated at 24 hours. The total water intake of the specimen, during the test, was 8 ml. The approximate rate of water intake from time 3 hours to 24 hours, was 0.27 ml/hour. It should be noted that the "wavy" appearance of the data is thought to be attributed to noise from the force transducer.

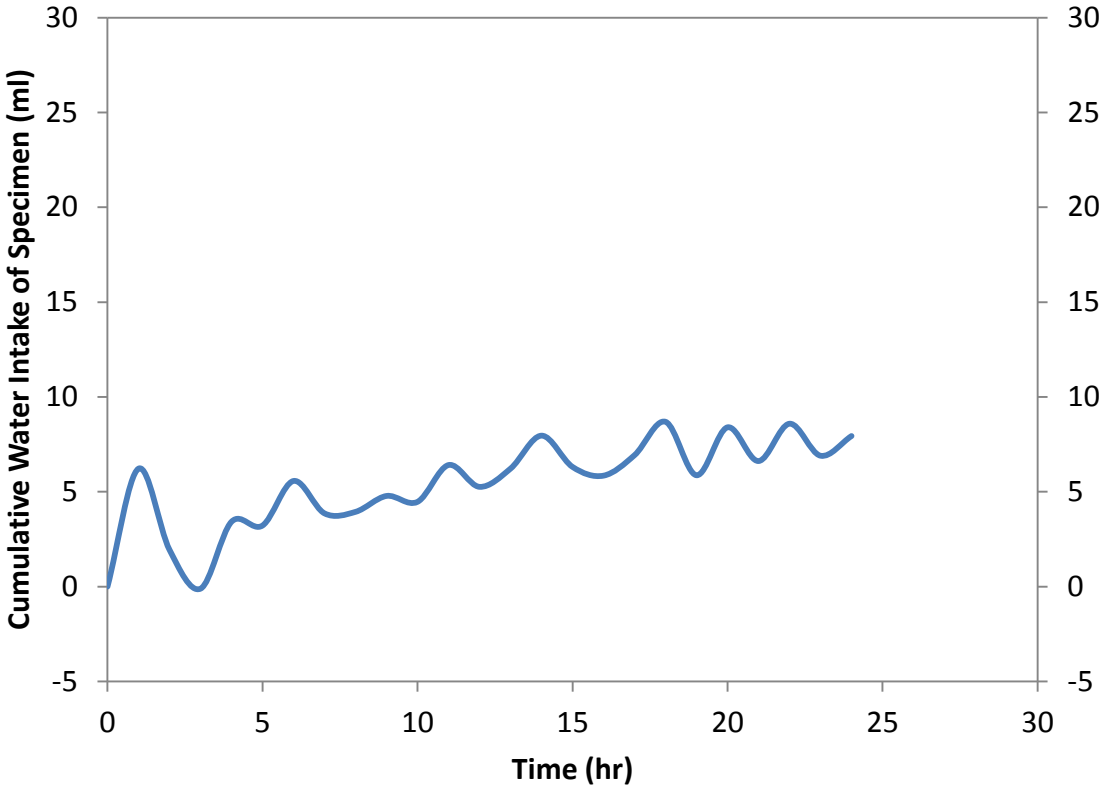

Figure 3.8 L05_S01 Cumulative Water Intake of Specimen vs. Time

3.1.5 PIV Results

Table 3.2 lists the data that corresponds to the subsets assigned to the images from Test L05_S01, and Figure 3.9 illustrates the subset layout.

Table 3.2 L05_S01 PIV Subset Data

PIV Subset Data	
Number of Subsets	286
Subset Size (pixel x pixel)	64 x 64
Number of Subsets per Row	13
Horizontal Subset Spacing (pixel)	32
Vertical Row spacing (pixel)	100
Number of Rows	22

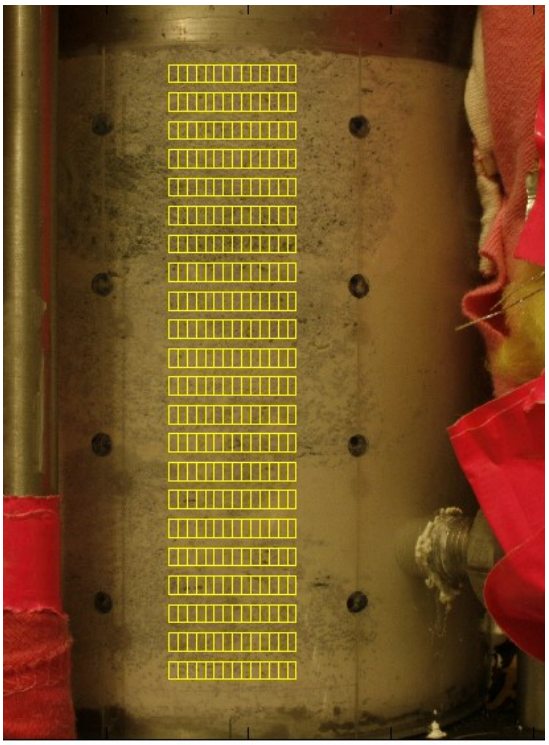

Figure 3.9 L05_S01 PIV Subsets

Figure 3.10 and Figure 3.11 illustrate the strain profiles in the specimen during hours 0 to 5, and hours 5 to 24, respectively. As the soil near the upper boundary condition froze, it appeared to undergo positive strain, followed by negative strain. This trend indicated that the soil underwent a period of consolidation, followed by expansion which was thought to be caused by the freezing of pore water. This was consistent with findings by Azmatch et al. (2008), and suction data presented in this chapter. Soil in the unfrozen zone showed an increase in positive strain, indicating a period of consolidation.

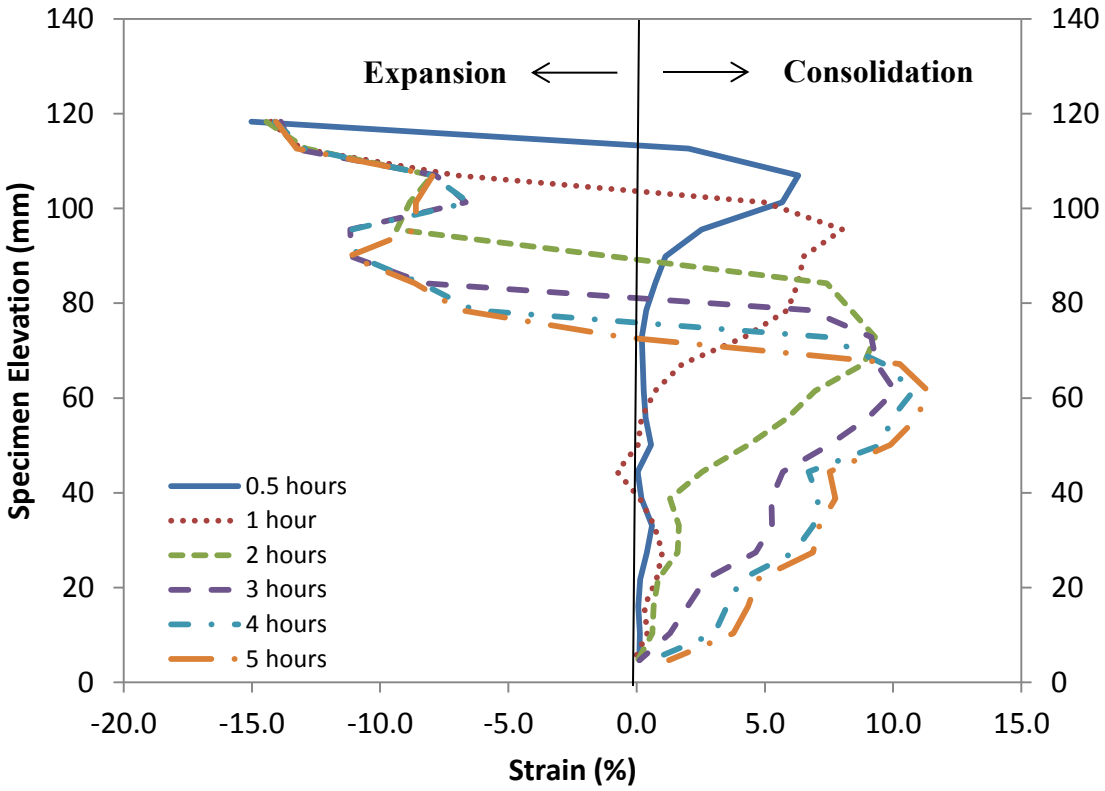

Figure 3.10 L05_S01 Specimen Elevation vs. Strain for 0 hours to 5 hours

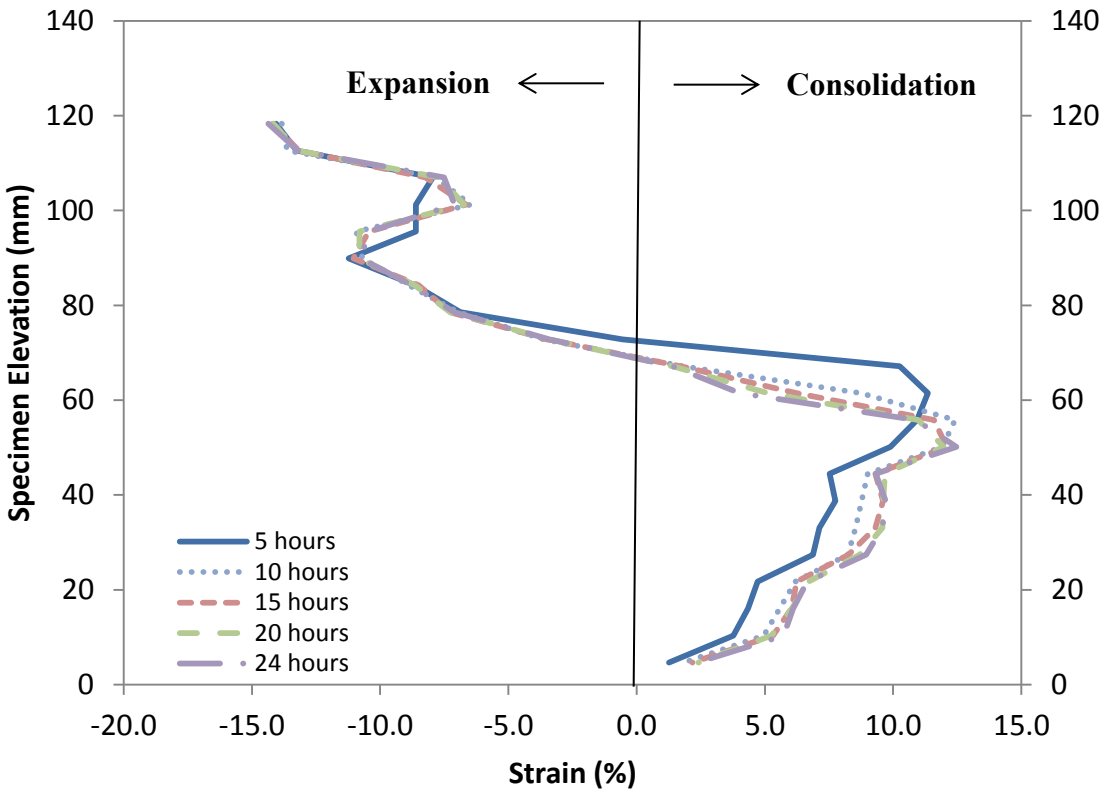

Figure 3.11 L05_S01 Specimen Elevation vs. Strain for 5 hours to 24 hours

Figure 3.12 and Figure 3.13 illustrate the void ratio profiles in the specimen during hours 0 to 5, and hours 5 to 24, respectively, as calculated from PIV results. As expected, the void ratio profiles followed a similar trend to that of the strain profiles. As the soil in the frozen zone froze, it showed a decrease in void ratio followed by an increase in void ratio. This was consistent with the soil undergoing consolidation, followed by expansion due to pore water freezing. Soil in the unfrozen zone showed a decrease in void ratio, consistent with freezing induced consolidation. This was generally consistent with void ratios calculated from water contents.

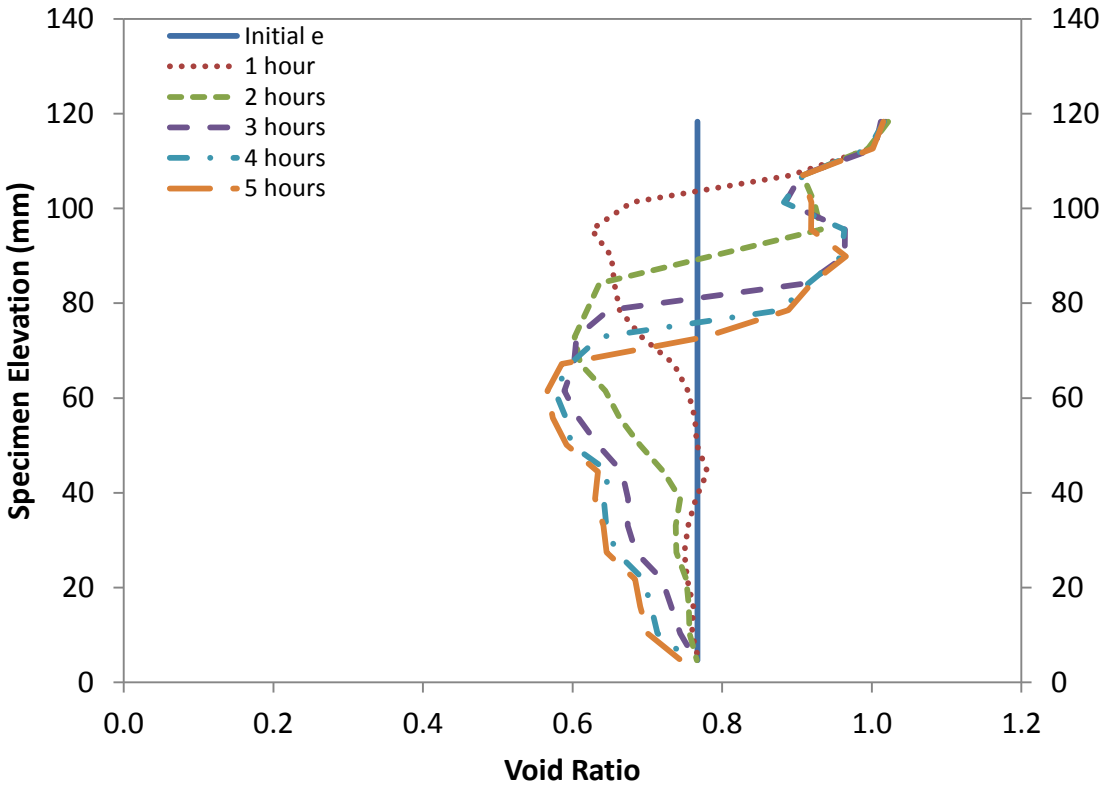

Figure 3.12 L05_S01 Specimen Elevation vs. Void Ratio for 0 to 5 hours

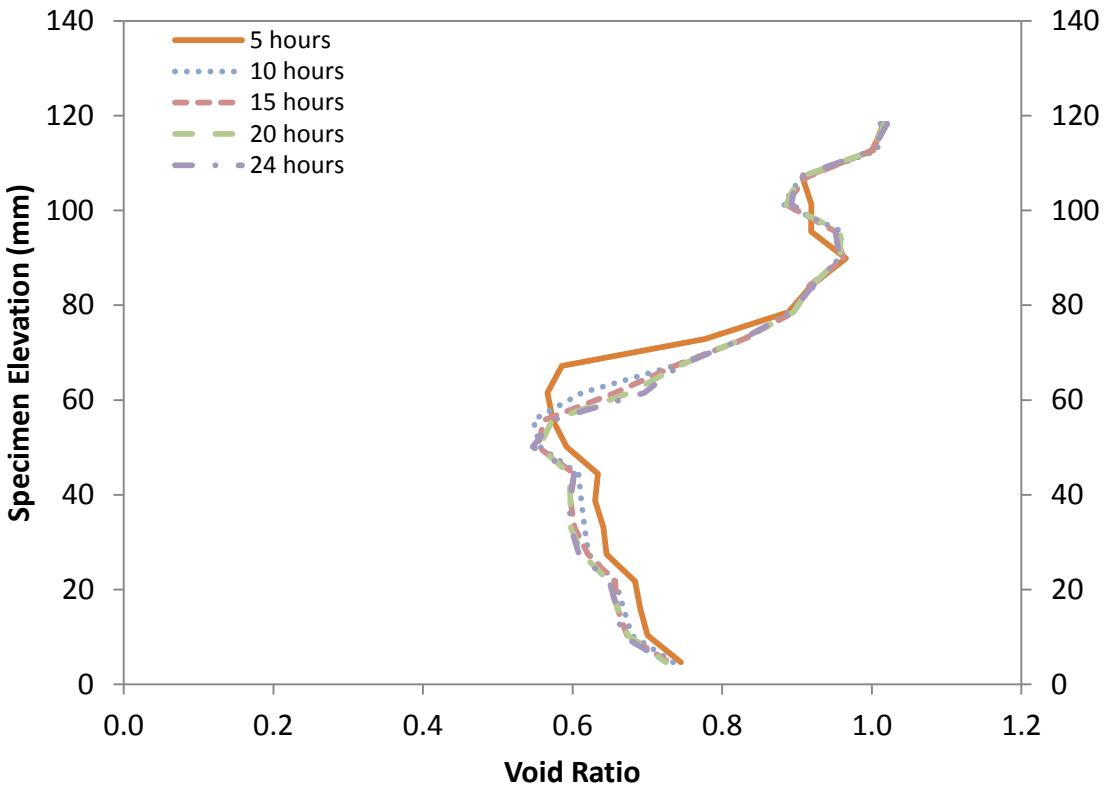

Figure 3.13 L05_S01 Specimen Elevation vs. Void Ratio for 5 to 24 hours

Figure 3.14 illustrates the depth of the frost front (i.e. zero degree isotherm) penetration in the specimen, as freezing progressed. The frost front penetrated the specimen approximately 72 mm, to an elevation of 55 mm. The frost front stopped advancing, and became approximately stationary, at this elevation at time 14 hours. For the purpose of this research, the frost front was determined to be stationary (and the onset of the final ice lens began) after 95% of the total heave had occurred. This was arbitrarily chosen, as the frost front continued to move very slightly after 10 to 15 hours. The location of the frost front was determined using a Matlab code that interpolated the location of the zero degree isotherm, throughout Stage C, from the TC data. It should be noted that the location of the zero degree isotherm, with time, was validated through visual observation of the freezing front. See Appendix B for an example of the comparison of the interpolation of the location of the zero degree isotherm with visual observations of the freezing front.

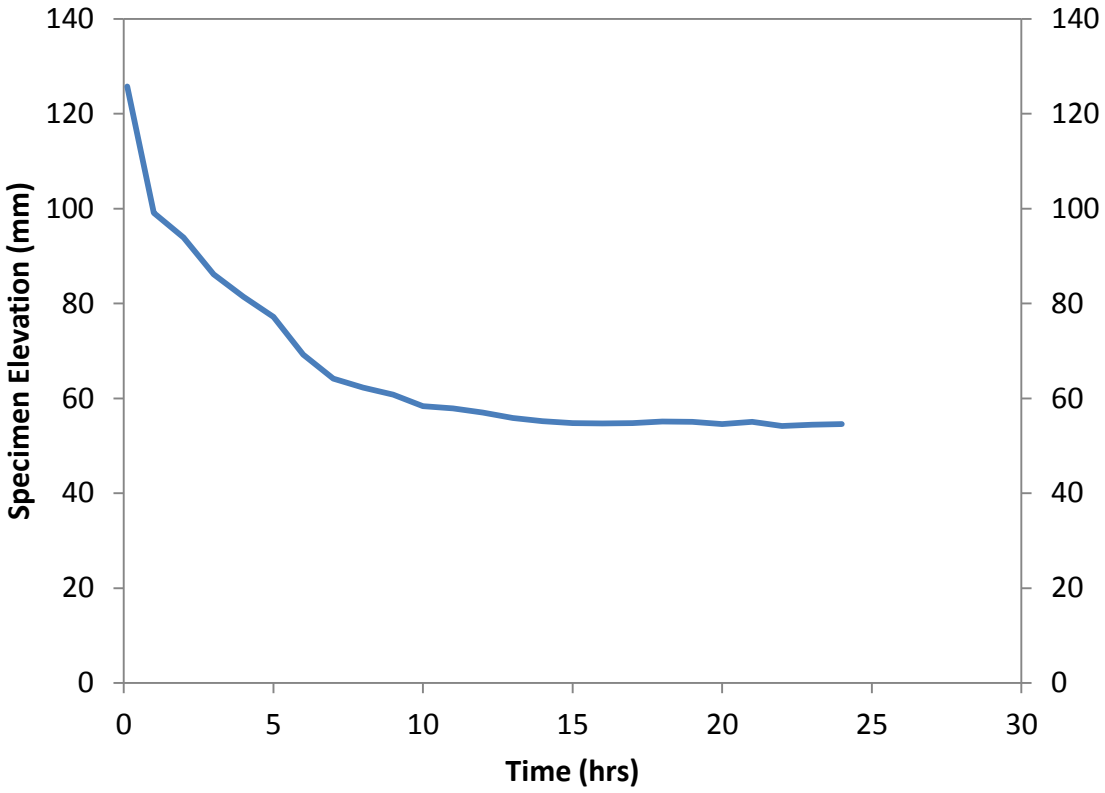

Figure 3.14 L05_S01 Frost Front Elevation in Specimen vs. Time

3.2 L06_S01 (PROCEDURE B)

3.2.1 Water Content and Void Ratio

The initial moisture content of the specimen prior to freezing conditions was 24%. After undergoing freezing, the moisture content of the frozen soil increased to an average of 30%, while the moisture content of the unfrozen soil decreased to an average of 22%. This trend in moisture redistribution was similar to that seen in Test L05_S01. Figure 3.15 illustrates the initial and final measured moisture profiles of the specimen, before and after the test. For this test, as well as Test L07_S02, improved accuracy was achieved when measuring moisture content and determining void ratio. As a result, there is less scatter compared to the data from Test L05_S01.

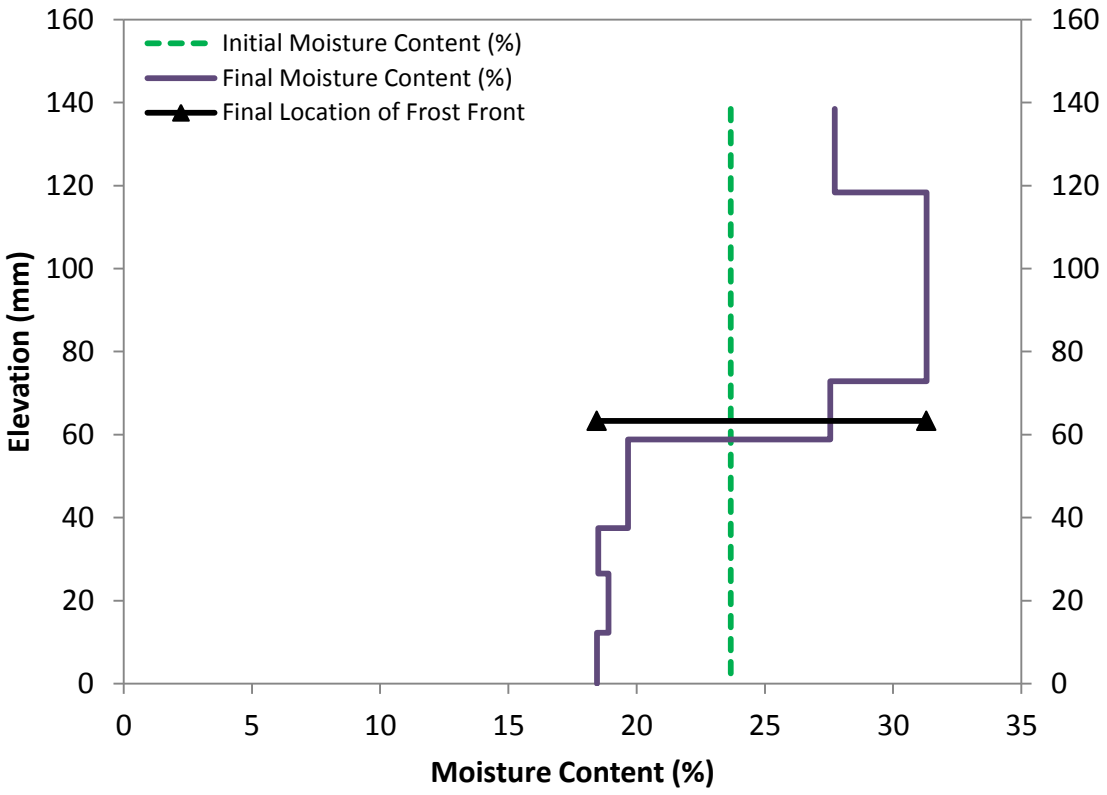

Figure 3.15 L06_S01 Specimen Elevation vs. Moisture Content

As shown in Figure 3.16, the initial void ratio of the specimen (calculated via phase relationships) was approximately 0.76. After undergoing freezing, the void ratio of the frozen soil increased to an average of 1.11, while the void ratio of the unfrozen soil decreased to an average of 0.68. This trend in void ratio was similar to that seen in Test L05_S01. Figure 3.16 illustrates the initial and final void ratio profiles of the specimen, before and after the test.

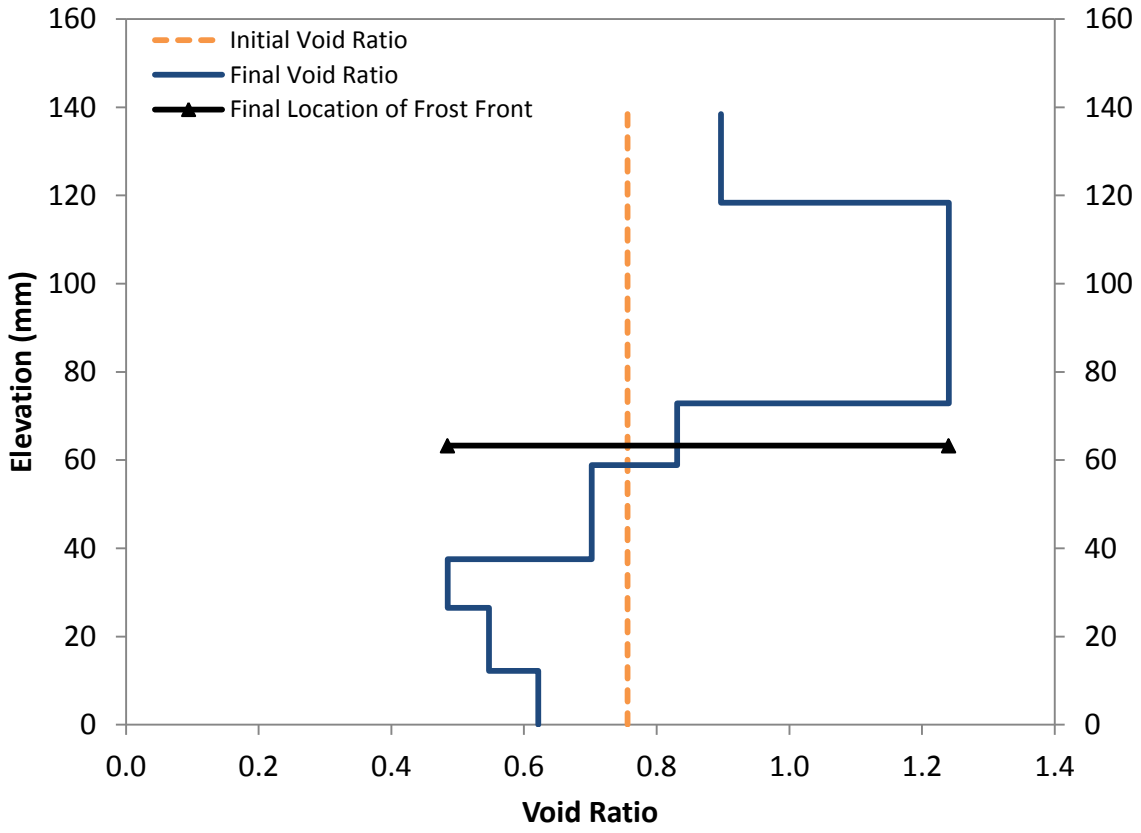

Figure 3.16 L06_S01 Specimen Elevation vs. Void Ratio

3.2.2 Temperature Results

Figure 3.17 and Figure 3.18 illustrate the temperature profiles at various elevations throughout the specimen during hours 0 to 5, and hours 5 to 26, respectively. At the beginning of Stage C (0 hours), the initial temperature in the specimen was measured between +2.3°C and +3.2°C. As freezing progressed, the temperature at the bottom of the

specimen gradually increased to +4.5°C. The temperature at the top of the specimen decreased to -6.3°C. As seen in the Test L05_S01, the slight increase in temperature at the bottom of the specimen, compared to the bottom boundary condition, was attributed to the peristaltic pump used for circulating the water through the bottom plate. The thermal profile across the specimen approached linearity at 10 hours into the test. The thermal trends were similar to those seen in Test L05_S01. In this test, however, the temperature in the specimen reached steady state 5 hours earlier than in Test L05_S01.

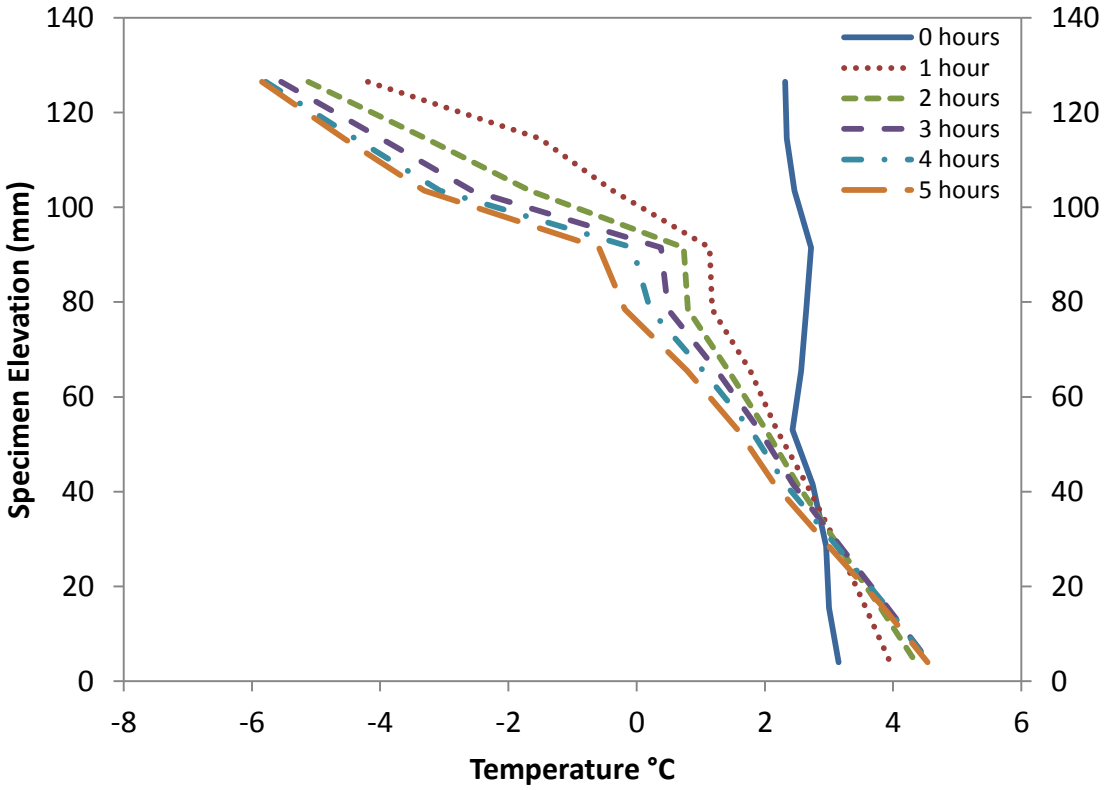

Figure 3.17 L06_S01 Specimen Elevation vs. Temperature for 0 to 5 hours

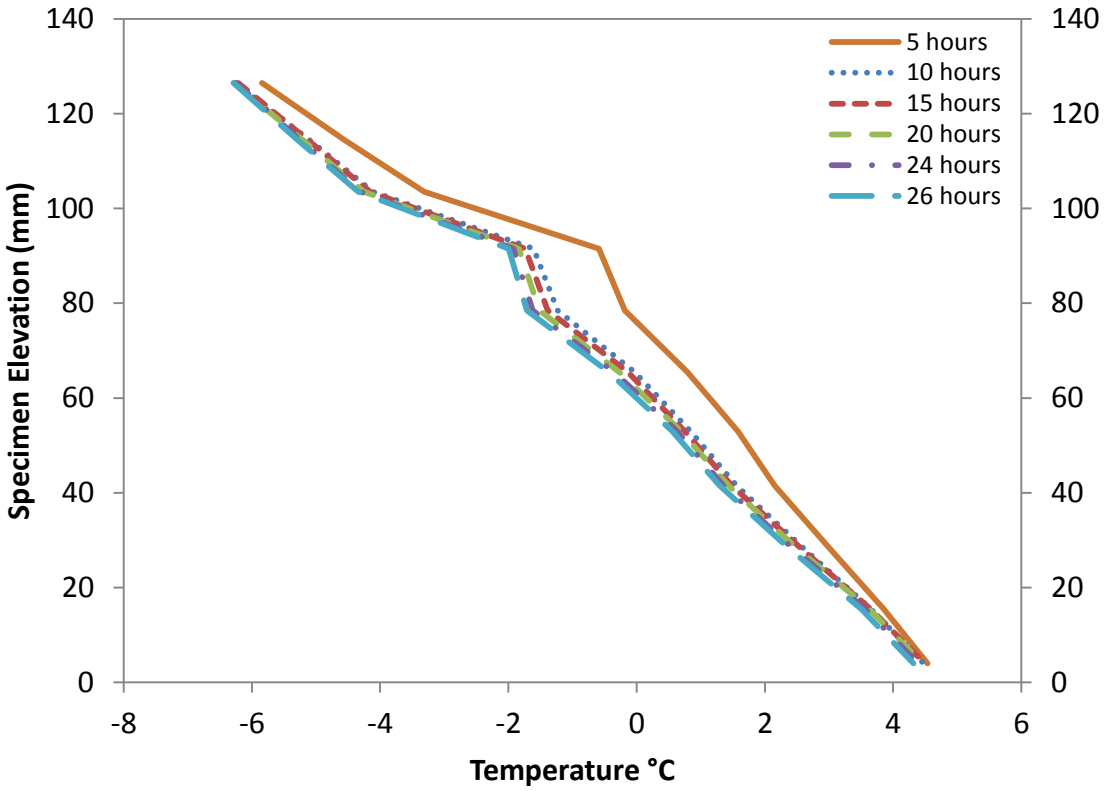

Figure 3.18 L06_S01 Specimen Elevation vs. Temperature for 5 to 26 hours

3.2.3 Suction Results

Figure 3.19 illustrates the suction versus time profiles in the specimen during Stage C. Figure 3.20 and Figure 3.21 illustrate the suction versus elevation profiles in the specimen during hours 0 to 5, and hours 5 to 26, respectively. Initial suction readings in all PPTs were approximately 0 kPa. Similar to results from Test L05_S01, during the first hour of the test PPT 01 and PPT 02 showed slight increases in pore water pressure due to freezing induced consolidation. PPT 01 reached a maximum suction of -25 kPa, 4.08 hours into the test. The suction then gradually decreased during the remainder of the test, reaching approximately -14 kPa when the test was terminated at 26 hours. PPT 02 reached a maximum suction of -59 kPa, 3.83 hours into the test. The suction then gradually decreased during the remainder of the test, reaching approximately -19.5 kPa when the test was terminated at 26 hours. Both PPT 01 and PPT 02 remained in the

unfrozen zone of soil for the entire test. PPT 03 reached a maximum suction of -198 kPa, 5.92 hours into the test, before cavitating. PPT 04 reached a maximum suction of -311 kPa, 1.92 hours into the test, before cavitating. Both PPT 03 and PPT 04 were in the frozen zone of soil at the termination of the test. The suction trends in this test were very similar to those observed in test L05_S01. PPT 03 and PPT 04, however, did not reach their maximum capacity prior to cavitation. This was likely a result of the ceramics not being fully saturated. It is also noted that following cavitation, the PPTs did not freeze during this test.

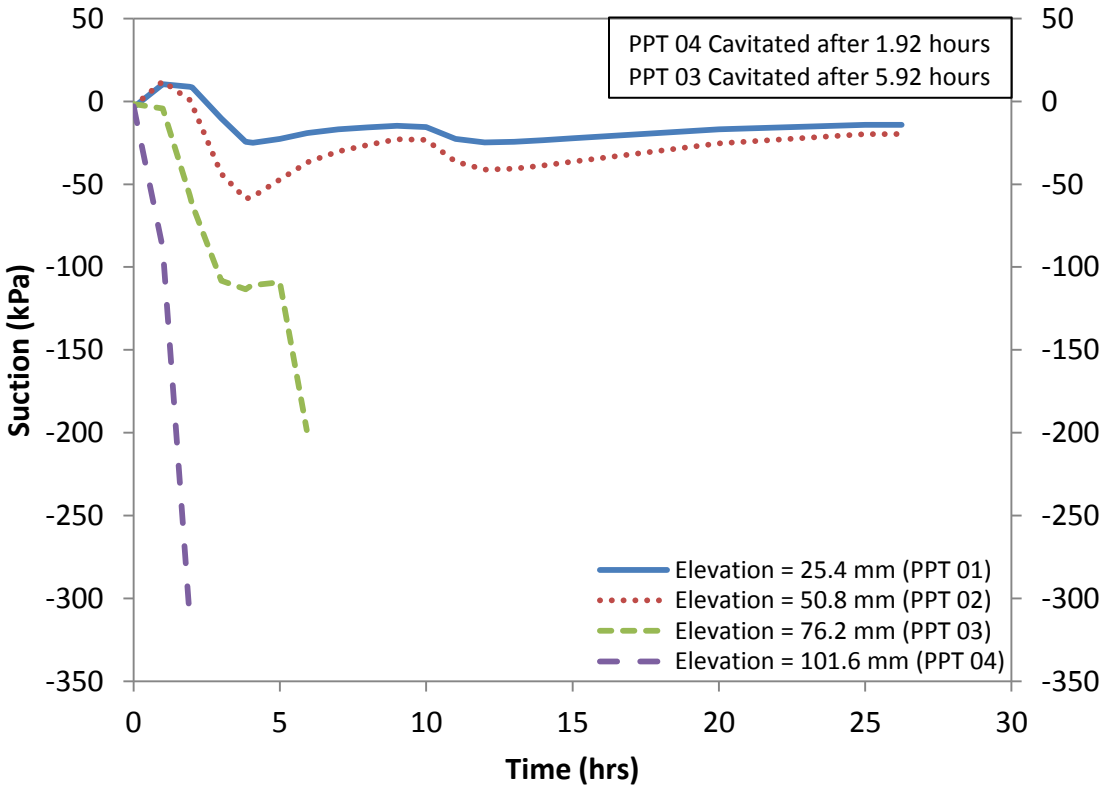

Figure 3.19 L06_S01 Suction vs. Time

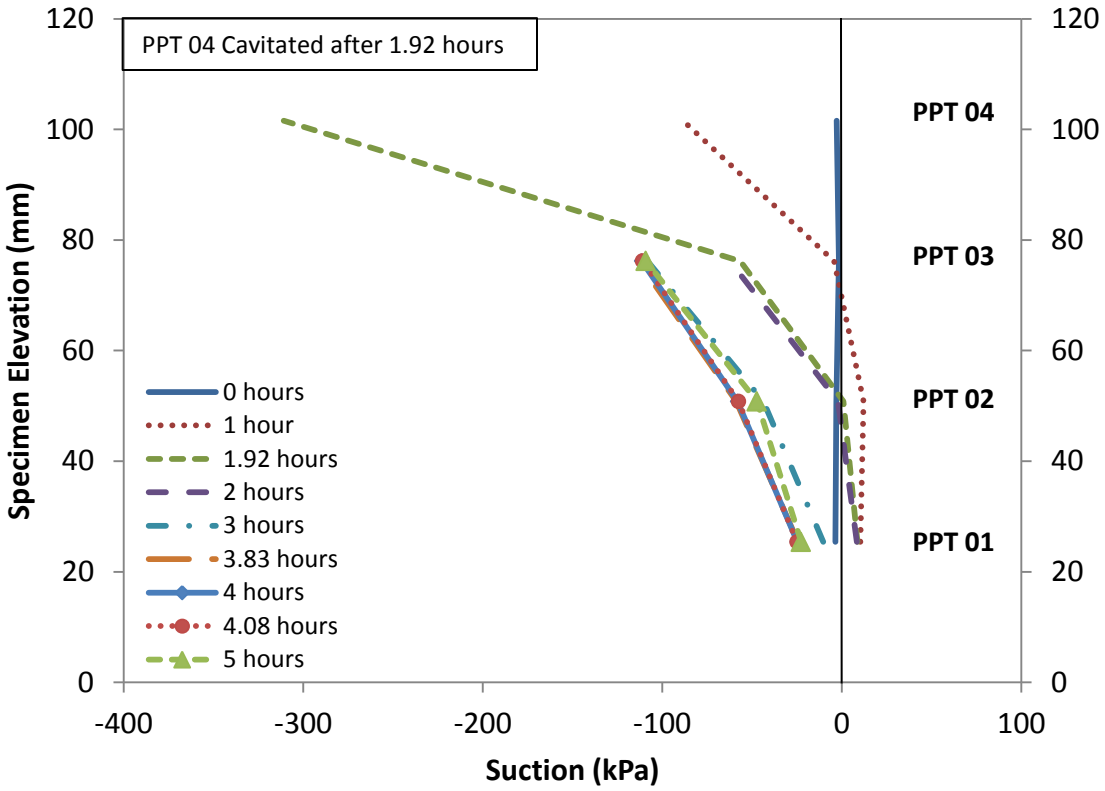

Figure 3.20 L06_S01 Specimen Elevation vs. Suction for 0 to 5 hours

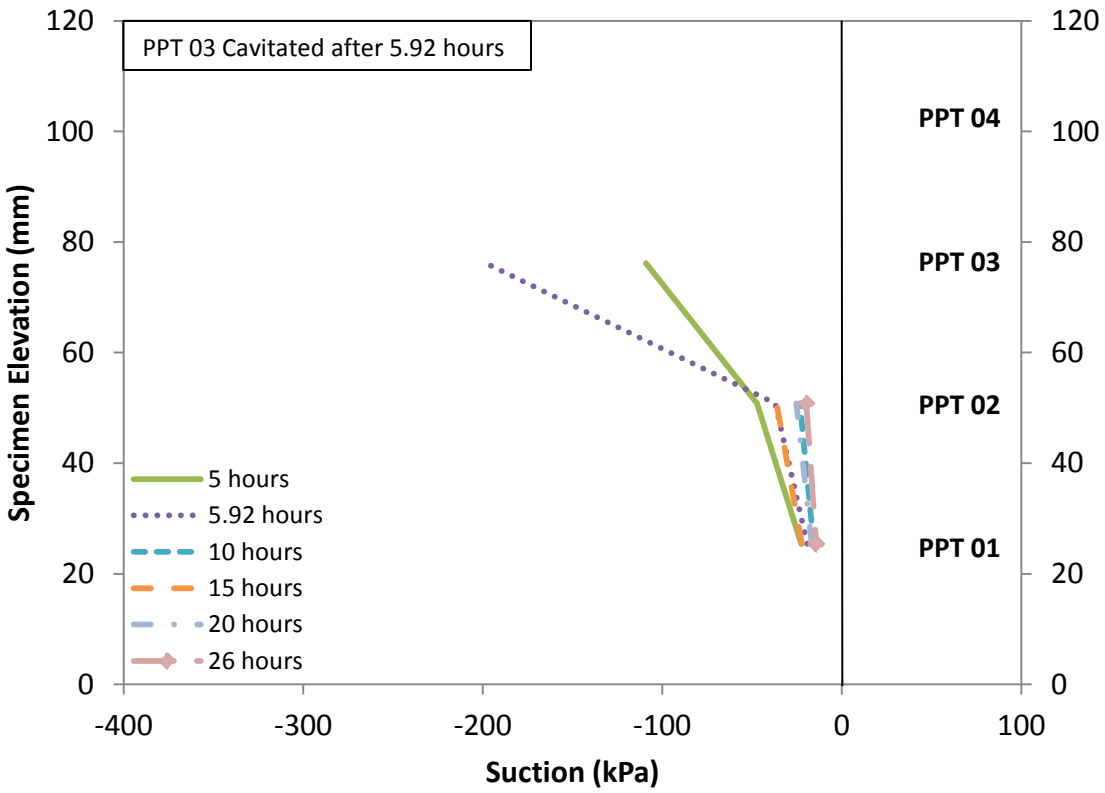

Figure 3.21 L06_S01 Specimen Elevation vs. Suction for 5 to 26 hours

3.2.4 Water Intake Results

During this test, the specimen was allowed to heave. Figure 3.22 illustrates the water intake of the specimen during Test L06_S01. The specimen took in approximately 4 ml of water during the first hour, and then expelled it by the two hour mark of the test. Since suction values were zero at the beginning of the test, this initial water intake was caused by the small head (30 mm) of water in the reservoir. As the soil froze, it underwent freezing induced consolidation in the unfrozen soil, causing an increase in pore water pressure (see Figure 3.20). The low permeability of the soil caused a lag in pore water pressure dissipation, which began to occur during hour two. During the third hour into the test, the specimen continued to expel an additional 2 ml of water. At this point (hour four) the soil had developed sufficient suction to create steady water intake. At approximately 9 hours into the test, the specimen had taken in enough water to be back at 0 ml of overall

water intake. At this time, the specimen continued to exhibit steady water intake until the test was terminated at 26 hours. The total water intake of the specimen, during the test, was 20 ml. The approximate rate of water intake from time 9 hours to 26 hours, was 1.12 ml/hour.

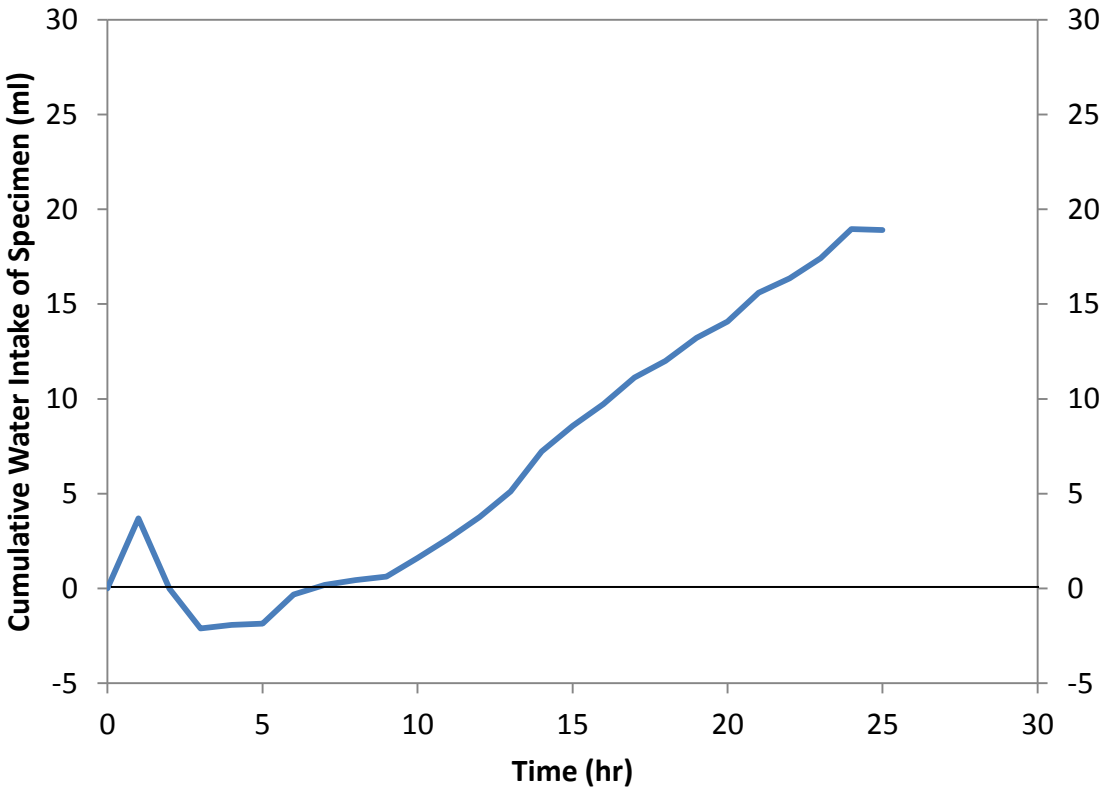

Figure 3.22 L06_S01 Cumulative Water Intake of Specimen vs. Time

3.2.5 PIV Results

Table 3.3 lists the data that corresponds to the subsets assigned to the images from Test L06_S01, and Figure 3.23 illustrates the subset layout.

Table 3.3 L06_S01 PIV Subset Data

PIV Subset Data	
Number of Subsets	286
Subset Size (pixel x pixel)	64 x 64
Number of Subsets per Row	13
Subset Spacing (pixel)	32
Row spacing (pixel)	100
Number of Rows	22

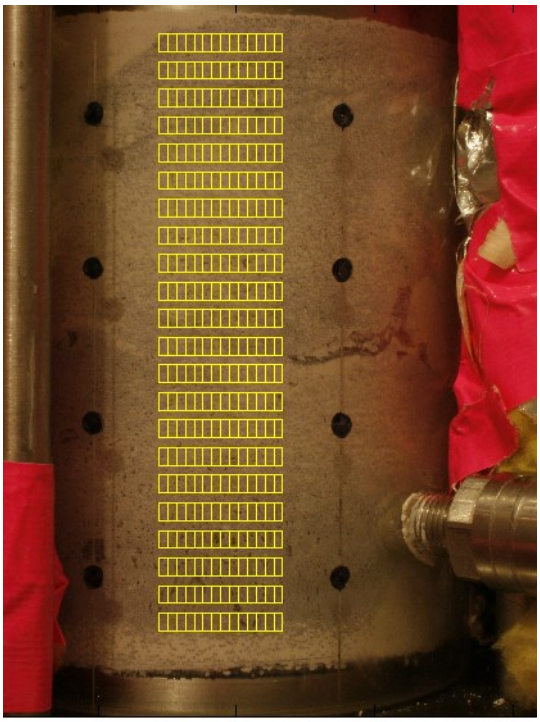

Figure 3.23 L06_S01 PIV Subsets

Figure 3.24 and Figure 3.25 illustrate the strain profiles in the specimen during hours 0 to 5, and hours 5 to 26, respectively. The strain profile trends were similar to those seen in L05_S01. In this test, however, large positive and negative strains were indicated between elevation 60 mm to 71.5 mm, beginning at hour 15. These strains, labeled "Crack", are not an accurate representation of the strains in the specimen, but rather indicate that the PIV image analysis detected a substantial movement of the subsets in this area. As a result, these subsets; at elevation 71.5 mm, 65.8 mm, and 60.1 mm, were

excluded from the profiles at 15 hours, 20 hours, and 26 hours. The "Crack" profile was plotted separately for these three times.

The movement of the subsets was thought to be caused by the onset of heave. Similar issues were reported by Arenson et al. (2007) and their recommendations for avoiding these issues were implemented, despite having a similar outcome. A visual analysis of the images from this time to the end of the test confirmed the presence of a large crack in the soil, due to heave.

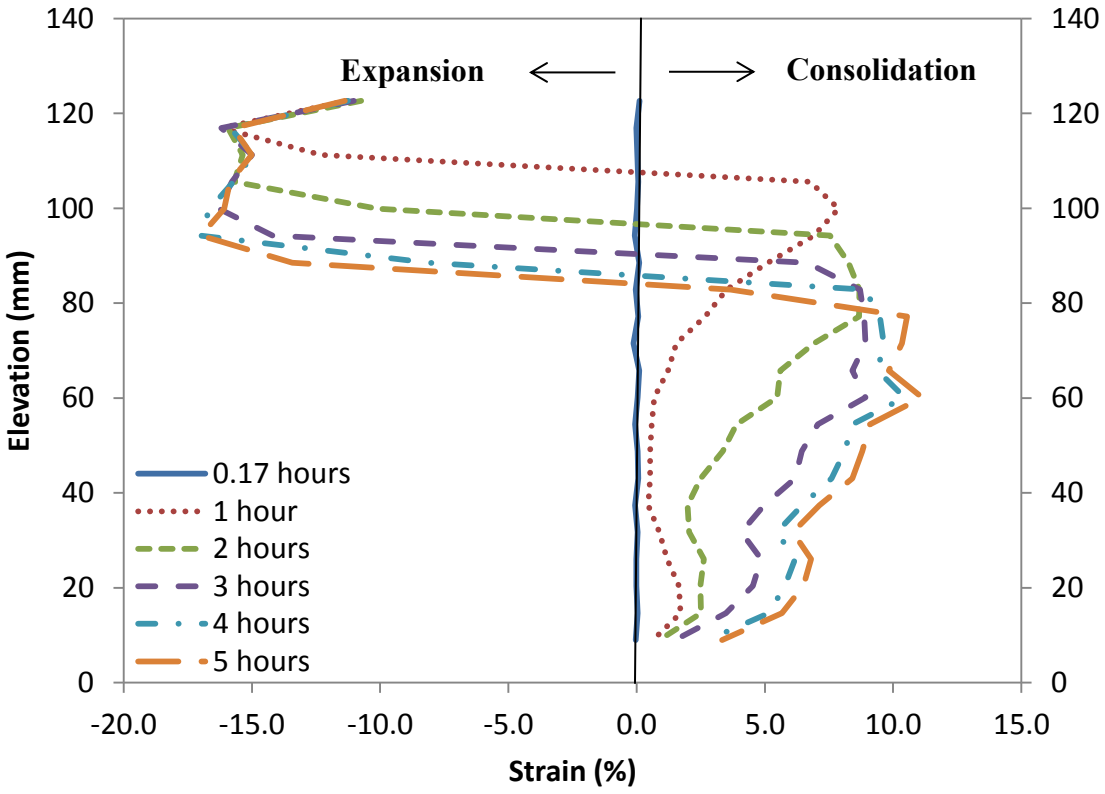

Figure 3.24 L06_S01 Specimen Elevation vs. Strain for 0 to 5 hours

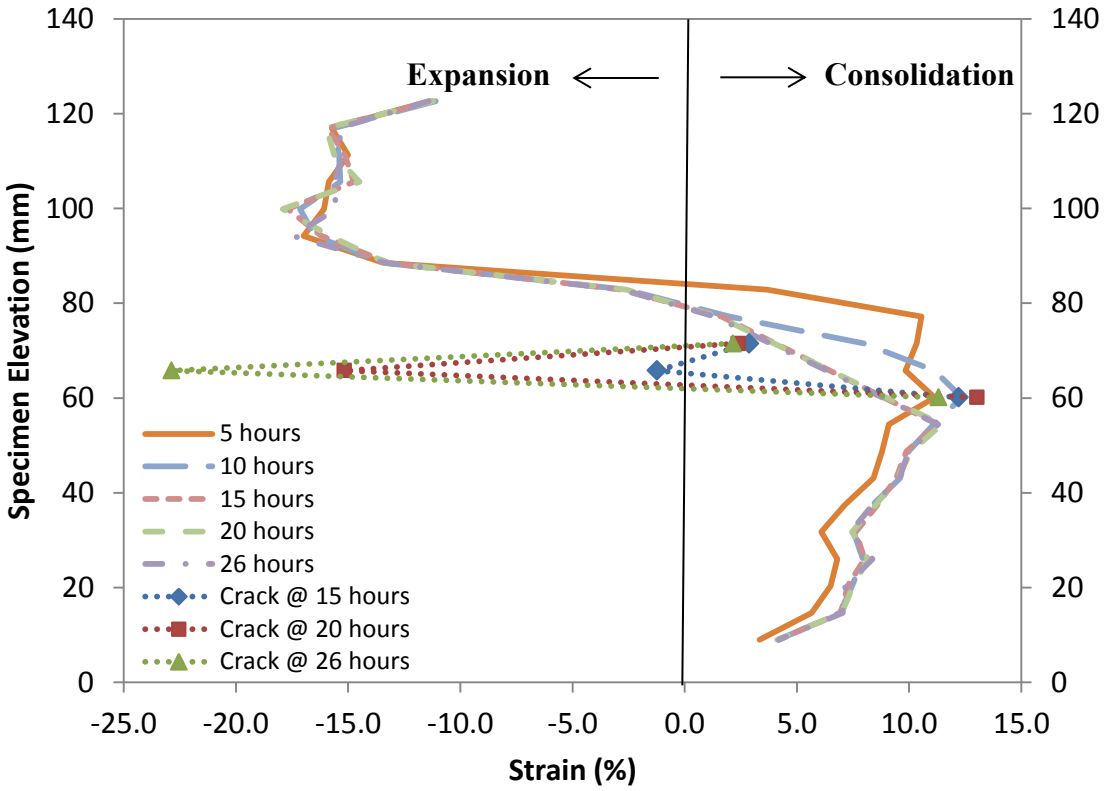

Figure 3.25 L06_S01 Specimen Elevation vs. Strain for 5 to 26 hours

Figure 3.26 and Figure 3.27 illustrate the void ratio profiles in the specimen during hours 0 to 5, and hours 5 to 26, respectively, as calculated from PIV results. As expected, the void ratio profiles followed a similar trend to that of the strain profiles. Trends are similar to those seen in L05_S01.

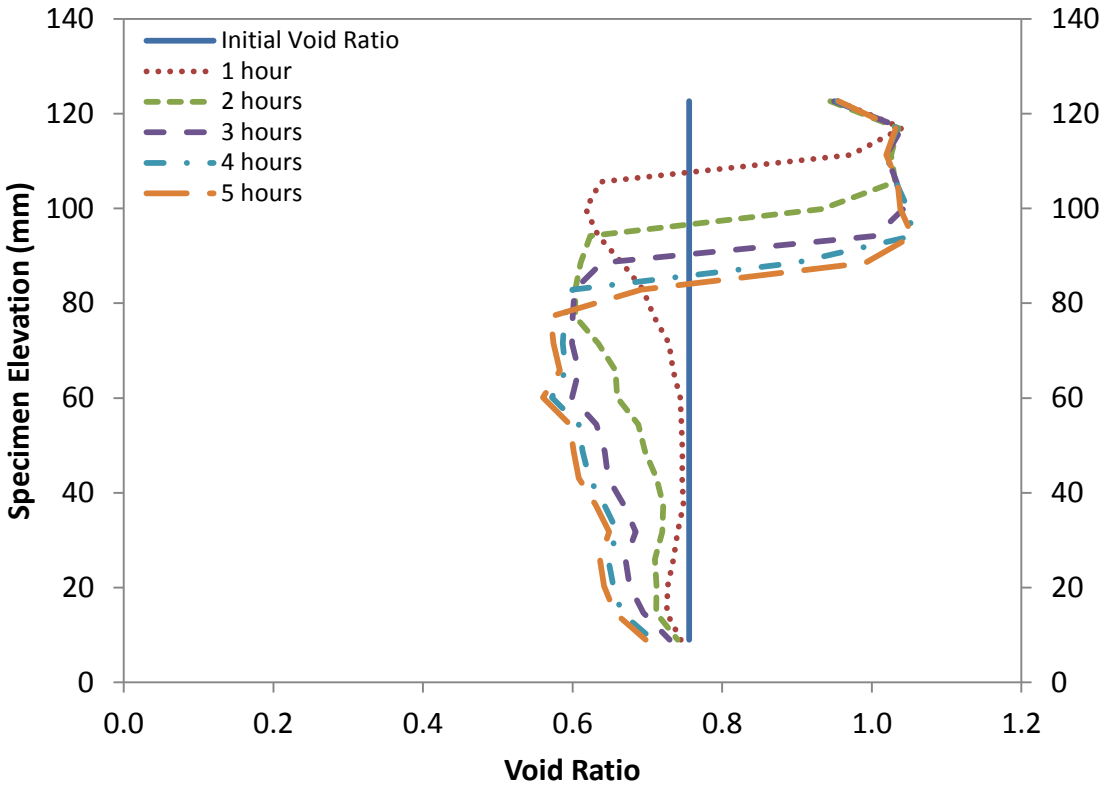

Figure 3.26 L06_S01 Specimen Elevation vs. Void Ratio for 0 to 5 hours

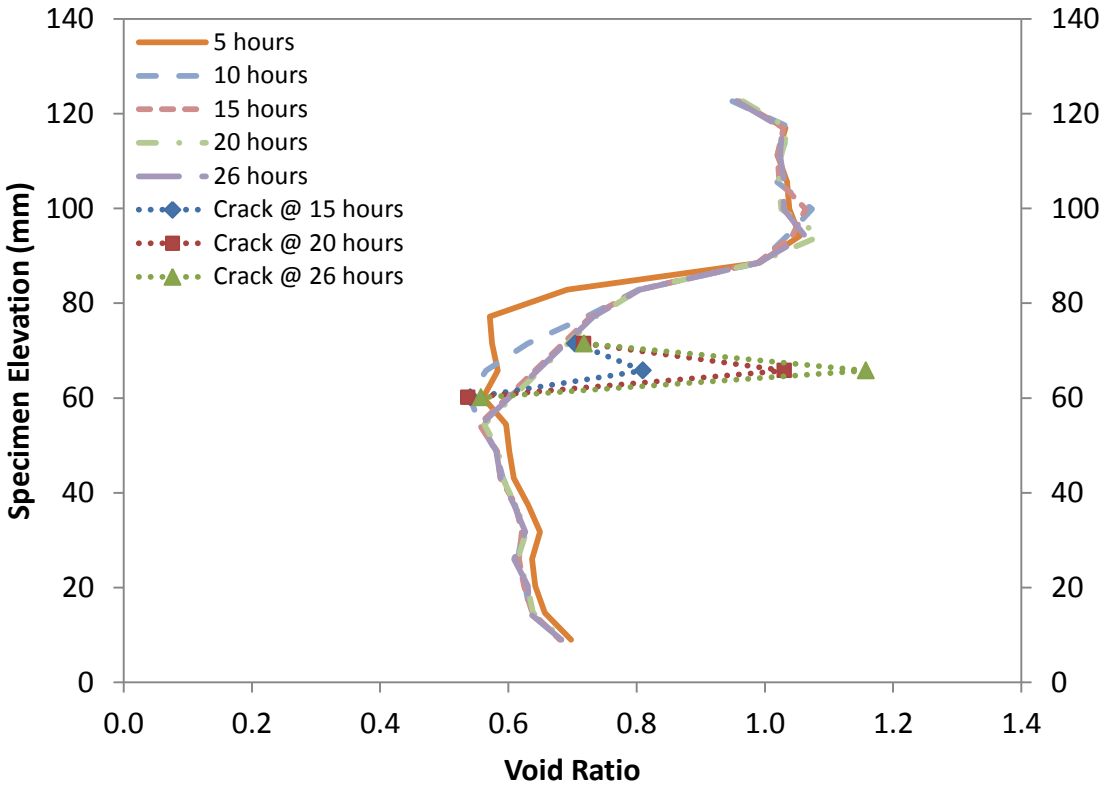

Figure 3.27 L06_S01 Specimen Elevation vs. Void Ratio for 5 to 26 hours

Figure 3.28 illustrates the depth of the frost front penetration in the specimen, as freezing progressed. The frost front penetrated the specimen approximately 71 mm, to an elevation of 63 mm. The frost front stopped advancing, and became approximately stationary, at this elevation at time 16 hours. The frost front penetration trend was similar to that seen in Test L05_S01.

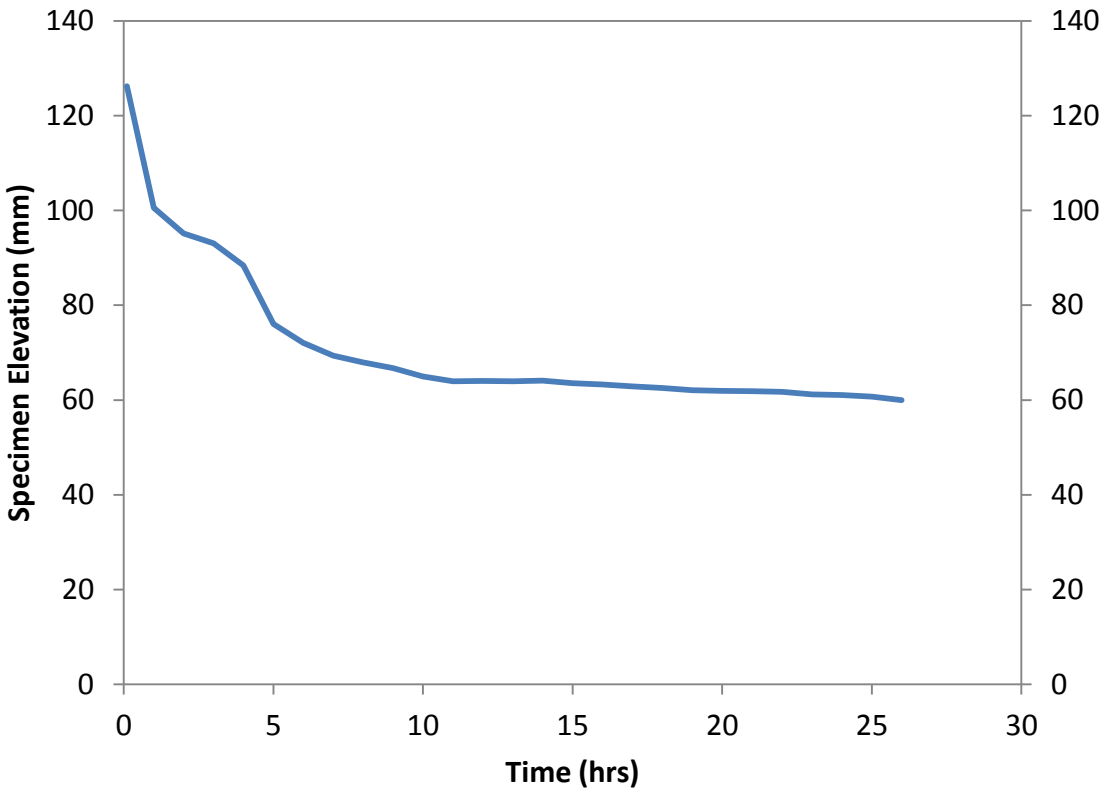

Figure 3.28 L06_S01 Frost Front Elevation in Specimen vs. Time

Figure 3.29 illustrates the rate of frost heave with time during Test L06_S01. The specimen appeared to consolidate by 0.25 mm in the first hour of the test, where it remained until hour ten. At ten hours into the test the specimen began to heave at a steady rate, reaching a maximum heave of 2.3 mm when the test was terminated at 26 hours. Taking into account the freezing induced consolidation, this indicated an overall heave of 2.55 mm. The average rate of heave from hours 10 to 26 was 0.15 mm/hour.

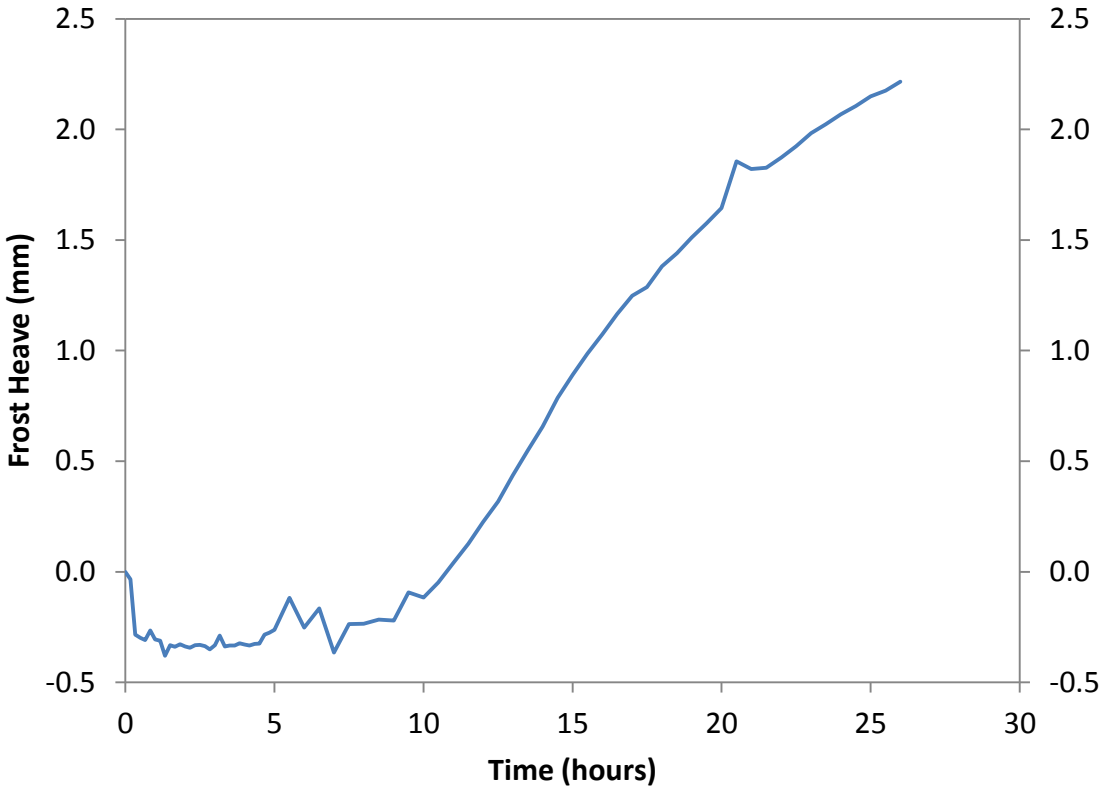

Figure 3.29 L06_S01 Frost Heave vs. Time

SP was calculated from temperature profile data and water intake data. SP = 40.4 mm^2/°C*d for Test L06_S01. According to Table 1.1, this soil falls in the mid-range of the low frost susceptibility class.

3.3 L07_S02 (PROCEDURE B)

Test L07_S02 was performed under the same conditions as Test L06_S01, in order to confirm the repeatability of data obtained from tests performed under Procedure B. The only difference between the two tests was their duration. Test L07_S02 was continued for 45 hours, whereas Test L06_S01 only had a duration of 26 hours. This was done in order to see the changes in rate of heave as the test progressed.

3.3.1 Water Content and Void Ratio

The initial moisture content of the specimen prior to freezing conditions was 23%. After undergoing freezing, the moisture content of the frozen soil increased to an average of 30%, while the moisture content of the unfrozen soil decreased to an average of 21%. These results were consistent with results from the other two tests. Figure 3.30 illustrates the initial and final measured moisture profiles of the specimen, before and after the test.

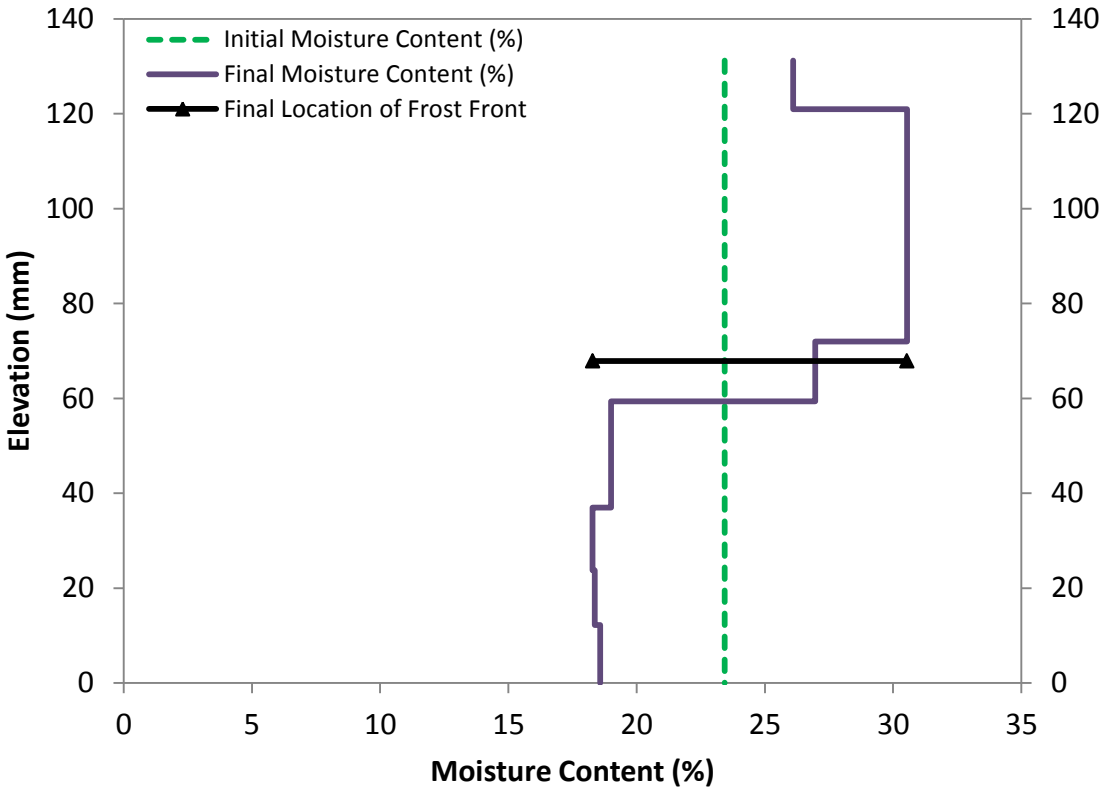

Figure 3.30 L07_S02 Specimen Elevation vs. Moisture Content

As shown in Figure 3.31, the initial void ratio of the specimen (calculated via phase relationships) was approximately 0.72. After undergoing freezing, the void ratio of the frozen soil increased to an average of 0.90, the void ratio of the unfrozen soil also increased slightly to an average of 0.73. This trend in void ratio redistribution was similar to that seen in Test L06_S01. The average final void ratio of the frozen soil in this test, however, was not as high as the other two tests. In addition, the average final void ratio of the unfrozen soil was slightly higher than the initial void ratio. This may be a result of the determined location of the frost front, which indicated the boundary between the frozen and unfrozen soil. Figure 3.32 illustrates the initial and final void ratio profiles of the specimen, before and after the test.

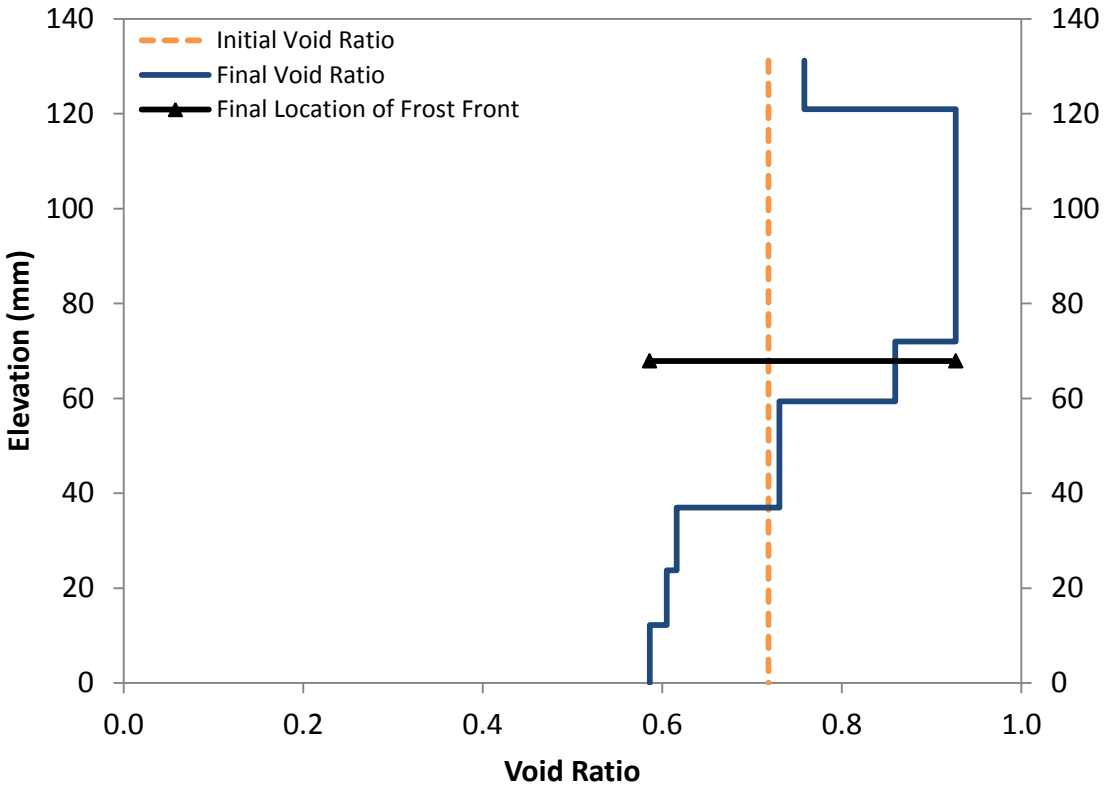

Figure 3.31 L07_S02 Specimen Elevation vs. Void Ratio

3.3.2 Temperature Results

Figure 3.32 and Figure 3.33 illustrate the temperature profiles at various elevations throughout the specimen during hours 0 to 5, and hours 5 to 45, respectively. At the beginning of Stage C (0 hours), the initial temperature in the specimen was measured between +2.8°C and +3.5°C. As freezing progressed, the temperature at the bottom of the specimen gradually increased to +4.6°C. The temperature at the top of the specimen decreased to -6.2°C. As seen in the other two tests, the slight increase in temperature at the bottom of the specimen, compared to the bottom boundary condition, was attributed to the peristaltic pump used for circulating the water through the bottom plate. The thermal profile across the specimen approached linearity at 10 hours into the test. These results are consistent with those seen in Test L06_S01.

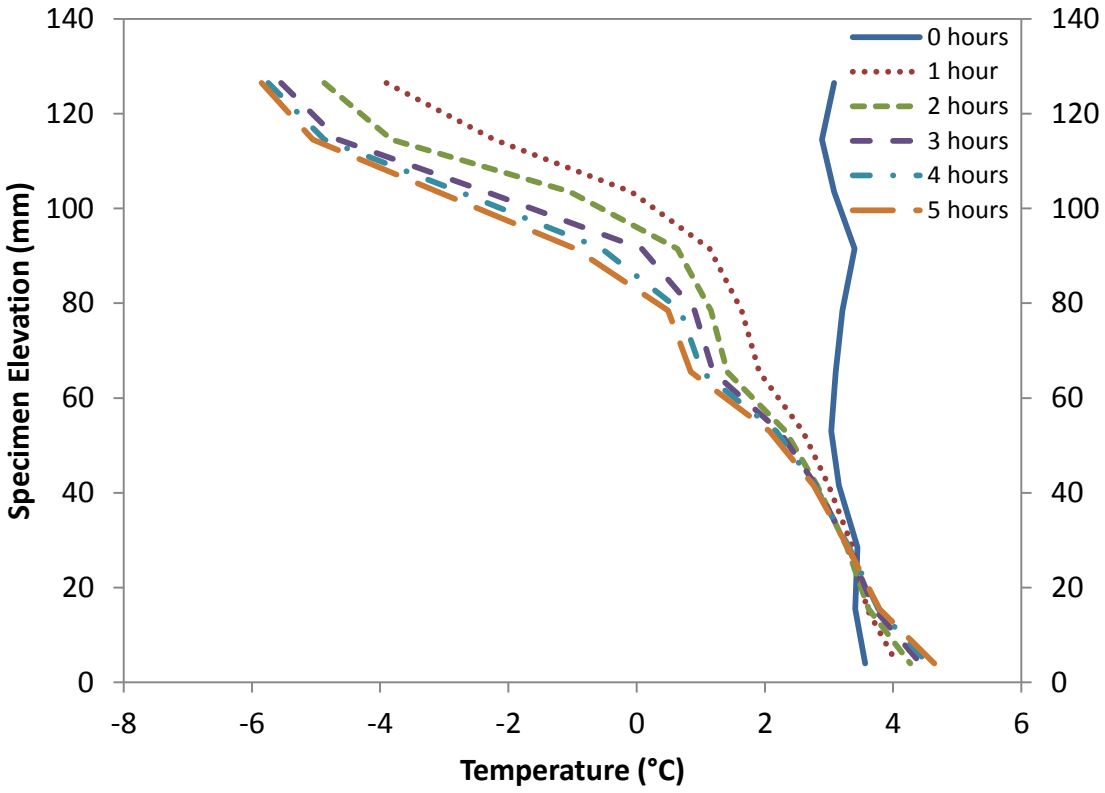

Figure 3.32 L07_S02 Specimen Elevation vs. Temperature for 0 to 5 hours

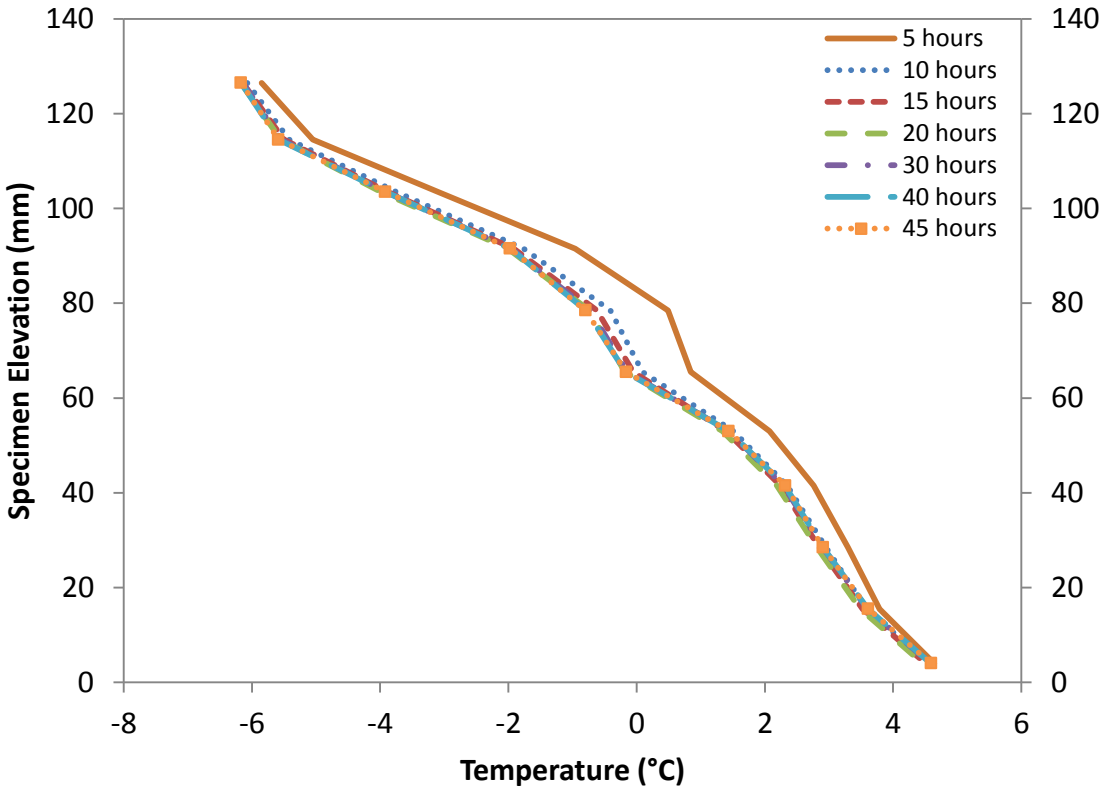

Figure 3.33 L07_S02 Specimen Elevation vs. Temperature for 5 to 45 hours

3.3.3 PIV Results

Table 3.4 lists the data that corresponds to the subsets assigned to the images from Test L07_S02, and Figure 3.34 illustrates the subset layout.

Table 3.4 L07_S02 PIV Subset Data

PIV Subset Data	
Number of Subsets	208
Subset Size (pixel x pixel)	64 x 64
Number of Subsets per Row	13
Subset Spacing (pixel)	32
Row spacing (pixel)	100
Number of Rows	15

Figure 3.34 L07_S02 PIV Subsets

Figure 3.35 and Figure 3.36 illustrate the strain profiles in the specimen during hours 0 to 5, and hours 5 to 45, respectively. The strain profiles were consistent with those seen in Test L06_S01. In this test, however, the large positive and negative strains caused by the onset of heave, were indicated between elevations 54 mm to 70 mm, beginning at hour 15. Similar to Test L06_S01, the subsets at elevation 69.2 mm, 61.6 mm, and 53.9 mm, were excluded from the profiles from 15 hours to 45 hours. The "crack" profile was plotted separately at the onset of the crack (15 hours) and at the end of the test (45.2 hours). This zone of soil influenced by heave was roughly the same magnitude as in Test L06_S01, but was located approximately 6 mm lower in the specimen.

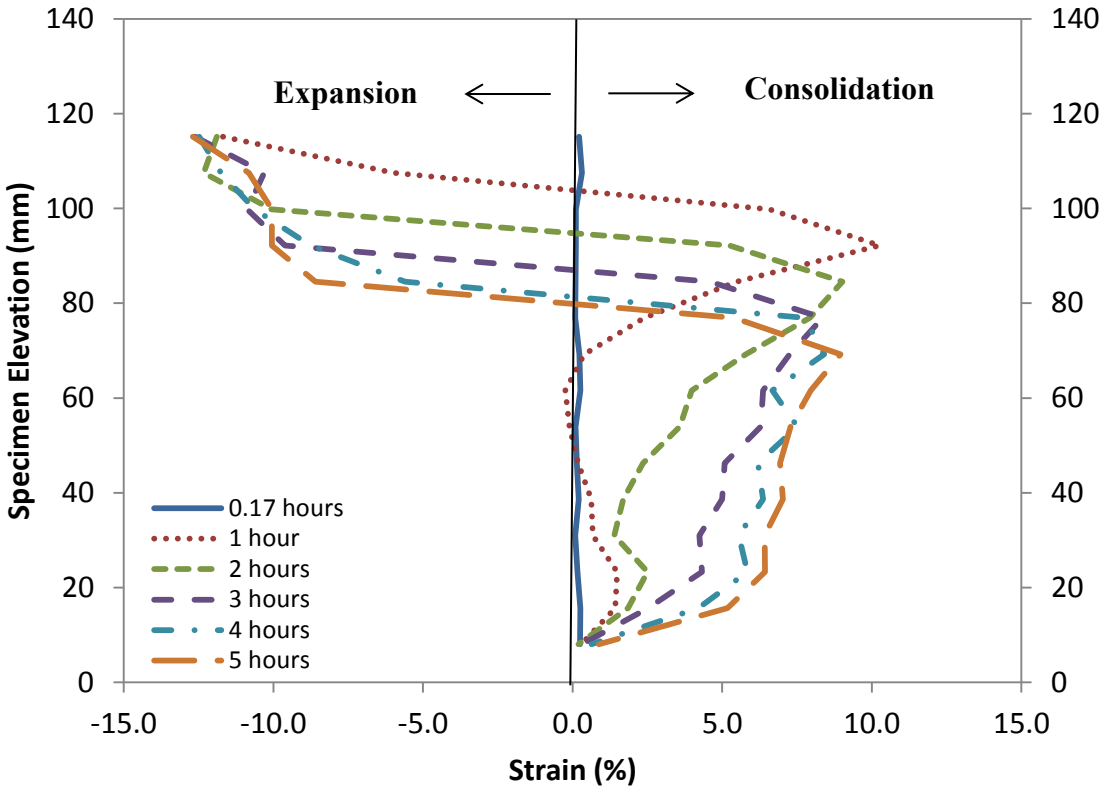

Figure 3.35 L07_S02 Specimen Elevation vs. Strain for 0 to 5 hours

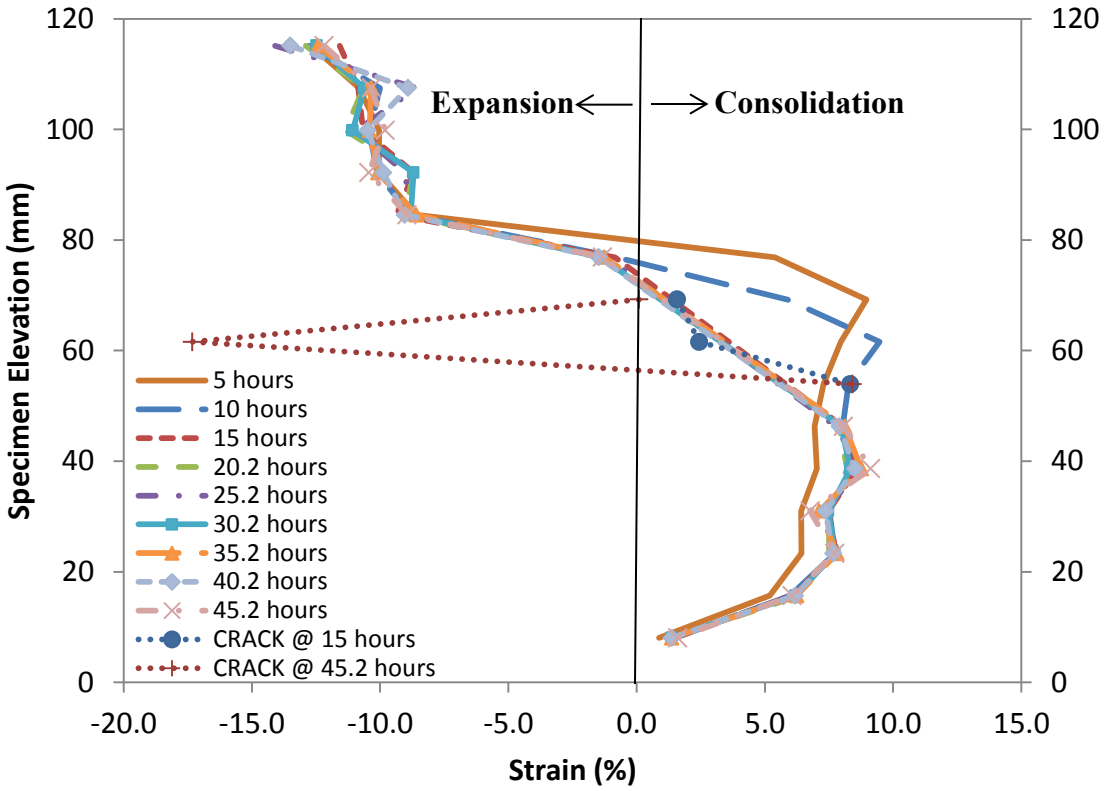

Figure 3.36 L07_S02 Specimen Elevation vs. Strain for 5 to 45 hours

Figure 3.37 and Figure 3.38 illustrate the void ratio profiles in the specimen during hours 0 to 5, and hours 5 to 45, respectively, as calculated from PIV results. As expected, the void ratio profiles were consistent with those seen in Test L06_S01.

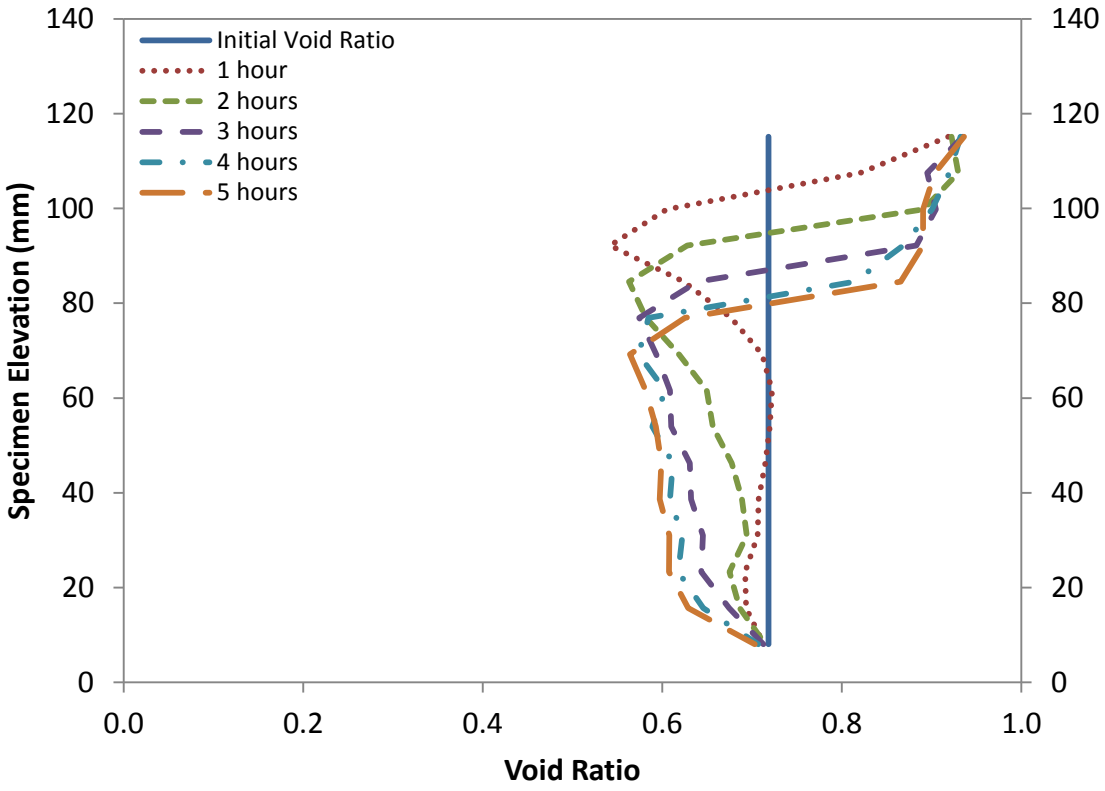

Figure 3.37 L07_S02 Specimen Elevation vs. Void Ratio for 0 to 5 hours

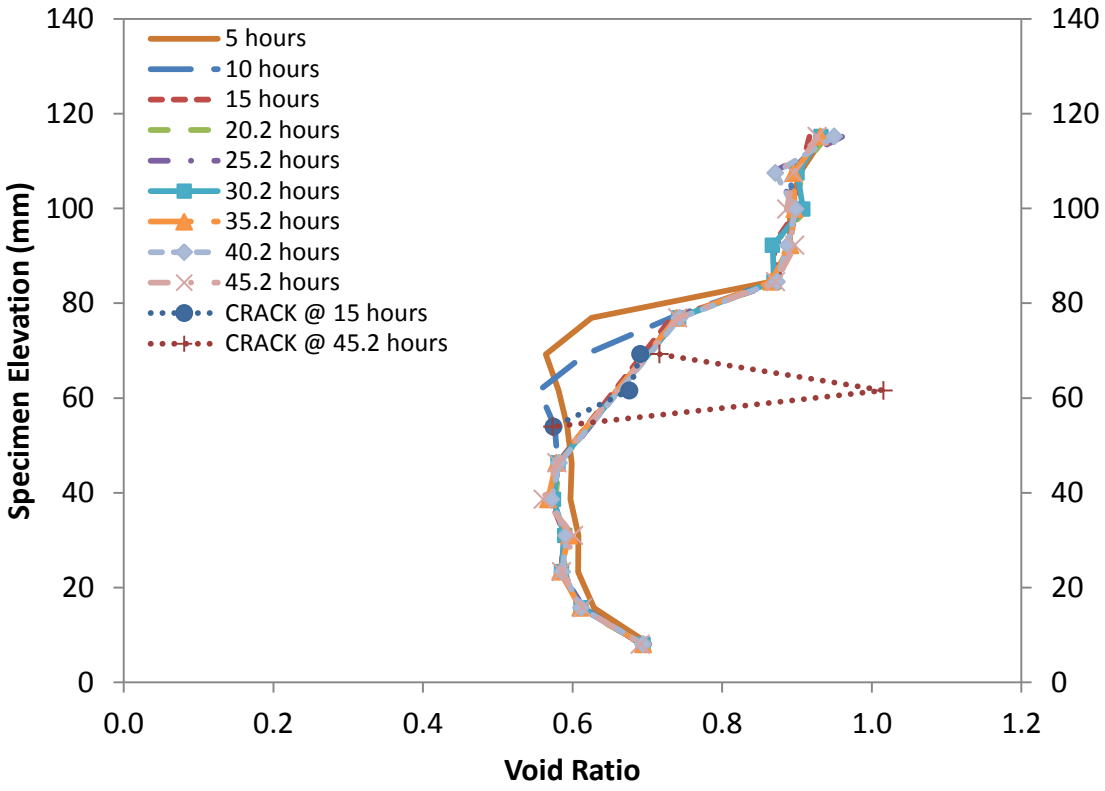

Figure 3.38 L07_S02 Specimen Elevation vs. Void Ratio for 5 to 45 hours

Figure 3.39 illustrates the depth of the frost front penetration in the specimen, as freezing progressed. The frost front penetrated the specimen approximately 59 mm, to an elevation of 68 mm. The frost front stopped advancing, and became approximately stationary, at this elevation at time 10 hours. The frost front penetration trend was similar to that seen in Test L06_01. In Test L07_S02, however, the frost front stopped penetrating after 10 hours.

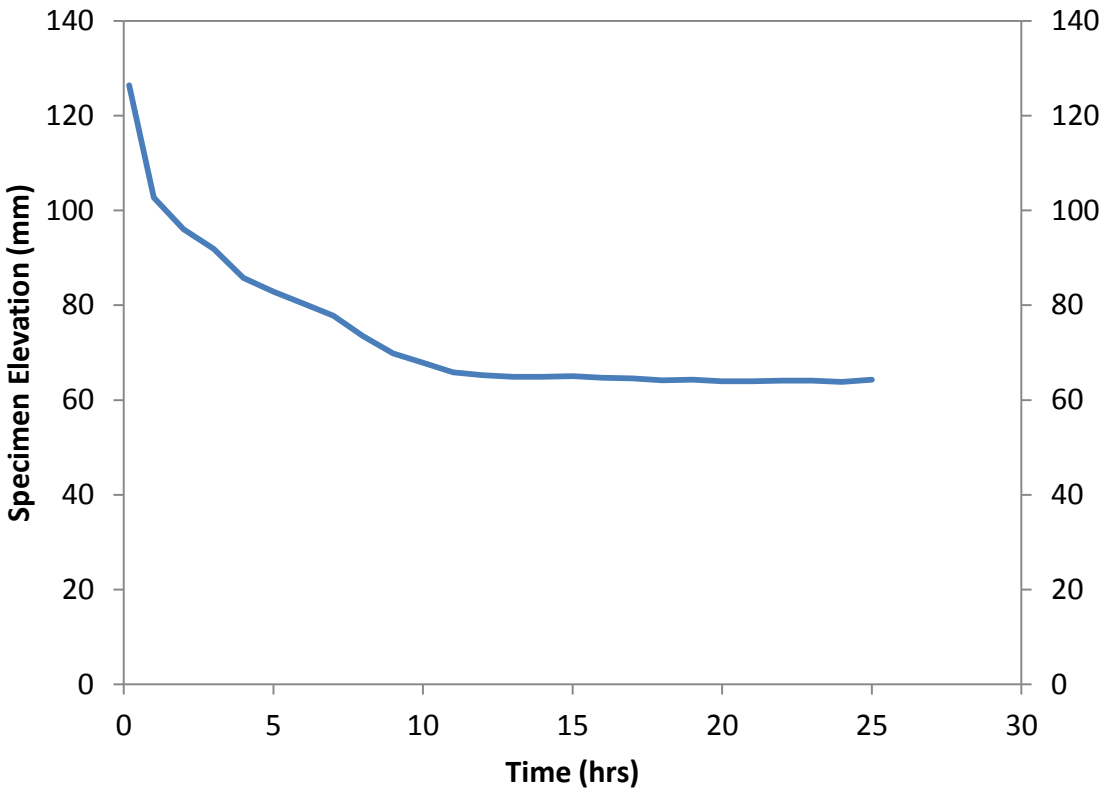

Figure 3.39 L07_S02 Frost Front Elevation in Specimen vs. Time

Figure 3.40 illustrates the rate of frost heave with time during Test L07_S02. In Test L06_S01, the specimen appeared to consolidate by 0.25 mm in the first hour of the test then began to heave at a steady rate at hour 10, reaching a maximum heave of 2.3 mm when the test was terminated at 26 hours. In Test L07_S02, however, the specimen did not appear to undergo an initial period of consolidation during the first hour of the test. The specimen did, however, begin to heave at a steady rate at hour 10. By hour 24.2, the specimen had heaved approximately 1.88 mm. The rate of heave between hours 10 and 24.2 was approximately 0.137 mm/hour. At hour 24.2, the rate of heave in the specimen decreased to approximately 0.033 mm/hour where it continued at a steady rate until the test was terminated at 45.2 hours. The total heave recorded by the specimen was 2.54 mm, which was consistent with the total heave measured in Test L06_S01.

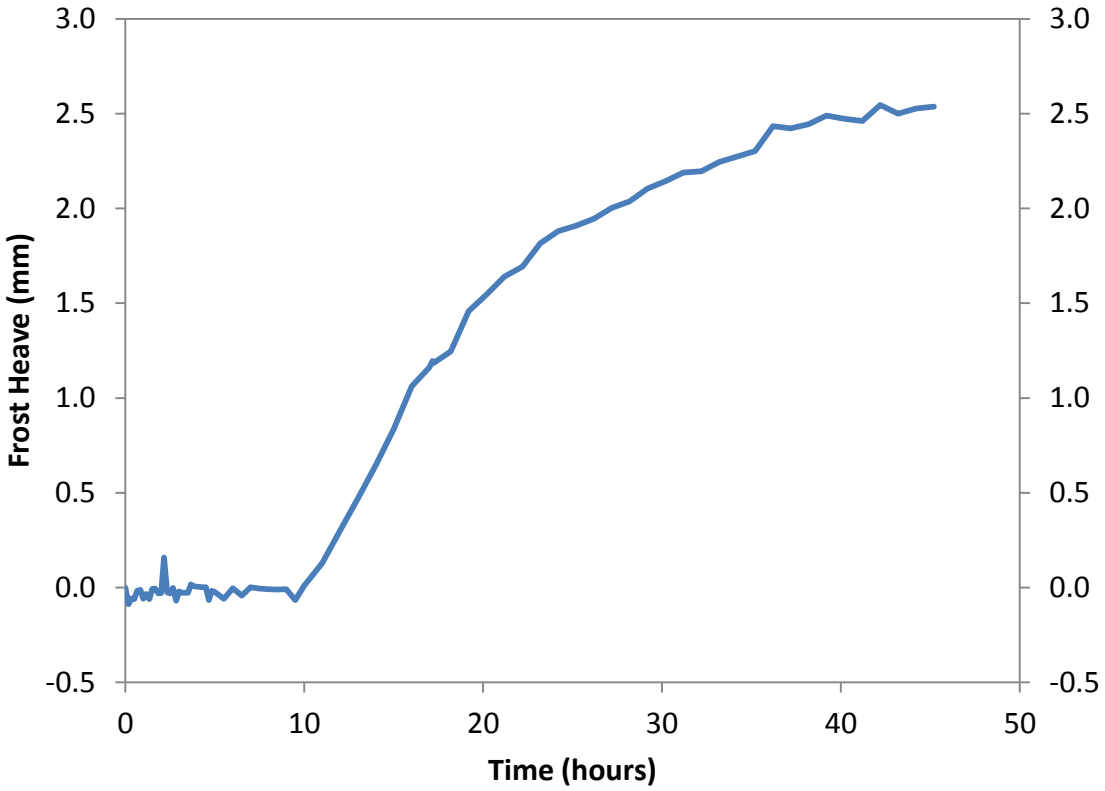

Figure 3.40 L07_S02 Frost Heave vs. Time

SP potential was not calculated for this test, as there was no water intake data available.

3.4 COMPARISON OF RESULTS

Table 3.5 summarizes the main results obtained from the three tests discussed in this chapter. This section will discuss comparisons among these results. The advantages of the test procedures developed for this research over those indicated in previous literature, as well as the repeatability of the results, will be indicated.

Table 3.5 Summary of Test Data

				Test No.		
				L05_S01	L06_S01	L07_S02
Water Content and Void Ratio	Moisture Content	Initial		24%	24%	23%
		Avg.	Frozen Zone	29%	30%	30%
		Final	Unfrozen Zone	19%	22%	21%
	Void Ratio	Initial		0.77	0.76	0.72
		Avg.	Frozen Zone	1.05	1.11	0.90
		Final	Unfrozen Zone	0.54	0.68	0.73
Data Acquisition System Measurements	Temperature Profile	Initial Settings	Top	-8°C	-8°C	-8°C
			Bottom	+2°C	+2°C	+2°C
		Initial	Top	+2.6°C	+2.3°C	+3.0°C
			Bottom	+2.8°C	+3.2°C	+3.6°C
		Final	Top	-6.9°C	-6.3°C	-6.2°C
			Bottom	+3.6°C	+4.3°C	+4.6°C
		Time to Reach Steady State		15 hours	10 hours	10 hours
	Suction Measurements	Maximum Suction		-565 kPa	-311 kPa	-
		Elevation of Max. suction		76.2 mm	76.2 mm	-
		Time of Max. Suction		5.67 hours	5.92 hours	-
	Water Intake	Rate of Water Intake		-	1.12 ml/hour	-
		Onset of Steady Rate of Intake		-	9 hours	-
		Cummulative Water Intake		-	20 ml	-
PIV Measurements	Strain Measurements	Onset of Heave Crack		-	15 hours	15 hours
		Elevation of Heave Crack		-	60 to 71.5 mm	54 to 70 mm
		Thickness of Heave Crack		-	11.5 mm	16 mm
	Void Ratio	Initial (measured)		0.77	0.76	0.72
		Avg.	Frozen Zone	0.91	0.96	0.87
		Final	Unfrozen Zone	0.63	0.61	0.60
	Frost Front	Onset of Stationary Frost Front		14 hours	16 hours	10 hours
		Depth of Frost Front Penetration		72 mm	71 mm	59 mm
		Final Elevation of Frost Front		55 mm	63 mm	68 mm
	Heave	Onset of Soil Heave		-	10 hours	10 / 24.2 hours
		Frost Heave Rate		-	0.15 mm/hour	0.137 / 0.033 mm/hour
		Total Heave		-	2.3 mm	2.54 mm
	Segregation Potential			-	40.4 $mm^2/°C*d$	-

3.4.1 Suction Results

Konrad and Morgenstern (1982a) predicted that the suction at the frost front of Devon silt could not exceed -80 kPa, without cavitation. Results from Test L05_S01 and Test L06_S01 indicated that suctions existed in this clay as low as -565 kPa and -311 kPa, respectively. These values indicated the limitations of the ceramics used to modify the pressure transducers to measure suction, and not necessarily the actual suctions in the soil. It is believed by the author that the suctions in this soil can reach values below that measured (i.e. -565 kPa). Reliable measurements of suctions in excess of those presented in this dissertation, requires the use of ceramics with higher AEVs.

The use of high capacity pressure transducers, to measure soil suction, is a considerable improvement over tensiometers and back pressure techniques. Results presented in this chapter indicated a consistent ability to measure soil suctions well in excess of what has been presented in previous literature. The use of this advanced technology to measure soil suction offers an improved methodology for the reliable measurement of soil suction.

3.4.2 PIV Results

In Tests L06_S01, and L07_S02, the strain profiles throughout the test were used to determine the onset, location, and magnitude of heave. In both tests, heave cracks were initiated at 15 hours into the tests, at approximately the same elevation as the location of the frost front at that time. The magnitude of the heave in both specimens was comparable.

PIV was also used to measure the void ratio of the soil throughout the freezing process. The final void ratio profile of each specimen was also determined from the measured moisture profile at the end of each test. Figure 3.41, Figure 3.42, and Figure 3.43 validate the use of PIV to accurately measure void ratio, through comparison of final measured values. It should also be noted that void ratio distribution did not change appreciably

from the onset of a steady state temperature profile, to the end of the test. The exception to this trend was at the location where heave occurred in Test L06_S01 and Test L07_S02. It should also be noted that the average final void ratio in the frozen zone was comparable in all three tests. Similarly, the average final void ratio in the unfrozen zone was also comparable in all three tests.

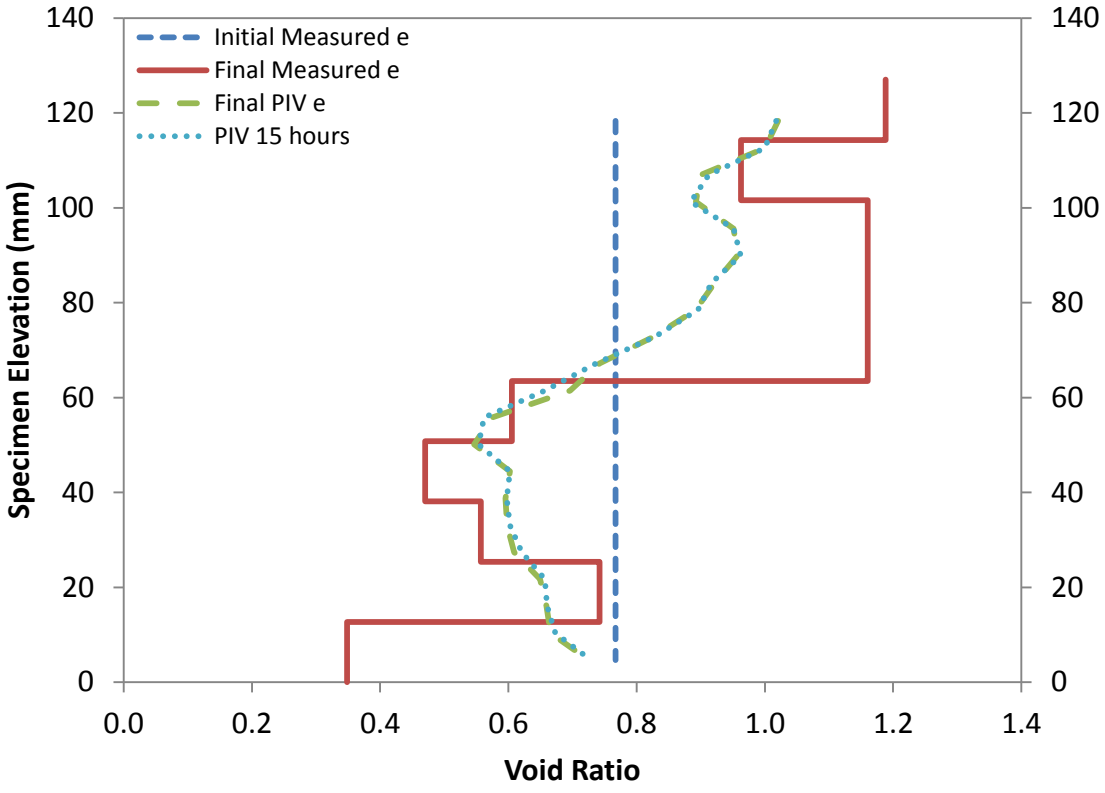

Figure 3.41 L05_S01 Void Ratio Comparison

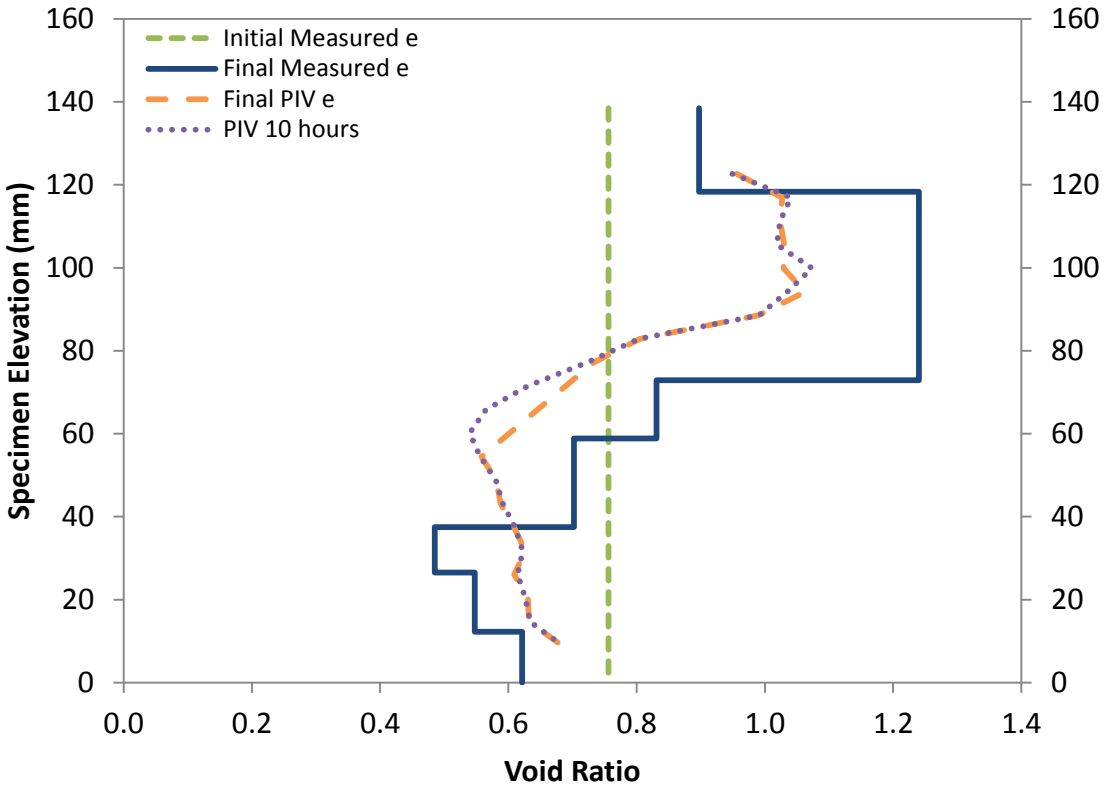

Figure 3.42 L06_S01 Void Ratio Comparison

Note that the data points at elevations 71.5 mm, 65.8 mm, and 60.1 mm, were excluded from the final profile, since the patches at those elevations were compromised.

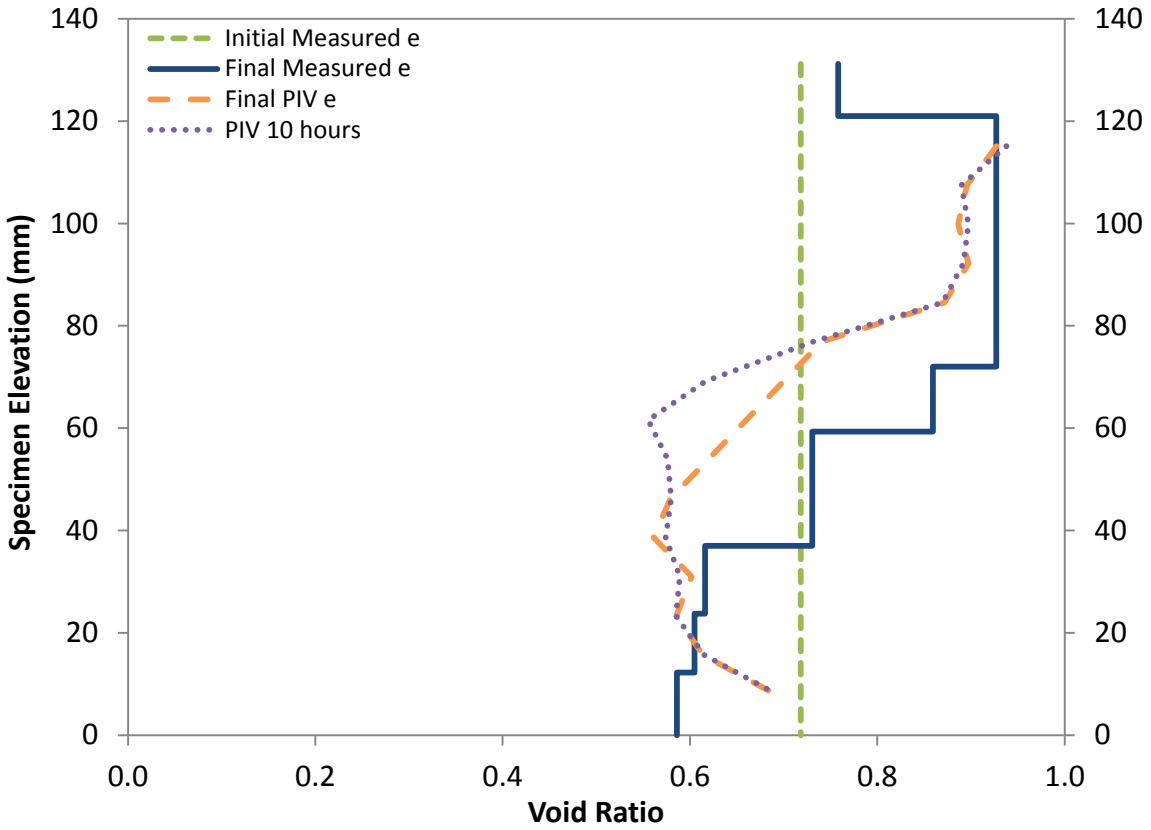

Figure 3.43 L07_S02 Void Ratio Comparison

Note that the data points at elevations 69.2 mm, 61.6 mm, and 53.9 mm, were excluded from the final profile, since the patches at those elevations were compromised.

Frost front data in Table 3.5 indicated that the onset of the frost front becoming stationary coincided with the onset of the temperature gradient reaching steady state for Tests L05_S01, and L07_S02. For Tests L06_S01, and L07_S02, the onset of the temperature gradient reaching steady state coincided with the onset of heave. This is consistent with Konrad and Morgenstern's findings (1982a). This makes sense since the frost front is synonymous with the zero degree isotherm, which would have become stationary when the temperature gradient reached steady state. As stated previously, this elevation is consistent with the elevation of the formation of the heave crack, which developed at hour 15, in Tests L06_S01, and L07_S02.

PIV allowed for the determination of multiple characteristics, simultaneously, from a set of images. PIV analysis was used in this research to calculate strain, void ratio, and heave throughout the entire freezing process. This offered a simplified and improved option over determining void ratio and strain from bulk measurements at the end of a test, and direct measurements of surface heave. Results from PIV analyses also provided a more complete understanding of strain development, void ratio redistribution, and rate of heave as freezing progressed. This was especially true for determination of the rate of heave, since Konrad and Seto (1993) indicated that the direct measurement of surface heave can be misleading and may underestimate heave by not accounting for freezing induced consolidation of the unfrozen zone of soil.

CHAPTER 4 DISCUSSION

4.1 DISCUSSION OF TEST CELL PERFORMANCE

The goal of this research was to develop a laboratory freeze cell experiment to measure suction development during frost heave damage in clayey material specimens and use Particle Image Velocimetry (PIV) to identify the mechanisms of ice lens formation. The freeze cell design was roughly based on similar apparatus from previous literature, but implemented a combination of testing techniques, using newly developed technology. The cell allowed for the successful measurement of suction, temperature, and water migration throughout the specimen, as well as the capture of images of the soil behaviour, throughout the test. The validity of the test cell performance was confirmed through obtaining repeatable test data.

The main issue encountered with the test cell, was the specimen's propensity to adfreeze to the sidewall of the cell, during Test Procedure A. This adfreezing produced an unknown confining stress on the specimen, changing the processes that took place. This confining stress created an increase in pore water pressure at the bottom of the specimen, making it difficult for the specimen to take in water.

Konrad and Morgenstern (1982b) froze specimens from the bottom upwards, to minimize the effects of side friction. This resulted in the unfrozen soil being pushed upwards, due to heave, as the frost front penetrated the soil. Results from those tests indicated that samples frozen from the bottom upwards showed no significant lateral friction. Identical samples, frozen from the top downwards, indicated an increased stress on the freezing front, due to lateral friction.

In order to overcome the effects of adfreezing in this experiment, Procedure B was developed where the cell sidewall was generously coated with a silicone lubricant prior to compaction of the specimen. Figure 3.29 illustrates the effectiveness of the lubricant, through the exhibited heave of the specimen. The initial lag in heave at the beginning of

the test, however, indicated that some friction may still exist. However, this delay could also have been partially caused by the freezing induced consolidation.

4.2 Discussion of Monitoring Equipment

4.2.1 Temperature Monitoring

The TCs used for this experiment provided sufficient temperature readings for calculating thermal gradients, and locating the zero degree isotherm. It is noted, however, that temperature sensors with a higher degree of accuracy do exist.

The type of TCs used was designed such that they could be inserted through the sidewall of the cell and extend laterally into the center of the specimen. This allowed for the measurement of temperatures at the center of the specimen, where the soil temperature should be the most consistent (i.e. least affected by ambient temperature effects).

A downside to the orientation of the TCs, however, was that when the soil heaved it had to shear past the TC wires. This added to the restriction of heave and/or consolidation.

4.2.2 Suction Monitoring

Results from two of the tests reported in this dissertation indicated large suctions in the soil near the cold side temperature boundary conditions, at the beginning of the tests. This was consistent with previous theories, however, no one has been able to reliably measure these suctions to date. Suctions observed were well in excess of -100 kPa, which was the maximum measured suction in previous literature. The ability to measure suctions, of this magnitude, in freezing soils gives valuable information about transient freezing.

The main issue encountered with the suction monitoring equipment was the tendency of the water inside the PPTs to freeze, or the ceramic tips of the PPTs to cavitate, during

transient freezing. These were limiting factors to the suction data that was able to be recorded during the test.

4.2.3 PIV Image Capture

Using PIV to analyse a freezing soil, provided more detailed soil measurements than other techniques in practice. Vertical strain and void ratio profiles were produced with time, instead of just reporting void ratio as a post-test measurement. Strain profiles illustrated that as the soil near the upper boundary condition froze, it appeared to undergo positive strain, followed by negative strain. This trend indicated that the soil underwent a period of consolidation, followed by expansion. This could have been caused by the freezing of pore water and/or the adfreezing of the soil to the cell wall and helped to explain the initial expulsion of water from the specimen. Void ratio profiles were very detailed and appeared to be more reliable than post-test measured void ratios. This may allow future researchers to perform a moisture balance on the soil throughout the test.

From the images used for PIV analysis, ice lenses were optically visible. This was useful for determining the transient elevation of the warmest ice lens (location of the frost front). Results from visual determination of the frost front location were reasonably similar to those obtained from the location of the zero degree isotherm.

PIV image analysis was also used to determine the soil displacement in terms of heave. In both Test L06_S01 and Test L07_S01, however, there was an initial lag in heave at the beginning of the test which may have been attributed to some remaining friction on the sidewall. As noted previously, the consolidation process may have also been responsible for a portion of this lag.

4.3 Discussion of Sample Preparation

Specimens were prepared using a compaction method for all tests. It should be noted that similar tests published in previous literature have been performed on consolidated

samples. Although consolidation may achieve more consistent soil samples than compaction, in terms of degree of saturation, initial suction, voids, etc., it would be a difficult and lengthy process especially for the given soil.

In order to perform an accurate PIV analysis, adequate texture was required in the images. Since the given soil consisted of fine white particles, it was necessary to add texture to the soil in the PIV window, in the form of Ottawa sand dyed black. This was easily accomplished by rolling each lift of soil in the black sand prior to compaction. Adding similar texture to a consolidated soil sample would be complicated by the consolidation process. After consideration of all of these issues, compaction was chosen to create reasonable specimens for this research.

4.4 Discussion of Test Environment and Boundary Conditions

Test environment and boundary conditions were chosen in order to replicate one dimensional step freezing tests. The test was performed in a cold room with an ambient temperature of +2°C. Glycol at -8°C was circulated through the top plate of the cell, using a chiller, to maintain a constant cold side boundary condition. Water at ambient temperature (+2°C) was circulated through the bottom plate of the cell, using a peristaltic pump, to maintain a constant warm side boundary condition. The boundary conditions were maintained such that only step freezing (not ramped freezing) tests could be performed. The bottom boundary temperature tended to rise by up to 2.6°C, likely as a result of the peristaltic pump adding heat to the water when circulating it. In addition, the uppermost TC (at the top of the specimen) never registered lower than -6.9°C. The accuracy of the cold room (+/-1°C) may have attributed to these temperature inconsistencies.

The cell was insulated (all but the PIV window) in an effort to maintain one dimensional freezing. It was necessary to leave the PIV window clear in order to obtain quality images for PIV analysis. It has not been verified that this changed the one dimensional freezing process appreciably.

One of the main issues with the test environment, that was overcome, was maintaining a constant temperature at the cold joint reference for the TCs. TCs work by measuring a voltage potential generated across two dissimilar wires that are twisted together at either end. This voltage potential translates to a temperature difference between the two wire junctions. These two junctions are represented by the tip of the TC (which is inserted in the soil) and the cold joint reference (where the wires connected to the analog input box). Since the cold joint references were located inside the cold room, they were subject to change when the cold room circulated hot or cold air to maintain the +2°C ambient temperature. This caused inconsistencies in the TC measurements since the cold joint references were changing. To overcome this, the analog input box was insulated.

4.5 Discussion of Post Test Measurements

Following the termination of the test, the specimens were extruded from the cell, and divided into horizontal slices. Slice thickness ranges from 11 mm to 50 mm, depending on the frozen/unfrozen state of the slice material and its proximity to the final ice lens. Moisture content, and void ratio profiles were determined from the slices. Slicing the specimen proved to be difficult. Due to the frozen nature of the soil, high moisture contents, and limited cutting equipment, it was almost impossible to create thin even slices whose dimensions could be reliably measured. Though data from these slices was not overly accurate, post-test void ratio profiles were reasonably similar to PIV void ratio profiles. Results from Konrad and Seto (1994) show post-test moisture profiles similar to those reported in this dissertation, reinforcing the need for a more reliable measurement system (i.e. PIV).

CHAPTER 5 CONCLUSIONS AND RECOMMENDATIONS

The goal of this research was to develop a laboratory freeze cell experiment to monitor frost heave in soil specimens and identify the mechanisms of ice lens formation under one-dimensional, open system freezing conditions. This test apparatus incorporated unique methods for assessing frost heave. Modified high capacity pressure transducers were used as an improved method to accurately, and reliably measure soil suctions. PIV was used as an improved method to accurately, and reliably measure strain, void ratio, and rate of heave of a soil during freezing. Reliable suction measurements in combination with detailed data from PIV offered an improved method for identifying the mechanisms of ice lens formation during one dimensional step freezing tests on clayey material. Results presented in this dissertation showed that the experiment developed for research produced repeatable test data.

Now that the large transient suctions during the initial stages of frost heave can be measured, as well as the transient changes in void ratio, the tools to investigate the complex mechanisms of transient freezing are available.

The following recommendations are suggested for future research:

- Ensure adequate (i.e. excessive) lubrication on the cell sidewall to prevent adfreezing of the specimen and increased friction
- Implement more precise temperature regulation of the fluids used to control the temperature boundary conditions
- Use TCs with a higher degree of accuracy than +/-0.5°C (i.e. Resistance Temperature Detectors (RTDs))
- Explore the possibility of using a glycol/water mix to saturate ceramic tips of PPTs to prevent the liquid inside the PPT from freezing. This may have implications for air AEVs of ceramics
- Be more strategic with the number of PPTs, and placement depending on whether suctions are measured during transient freezing, or at the final ice lens

- If measuring suctions during transient freezing, use ceramic tips with higher AEVs since transient suctions are very large at the beginning of freezing
- If measuring suctions directly above and/or below the final ice lens, use ceramics with lower AEVs for ease of saturation, since large suctions will not develop
- Capture PIV images frequently (i.e. 5 minute intervals) at the beginning of the test (first 5 hours), then less frequently (i.e. 30 minute intervals) for the duration of the test
- Study the effects of a fully insulated cell, versus an insulated cell with an uninsulated PIV window
- Explore the possibility of leaving the PIV window uninsulated at the beginning of the test, but insulated once the image frequency is increased to 30 minute intervals (insulation on PIV window will have to be briefly removed to capture each subsequent image)
- Explore the use of consolidated samples (must add texture)
- Unless an improved method for post-test slicing of the specimen is developed, explore the use of PIV to determine changes in void ratio, instead of measured values

BIBLIOGRAPHY

Andersland, O.B., and Ladanyi, B. 2004. Frozen ground engineering second edition. John Wiley and Sons, Inc., Hoboken, New Jersey.

Arenson, L.U., Firew Azmatch T., and Sego, D.C. 2008. A new hypothesis on ice lens formation in frost susceptible soils. Proceedings of the Ninth International Conference on Permafrost, Fairbanks, Alaska, pp. 59-64.

Arenson, L.U., and Sego, D.C. 2004. Freezing processes for a coarse sand with varying salinities. Proceedings of the International Symposium on Cold Regions Engineering, Canada, Vol. 12, 0-unpaginated.

Arenson, L.U., Sego, D.C., and Take, W.A. 2007. Measurement of ice lens growth and soil consolidation during frost penetration using particle image velocimetry (PIV). Proceedings of the 60th Canadian Geotechnical Conference, Ottawa, ON, pp. 2046-2053.

Arenson, L. U., Xia, D., Sego, D. C., and Biggar, K. W. 2006. Change in ice lens formation for saline and non-saline devon silt as a function of temperature and pressure. Proceedings of the International Symposium on Cold Regions Engineering, Vol. 13, pp. 1-11.

Azmatch, T. F., Arenson, L. U., Sego, D. C., & Biggar, K. W. 2008. Measuring ice lens growth and development of soil strains during frost penetration using particle image velocimetry (GeoPIV). Proceedings of the International Conference on Permafrost, United States, Vol. 9, pp. 89-93.

Beddoe, R.A., Take, W.A., and Rowe, R.K. 2010. Development of suction measurement techniques to quantify the water retention behaviour of GCLs. Geosynthetics International, **17**(5): 301-312.

Conax Technologies. 2013. Technical Data – Tolerance of Thermocouples [Internet]. [Cited 20 March 2013], available from World Wide Web: http://www.conaxtechnologies.com

Ito, Y., Vinson, T. S., Nixon, J. F. D., & Stewart, D. 1998. An improved step freezing test to determine segregation potential. Proceedings of the Permafrost; Seventh International Conference, Yellowknife, Canada, Collection Nordicana, Vol. 67, pp. 509-516.

Konrad, J. M. 1994. Sixteenth canadian geotechnical colloquium; frost heave in soils; concepts and engineering. Canadian Geotechnical Journal, 31(2): 223-245.

Konrad, J.M. 1987. Procedure for determining the segregation potential of freezing soils. ASTM Geotechnical Testing Journal, 10(2): 51-58.

Konrad, J. M., and Morgenstern, N.R. 1980. A mechanistic theory of ice lens formation in fine-grained soils. Canadian Geotechnical Journal, 17(1): 473-486.

Konrad, J.M., and Morgenstern, N. R. 1981. The segregation potential of a freezing soil. Canadian Geotechnical Journal, 18(4): 482-491.

Konrad, J.M., and Morgenstern, N.R. 1982a. Prediction of frost heave in the laboratory during transient freezing. Canadian Geotechnical Journal, 19(3): 250-259.

Konrad, J.M., and Morgenstern, N.R. 1982b. Effects of applied pressure on freezing Soils. Canadian Geotechnical Journal, 19(4): 494-505.

Konrad, J. M.,and Seto, J. T. C. 1994. Frost heave characteristics of undisturbed sensitive champlain sea clay. Canadian Geotechnical Journal, 31(2), 285-298.

Penner, E. and Ueda, T. 1977. The dependence of frost heaving on load application – preliminary results. Proceedings of the International Symposium on Frost Action in Soils, Lulea, Vol. 1, pp. 92-101.

Penner, E. 1986. Aspects of ice lens growth in soils. Cold Regions Science and Technology, 13: 91-100.

Saarelainen, S. 1996. Pavement design applying allowable frost heave. Proceedings of the International Conference on Cold Regions Engineering, Fairbanks, AL, USA, pp. 890-898.

Take, W. A., and Bolton, M. D. 2003. Tensiometer saturation and the reliable measurement of soil suction. Geotechnique, 53(2): 159-172.

Thermx Southwest. 2013. Pressure transducers – Druck PDCR 4000 Series [Internet]. [Cited 20 March 2013], available from World Wide Web: http://www.thermx.com

White, D.J., Take, W.A., and Bolton, M.D. 2003. Soil deformation measurement using particle image velocimetry (PIV) and photogrammetry. Geotechnique, 53(7): 619-631

APPENDIX A Compaction Curve

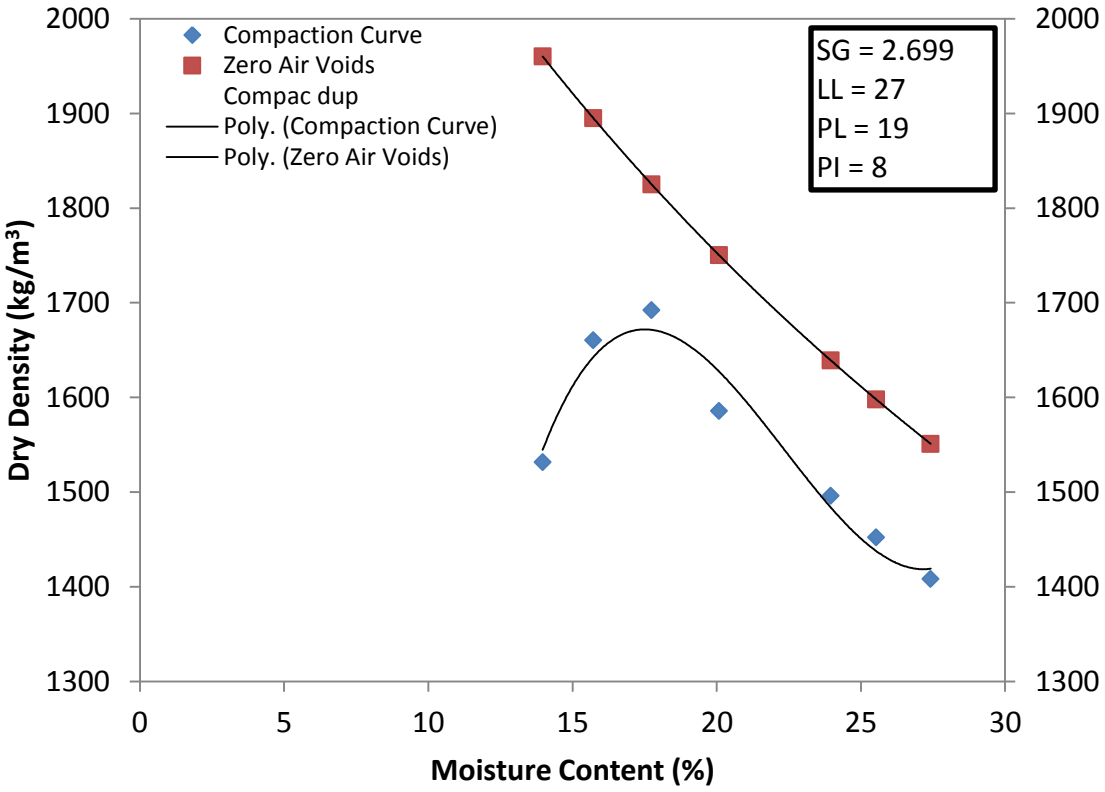

Figure A.1 Compaction Curve

APPENDIX B Comparison of Zero Degree Isotherm Location with Visual Observations of Freezing Front

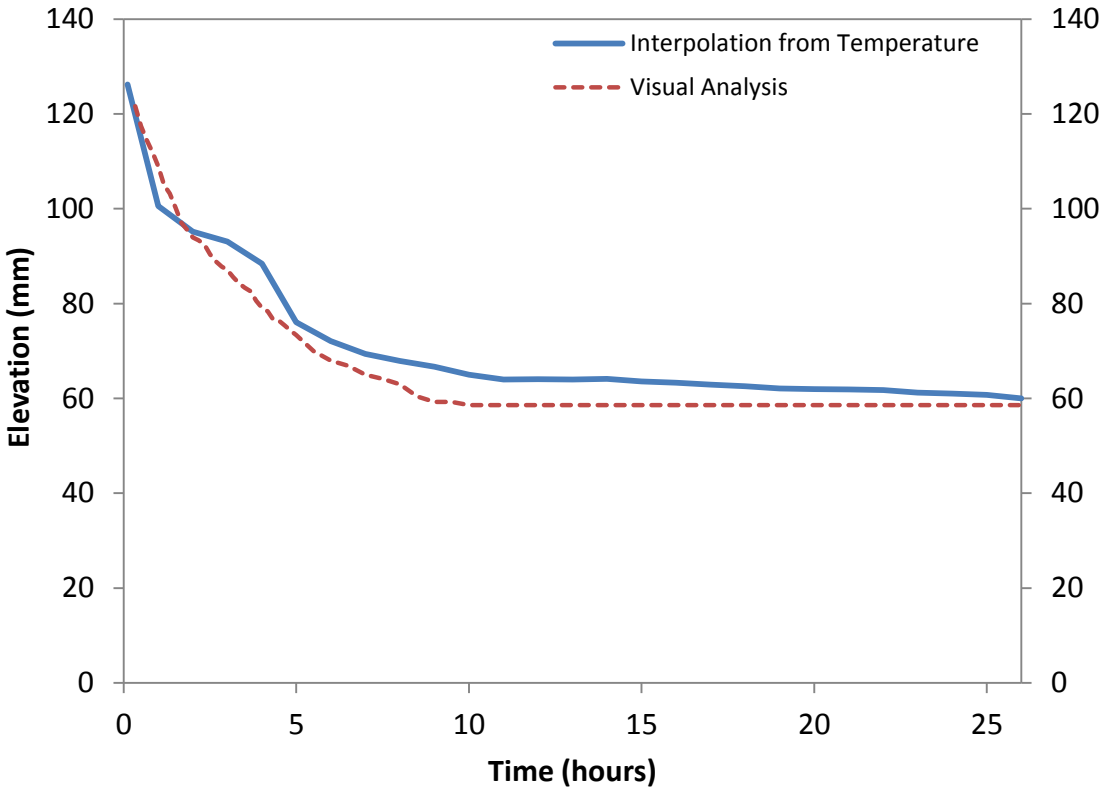

Figure B.1 Comparison of zero degree isotherm location with visual observations of freezing front